Università degli Studi di Pisa

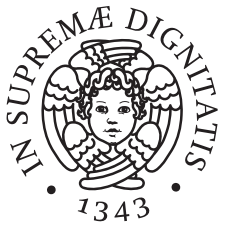

Facoltà di Scienze Matematiche, Fisiche e Naturali

Corso di Laurea in Fisica

Non-Local Gravity and Dark Energy

April 22, 2014

Tesi di Laurea Magistrale

Candidato
Michele Mancarella
mancarell@gmail.com

Relatore
Prof. Michele Maggiore
Université de Genève

Relatore interno
Dott. Giancarlo Cella
Università di Pisa

Anno Accademico 2012/2013

Contents

Introduction and summary

The observation of the accelerated expansion of the Universe in 1998 is without any doubt the most striking result in modern cosmology. Standard Cosmology is based on General Relativity (GR), a theory of impressive beauty, power and simplicity, which is supported by a number of tests at Solar System scales. However, Einstein's theory maintains untouched the Newtonian intuition that gravity should be attractive, hence leading to a *decelerating* Universe. An accelerated expansion hence requires some modification, at least at cosmological scales. A possible explanation, consistent with existing data, is provided by the introduction of a "cosmological constant" term Λ in the field equations. The value of the energy stored in such constant today, generally called "Dark Energy" (DE), has to be of the order of the critical density, $\rho_\Lambda \sim 10^{-12}\, eV^4$, a ridiculously small value that still leaves open a number of questions. In particular, in QFT a cosmological constant term can emerge from vacuum fluctuations, but there is no hint of why one should get the observed scale $10^{-3} eV$. Rather on the contrary, naive estimates leads to $\rho_{vac} \sim k_{max}^4$, where k_{max} is the UV cutoff of the theory. Also, a constant vacuum energy would have been negligibly small in the whole past history of the Universe, since it is constant in time, while matter and radiation density evolve as a^{-3} and a^{-4}, respectively (where a is the scale factor). So, it is quite puzzling that matter density and vacuum energy density become comparable just at the present epoch. This latter issue is often referred to as the "Cosmic coincidence problem".

Hence, there are many reasons to consider a dynamical dark energy as an alternative to a cosmological constant. First, it is a logical possibility which might be correct, and can be constrained by observation. Secondly, it is consistent with the hope that the ultimate vacuum energy might actually be zero. But most interestingly, one might wonder whether replacing a constant parameter Λ with a dynamical field could allow us to relax the fine-tuning that inevitably accompanies the cosmological constant. On the other hand, recent observations opened the possibility of a slight deviation from an equation of state $w_{DE} = -1$, suggesting in particular that a "phantom" (i.e. $w_{DE} < -1$) behaviour could explain the tension between different measurements, though these results should be interpreted just as preliminary hints that have to be supported by more precise measurements that will become available in the near future.
The nature of Dark Energy can be in principle approached in two ways. One is to add some exotic field to the matter content on the right hand side of Einstein's equations, contributing to the energy-momentum tensor with a negative pressure term. Alternatively, one could try a modified gravity model, in which the modification is made on the left hand side of the equations, i.e. on the Einstein tensor. Of course, from the point of view of gravitation itself, there is no way to distinguish the two using only gravitational interactions, since any modification to the Einstein tensor con be re-formulated into an "effective energy-momentum tensor" by moving it on the right hand side, and vice versa.
In recent years, a few authors explored the possibility of using non-local terms to produce mod-

ifications of General Relativity in the infrared with different motivations, e.g. the degravitation mechanism or the possibility to give mass to the graviton without breaking the gauge invariance of the massless theory.

In this work, we propose a modification of gravity obtained adding a term $m^2\, R\Box^{-2}R$ to the Einstein-Hilbert action. The resulting theory should be understood as a classical effective one. We find that the mass parameter m only affects the non-radiative sector of the theory, while the graviton remains massless, there is no propagating ghost-like degree of freedom, no vDVZ discontinuity, and no Vainshtein radius below which the theory becomes strongly coupled. For $m = \mathcal{O}(H_0)$ (where H_0 is the present value of the Hubble constant, $H_0 \sim 70\,\mathrm{Km\,s^{-1}\,Mpc^{-1}}$) the theory therefore recovers all successes of GR at solar system and lab scales, and only deviates from it at cosmological scales. We examine the cosmological consequences of the model and we find that it automatically generates a dynamical Dark Energy and a self-accelerating evolution. After fixing our only free parameter m so to reproduce the observed value of the Dark Energy density today, we get a pure prediction for the Dark Energy equation of state, $w_{DE} \approx -1.14$. This value is in excellent agreement with the Planck result $w = -1.13 + 0.13$ and would also resolve the existing tension between the Planck data and local measurements of the Hubble parameter. These original results have been recently published on the arXiv [1].

In chapter 1 we recall some basics aspects of the standard FRW cosmology, without giving a complete treatment, but rather underlying the aspect more relevant for the subsequent discussion, since the existence of a Dark Energy and its domination today are confirmed by a number of observations relying on the cosmological model we assume. In chapter 2 we present the most robust evidences of the accelerated expansion, Type Ia Supernovae (SnIa), Baryon Acoustic Oscillations (BAO), and the Cosmic Microwave Background (CMB), and we comment about the most recent experimental results. We then introduce our original non-local model in which a dynamical Dark Energy naturally emerges. We present in detail the cosmological consequences, and we comment on its predictive power and testability, comparing it to already existing models; we also show that the model smoothly reduces to GR at Solar System scales, hence recovering its experimental successes. We discuss in detail the conceptual aspects related to the introduction of non-local operators and their proper interpretation. Finally, in chapter 4 we discuss some possible extensions of the model.

Chapter 1

Basics of FRW cosmology

Throughout the text we shall assume the reader to be familiar with General Relativity and the basic cosmological picture, including thermal history and the need for an inflationary phase.

In this chapter we shall recall the basics of standard FRW cosmology. Rather than to provide a complete treatment, which can be found in every textbook such as [2], the aim is to fix the notation and to highlight a few concepts and definitions we shall need below.

1.1 FRW metrics

Standard Big Bang cosmology relies on the Cosmological Principle, the statement that the Universe is homogeneous and isotropic on large scales ($\ell \geq 100\,\mathrm{MpC}$), that can be formulated as follows: "*At any epoch, the Universe appears the same to all observers regardless of their individual locations*". This leads to the choice of a manifold of the form $R \times \Sigma$, where R is the time and Σ a three-manifold. The metric on it can be written in the general form

$$ds^2 = -dt^2 + a^2(t)\gamma_{ij}(x)dx^i dx^j \tag{1.1.1}$$

Here $a(t)$ is a function of time and γ_{ij} is the metric on Σ. We stress that, throughout the work, we shall use the "mostly +" convention for the metric (i.e. with signature $(-1, 1, 1, 1)$), as it is clear from the above expression. Since space is homogeneous, it must have the same curvature everywhere: as for the more familiar case of a two-dimensional manifold in a 3D space, the only three possible geometries with constant curvature are flat (a plane), positively curved (the surface of a sphere), negatively curved (a saddle). The most general expression of the metric can be shown to be [2] the Friedmann-Robertson-Walker (FRW) metric, which, in a suitable coordinate system, can be written as

$$ds^2 = -dt^2 + dl^2 = -dt^2 + a^2(t)\left(\frac{dr^2}{1-kr^2} + r^2 d\theta^2 + r^2 \sin^2\theta d\phi^2\right) \tag{1.1.2}$$

Here, $a(t)$ is the scale factor with cosmic time t and (r, θ, ϕ) are comoving coordinates, i.e., any observer at (r_0, θ_0, ϕ_0) will maintain the values of such coordinates fixed while the physical distances will grow isotropically as $a(t)$. The value of k describes the geometry of the spatial section of space-time, with

$$k = 1 \qquad \text{hypersphere ("open" universe)} \tag{1.1.3}$$
$$k = 0 \qquad \text{no curvature ("flat" universe)} \tag{1.1.4}$$
$$k = -1 \qquad \text{3-hyperboloid ("closed" universe)} \tag{1.1.5}$$

We shall re-cast 1.1.2 in the more convenient form

$$ds^2 = dt^2 - dl^2 = dt^2 - a^2(t)\left(d\chi^2 + S_k^2(\chi)\, d\Omega^2\right) \tag{1.1.6}$$

where

$$S_k(\chi) = \begin{cases} \sin\chi & k = 1 \\ \chi & k = 0 \\ \sinh\chi & k = -1 \end{cases} \tag{1.1.7}$$

or, in a unified notation,

$$S_k(\chi) = \frac{1}{\sqrt{-k}} \sinh\left(\sqrt{-k}\,\chi\right) \tag{1.1.8}$$

The case of a flat Universe is recovered by taking the limit $k \to 0$.

In some cases it is convenient to work in terms of the conformal time

$$d\eta = \frac{dt}{a(t)} \tag{1.1.9}$$

so that the metric becomes

$$ds^2 = a^2(\eta)[-d\eta^2 + d\chi^2 + S_k^2(\chi)\, d\Omega^2] \tag{1.1.10}$$

The unknown variables are the curvature k and the scale factor $a(t)$. These are determined by gravity - through Einstein's equations - and thermodynamics - through the equation of state of matter and radiation.

1.2 Kinematics: Cosmological redshift and Hubble's law

Since the observations of Hubble in the 20's, it is known that the observed wavelength λ_{obs} of absorption lines of a distant object is larger than the wavelength λ_{em} at emission.
We define the redshift as

$$z = \frac{\lambda_{obs} - \lambda_{em}}{\lambda_{em}} \tag{1.2.1}$$

Consider a wave coming from a source at radial distance χ. Since light travels on geodesics, $ds^2 = 0$, we have for incoming light $a(t)d\chi = -dt$ so

$$\chi = -\int_{t_{obs}}^{t_{em}} \frac{dt}{a(t)} = \int_{t_{em}}^{t_{obs}} \frac{dt}{a(t)} \tag{1.2.2}$$

If the next crest is emitted after an interval $\delta t_{em} = 1/\nu_{em}$ and received after an interval $\delta t_{obs} = 1/\nu_{obs}$, since the comoving distance is fixed we have also

$$\chi = \int_{t_{em}+\delta t_{em}}^{t_{obs}+\delta t_{obs}} \frac{dt}{a(t)} \tag{1.2.3}$$

This is true only if

$$\frac{\delta t_{obs}}{a(t_{obs})} = \frac{\delta t_{em}}{a(t_{em})} \tag{1.2.4}$$

so we get the fundamental relations

$$1 + z \equiv \frac{\nu_{em}}{\nu_{obs}} = \frac{a(t_{obs})}{a(t_{em})} = \frac{\delta t_{obs}}{\delta t_{em}} \tag{1.2.5}$$

The redshift gives then the amount of time dilation, as well as the ratio between the radius of the Universe at different epochs.

The dynamical explanation of the redshift is instead given by the Doppler shift expression in a locally Lorenzian frame

$$z = \left(\frac{1+\beta}{1-\beta}\right)^{1/2} \overset{\beta<<1}{\simeq} \beta \tag{1.2.6}$$

From Hubble's law, $z = H_0\, d/c$, we can relate the physical distance $d = a(t)\chi$ with the redshift and thus to the recession velocity by $v = H_0\, d$. On the other hand, from FRW metrics we have

$$v = \dot{d}(t_0) = \dot{a}(t_0)\chi = \dot{a}_0\chi = \frac{\dot{a}_0}{a_0} d \tag{1.2.7}$$

from which we read $H_0 = \dot{a}_0/a_0$, so we can define, at any time, $H(t) = \dot{a}(t)/a(t)$.

1.3 Dynamics: The Friedmann Equations

The scale factor $a(t)$ can be related to the energy-momentum density through Einstein's equations, which we shall write in the form

$$R_{\mu\nu} + g_{\mu\nu}\Lambda = 8\pi G \left(T_{\mu\nu} - \frac{1}{2} T g_{\mu\nu}\right) \tag{1.3.1}$$

We have included the "cosmological constant" term, $g_{\mu\nu}\Lambda$, in order to illustrate clearly its consequences on the background evolution.

We shall consider matter and energy as a perfect fluid at rest in comoving coordinates, so that the energy-momentum tensor

$$T_{\mu\nu} = (\rho + p) U_\mu U_\nu + p g_{\mu\nu}, \qquad U_\mu = (1, 0, 0, 0) \tag{1.3.2}$$

can be put in the convenient form

$$T^\mu_\nu = diag(-\rho, p, p, p) \tag{1.3.3}$$

In FRW, the curvature terms in d spatial dimensions become ($H \equiv \dot{a}/a$)

$$\begin{aligned} R^0_0 &= d(\dot{H} + H^2) = d\frac{\ddot{a}}{a} \\ R^i_j &= \left(\dot{H} + dH^2 + (d-1)\frac{k}{a^2}\right)\delta^i_j = \left(\frac{\ddot{a}}{a} + (d-1)\frac{\dot{a}^2}{a^2} + (d-1)\frac{k}{a^2}\right)\delta^i_j \\ R &= 2d\left(\dot{H} + \frac{d+1}{2}H^2 + \frac{k}{a^2}\right) = 2d\left(\frac{\ddot{a}}{a} + \frac{\dot{a}^2}{a^2} + \frac{k}{a^2}\right) \end{aligned} \tag{1.3.4}$$

The $(0,0)$ and (i,j) components of 1.3.1 in $d=3$ give the Friedmann equations

$$\left(\frac{\dot{a}}{a}\right)^2 = \frac{8\pi G}{3}\rho - \frac{k}{a^2} + \frac{\Lambda}{3} \tag{1.3.5}$$

$$\frac{\ddot{a}}{a} = -\frac{4\pi G}{3}(\rho + 3p) + \frac{\Lambda}{3} \tag{1.3.6}$$

Introducing the standard definitions of critical density and density parameter

$$\rho_c(t) = \frac{3H^2(t)}{8\pi G} \tag{1.3.7}$$

$$\Omega(t) = \frac{8\pi G}{3H^2(t)}\rho(t) = \frac{\rho(t)}{\rho_c(t)} \tag{1.3.8}$$

the Friedmann equation 1.3.5 becomes

$$\Omega(t) - 1 = \frac{k}{H^2 a^2} \tag{1.3.9}$$

where we have defined $\rho_\Lambda = \Lambda/8\pi G$. The density parameter, which can be observationally constrained, fixes the geometry of the universe:

$$\begin{aligned} &\rho < \rho_{crit} \Leftrightarrow \Omega < 1 \Leftrightarrow k < 0 \Leftrightarrow \text{open} \\ &\rho = \rho_{crit} \Leftrightarrow \Omega = 1 \Leftrightarrow k = 0 \Leftrightarrow \text{flat} \\ &\rho > \rho_{crit} \Leftrightarrow \Omega > 1 \Leftrightarrow k > 0 \Leftrightarrow \text{close} \end{aligned} \tag{1.3.10}$$

The second of the Friedmann equations, (1.3.6) implies that, in absence of a cosmological constant, an accelerated expansion can occur only if $\rho + 3p < 0$. In the usual case $p > 0$, $\rho > 0$, Einstein's GR maintains untouched the Newtonian intuition that gravity should be attractive, $\ddot{a} < 0$. On the contrary, if we stick to GR, an accelerating expansion could come from the pressure term - which is an entirely relativistic effect - only requiring a large negative value. As one can see from the Friedmann equations, the cosmological constant indeed does the job, since it can be considered as an energy component with mass density $\rho_\Lambda = \Lambda/8\pi G$ and pressure $p_\Lambda = -\rho_\Lambda$.

To make progress we can choose an equation of state. The perfect fluids relevant for cosmology obey the simple relation

$$p = w\,\rho \tag{1.3.11}$$

From energy-momentum covariant conservation $\boldsymbol{\nabla}_\mu T^{\mu\nu} = 0$ we read the continuity equation

$$\dot{\rho} + 3H(\rho + p) = 0 \tag{1.3.12}$$

which using 1.3.11 can be integrated assuming a constant w to yield

$$\rho = \sum_i \rho_{0,i}\left(\frac{a}{a_0}\right)^{-3(1+w_i)} = \sum_i \rho_{0,i}(1+z)^{3(1+w_i)} \tag{1.3.13}$$

The sum runs over the species that contribute to the energy-momentum density, non-relativistic particles ($w_M = 0$), relativistic particles ($w_R = 1/3$), cosmological constant ($w_\Lambda = -1$). The

ΛCDM model is defined by $w_\Lambda = -1$.

Given the nature of our discussion, it is more convenient to introduce a form of Dark Energy which allows for an arbitrary equation of state of the form $P = w(z)\,\rho$. In this case the continuity equation is integrated to give $\Omega_{DE}(z) = \Omega_{DE}\, f(z)$, where the dimensionless Dark Energy density is

$$f(z) = \exp\left[3\int_0^z \frac{1+w(z')}{1+z'}\,dz'\right] \tag{1.3.14}$$

From equation 1.3.5 we can now read how the Hubble parameter is determined by the energy content of the Universe. Introducing the more general dynamical EOS for the Dark Energy instead of the cosmological constant, we can put it in the convenient form

$$H^2(t) = H_0^2\left[\Omega_R(1+z)^4 + \Omega_M(1+z)^3 + \Omega_{DE}\, f(z) + \Omega_k(1+z)^2\right] \tag{1.3.15}$$

where we have defined $\Omega_k = -k/(a_0^2 H_0^2)$ and we denote by Ω_i the energy density of the different species at the present time.

We finally introduce the function

$$E(z) = \left[\Omega_R(1+z)^4 + \Omega_M(1+z)^3 + \Omega_{DE}\, f(z) + \Omega_k(1+z)^2\right]^{1/2} \tag{1.3.16}$$

so that $H(z) = H_0 E(z)$.

In the following, we shall use the term "Dark Energy" to indicate everything that is not ordinary matter-radiation or curvature and that could lead to an accelerated expansion. The case of a cosmological constant is included in this definition. Conversely, we may use the definition "cosmological constant" referring to something that is actually a dynamical Dark Energy. In conclusion, the two terms may be used interchangeably.

1.4 Distances

Consider an object with absolute luminosity L at physical distance d. In a flat space, the observed flux would be $F = L/S$ where S is the surface of the sphere of radius d, $S = 4\pi d^2$. In an expanding Universe however, we have $S = 4\pi a_0^2 S_k^2(\chi)$ and we must also account for the expansion. According to 1.2.5, we have two effects: the redshifted frequency of the photons and the reduction of the detection rate due to the stretching of time intervals. These two effects will reduce the observed flux by a factor of $(1+z)$ each. Then the detected apparent luminosity is

$$F = \frac{L}{4\pi a_0^2 S_k^2(\chi)\,(1+z)^2} \tag{1.4.1}$$

To recover the same functional form as in flat space, we define the **luminosity distance** by

$$d_L = a_0\, S_k(\chi)\,(1+z) \tag{1.4.2}$$

For a photon moving on a geodesic, $ds^2 = 0$, we have $d\chi = -dt/a(t)$. Using the definition of H and the expression 1.2.5 for the redshift we have

$$\frac{d}{dt} = \dot{a}\frac{d}{da} = \dot{a}\frac{dz}{da}\frac{d}{dz} = -H\,(1+z)\,\frac{d}{dz} \tag{1.4.3}$$

so we find that the comoving distance is given by

$$\chi = \int_0^t \frac{dt}{a(t)} = \int_0^z \frac{dz}{H(z)\,a\,(1+z)} = \frac{1}{a_0 H_0}\int_0^z \frac{dz'}{E(z')} \tag{1.4.4}$$

where we used equations 1.4.3 and 1.2.5 and the definition 1.3.16 of $E(z)$.
Note that this is also the maximum comoving distance light can propagate between initial time 0 and time t and is called the *(comoving) particle horizon*. The physical size is $d(t) = a(t)\,\chi$.

Finally, using the definition 1.1.8 of $S_k(\chi)$ we read from 1.4.2 the general expression

$$d_L(z) = \frac{(1+z)}{H_0\sqrt{\Omega_k}} \sinh\left(\sqrt{\Omega_k}\int_0^z \frac{dz'}{E(z')}\right) \tag{1.4.5}$$

Through equation 1.3.15 we are able to determine the dependence of the luminosity distance from the energy and geometry evaluating 1.4.5.
We illustrate such dependence with an explicit example (see e.g. [3]). Let us consider a two component Universe with a non-relativistic fluid and a cosmological constant. The function $\int_0^z \frac{dz'}{E(z')}$ can be expanded for $z << 1$ as

$$\int_0^z \frac{dz'}{E(z')} = z - \frac{E'(0)}{2}z^2 + \frac{1}{6}\left[2E'(0)^2 - E''(0)\right] z^3 + \mathcal{O}(z^4) \tag{1.4.6}$$

Plugging in 1.4.5 and expanding $\sinh x = x + x^3/3 + \mathcal{O}(x^5)$ we find

$$\begin{aligned} d_L &= \frac{1}{H_0}\left[z + \left(1 - \frac{E'(0)}{2}\right) z^2 + \frac{1}{6}\left(2E'(0)^2 - E''(0) - 3E'(0) + \Omega_k\right) z^3 + \mathcal{O}(z^4)\right] \\ &= \frac{1}{H_0}\left[z + \frac{1}{4}\left(1 - 3w_{DE}\Omega_{DE} + \Omega_k\right) z^2 + \mathcal{O}(z^3)\right] \end{aligned} \tag{1.4.7}$$

Since $w_{DE} < 0$ and $\Omega_{DE} > 0$, the luminosity distance becomes larger in presence of a cosmological constant. The same happens in an open Universe - $k < 0$ - with respect to a flat one. In figure 1.1 we show three different cases.

Another useful notion of distance is the distance we infer from the intrinsic and observed size of a source, called the **angular diameter distance**; it is defined to be

$$d_A = \frac{R}{\theta} \tag{1.4.8}$$

where R is the proper size and θ is the observed angular diameter. It is easy to check that this distance is related to d_L by

$$d_L = (1+z)^2 d_A \tag{1.4.9}$$

1.5 Age of the Universe

From 1.4.3 we have the relation

$$dt = -\frac{dz}{H(z)\,(1+z)} \tag{1.5.1}$$

which integrates to

$$t_0 = \int_0^{t_0} dt = \frac{1}{H_0}\int_0^\infty \frac{dz}{E(z)\,(1+z)} \tag{1.5.2}$$

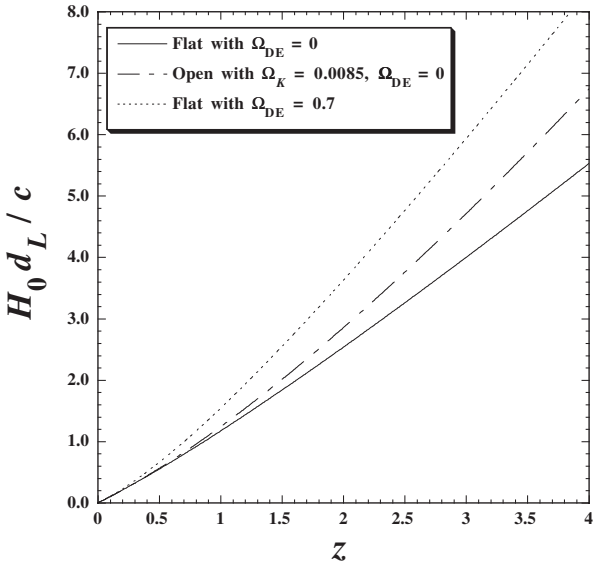

Figure 1.1: Luminosity distance d_L for a two-component flat Universein the cases: (1) flat Universe without Dark Energy, (2) open Universe without Dark Energy, (3) flat Universe with cosmological constant. Figure from ref. [4]

We shall anticipate the discussion of chapter 2 integrating equation 1.5.2 in the case of a flat Universe with a negligible amount of relativistic matter, $\Omega_M + \Omega_{DE} = 1$. Then

$$t_0 = \frac{1}{3\,H_0\,\sqrt{1-\Omega_M}}\,\log\left(\frac{1+\sqrt{1-\Omega_M}}{1-\sqrt{1-\Omega_M}}\right) \tag{1.5.3}$$

This equation makes evident that t_0 increases for decreasing Ω_M (in the limit $\Omega_M \to 0$ we have $t_0 \to \infty$), while in absence of Dark Energy we get $t_0 = 2/(3H_0)$.

It could be possible to make the cosmic age larger also in an open Universe without Dark Energy. Setting $\Omega_{DE} = 0$, $\Omega_M + \Omega_k = 1$ we get from 1.5.2

$$t_0 = \frac{1}{H_0\,(1-\Omega_M)}\left[1 + \frac{\Omega_M}{2\sqrt{1-\Omega_M}}\,\log\left(\frac{1-\sqrt{1-\Omega_M}}{1+\sqrt{1-\Omega_M}}\right)\right] \tag{1.5.4}$$

The limit $\Omega_M \to 1$ is again $t_0 = 2/(3H_0)$, while the opposite case $\Omega_M \to 0$ gives $t_0 = H_0^{-1}$.

Chapter 2

Dark Energy: Observational Evidences

In this chapter we review the most significant observations supporting the existence of a Dark Energy component. We shall concentrate on the most mature and well-studied probes of an accelerated expansion: Type Ia Supernovae (SnIa), Baryon Acoustic Oscillations (BAO), and the Cosmic Microwave Background (CMB). Being purely geometrical and statistically independent, they are the most robust measurements currently available.

2.1 Age of the Universe

The computation of the age of the Universe can be directly compared with the oldest known stellar populations. The data of a number of groups are available: Jimenez *et al.* determined the age of Globular clusters in the Milky way as $t = 13.5 \pm 2\, Gyr$ [5], while Caretta *et al.* obtained $12.9 \pm 2.9\, Gyr$ [6], Richer *et al.* and Hansen *et al.* [7] constrained the age of the Globular cluster M4 to $t = 12.7 \pm 0.7\, Gyr$. A more recent measurement by Bond *et al.* has determined the age of the nearby sub-giant HD-140283 to be $14.5 \pm 0.8\ Gyr$ [8].
On the other hand, bounds on the value of H_0 do put constraints on the age of the universe computed by 1.5.2, since $t_0 \sim H_0^{-1}$.

For example, taking the constraint already given in 2001 by the Hubble Space Telescope Key project [9], $H_0 = 72 \pm 8\, km\, s^{-1}\, Mpc^{-1}$, for a Universe without Dark Energy ($t_0 = 2/(3H_0)$), see section 1.5), we get $t_0 \sim 8 - 10\ Gyr$, which does not satisfy the stellar age bound. This is indeed the first serious problem that a flat Universe without a cosmological constant suffers, and has been indeed known even since before the SN measurements of 1998.
Current observations constraint the age of the Universe to be around $t_0 \sim 13.8\, Gyr$ - 9 year WMAP [10] gives 13.88 ± 16 while Planck gives 13.817 ± 0.048 [11].

The age problem can be elegantly solved in presence of a cosmological constant. In figure 2.1 we show the cosmic age versus Ω_M in the two cases of a flat Universe with cosmological constant and of an open Universe without cosmological constant, computed in section 1.5. If the curvature $|\Omega_k|$ is constrained to be small, which is the present case (see below), we see that an open Universe without Dark Energy can't manage to satisfy the stellar age bound, whereas a flat one in presence of a cosmological constant can account for the observations - e.g. with

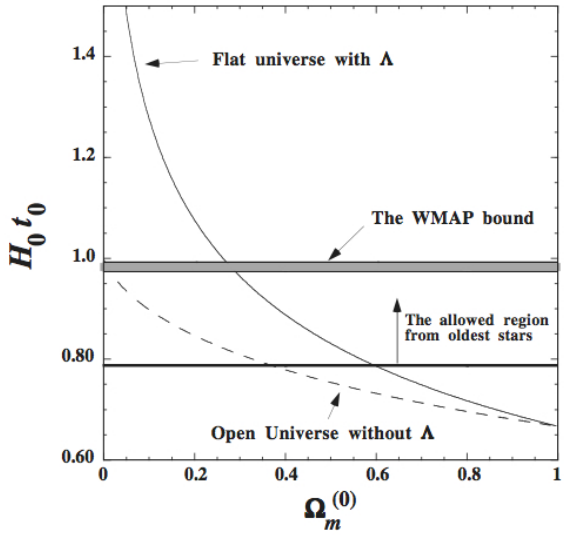

Figure 2.1: Cosmic age as a function of the matter density Ω_M in a flat Universe with Dark Energy (solid line), and in an open Universe in absence of Dark Energy (dashed line). The bounds from stellar age and WMAP 5-year data with h=0.70 [12] are also included. Figure from reference [4]

$\Omega_M = 0.3$, $\Omega_\Lambda = 0.7$ we have $t_0 = 0.964\, H_0$, or $t_0 = 13.1\, Gyr$ for $h = 0.72$.

2.2 Constraints from SnIa

2.2.1 SnIa as Standard Candles

In section 1.4 we saw how the observable luminosity distance is connected to the theoretically predictable Hubble expansion history. The deduction of $H(z)$ from d_L relies then on the measured luminosity distance as a function of redshift

$$d_L(z) = \sqrt{\frac{L}{4\pi\, F(z)}} \tag{2.2.1}$$

where $F(z)$ is the observed flux from an object with intrinsic luminosity L at a redshift z. This requires knowing a priori the absolute luminosity, so that the object in question can be used as a distance indicator. Objects whose intrinsic luminosity is known are referred to by astronomers as "Standard Candles ".
In practice, rather than referring to the fluxes, astronomers does instead make use of the apparent magnitude, defined so that the measured fluxes F_1 and F_2 of two stars are related by

$$m_1 - m_2 = -\frac{5}{2} \log_{10}\left(\frac{F_1}{F_2}\right) \tag{2.2.2}$$

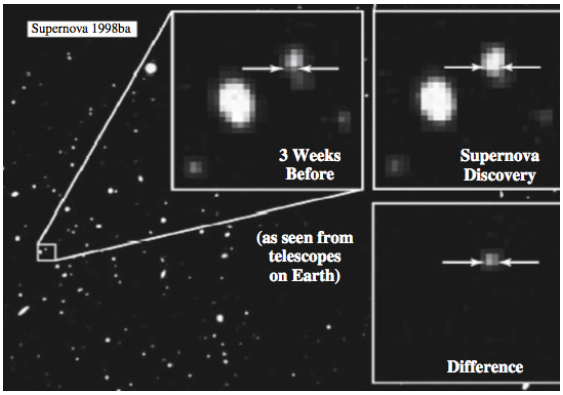

Figure 2.2: An example of supernova discovery. Figure from reference [13]

The absolute magnitude $\mathcal{M}$ is defined as the apparent magnitude an object would have if it were located at a luminosity distance $d_L = 10\,pc$ from the observer:

$$\mathcal{M} = m - 5\log_{10}\left(\frac{d_L}{10\,pc}\right) \tag{2.2.3}$$

Among the known standard candles, the best indicators for cosmology are Type Ia supernovae (SnIa) (see [13] for a discussion).
The explosion of a supernova is an extremely luminous event that emits a burst of radiation. These events can have different origin and are classified according to the absorption lines in the spectrum. In particular, what discriminates Sn of Type I from Sn of Type II is the absence in the former of spectral lines of hydrogen, while among Type I Sn one can further classify Type Ia (with an absorption line of singly ionized silicon), Type Ib (containing a line of helium) or Ic (without both silicon and helium).
Type Ia supernovae are phenomena that occur in binary systems where one of the stars has a mass below the Chandrasekhar limit of $1.4\,M_\odot$ and therefore ends up (after hydrogen and helium burning - then the absence of the absorption lines in the spectrum) as a white dwarf - the dense, carbon remain of the original star. When the companion star reaches its red giant phase, the white dwarf will begin to pull material off it, adding that matter to itself and accreting mass until it reaches the Chandrasekhar mass. Then a nuclear chain reaction occurs, causing the white dwarf to explode. The resulting magnitude is 5 billion times than that of the Sun (the peak absolute magnitude is typically $\mathcal{M} \simeq -19$, approximately $10^{10}\mathcal{M}_\odot$) and is detected with a light curve that increases luminosity in a few weeks and subsequently fades away in 1-2 months. In figure 2.2 we show an example of a Sn discovery.

Several reasons make SnIa good distance indicators. The first is the already mentioned exceptional luminosity. Moreover, the explosion mechanism is fairly well understood and uniform: because the chain reaction always happens in the same way, and at the same mass, the brightness of these Type Ia supernovae are also always the same - there isn't any known mechanism of cosmic evolution of the explosion mechanism. Finally, a number of nearby SnIa has been found that makes possible to calibrate the corrections for minor intrinsic luminosity differences and radiation extinction. Type Ia supernovae observed nearby show a relationship between their peak absolute luminosity and the timescale of their light curve: the brighter supernovae are slower and the fainter supernovae are faster; it has been found that a simple linear relation between the absolute

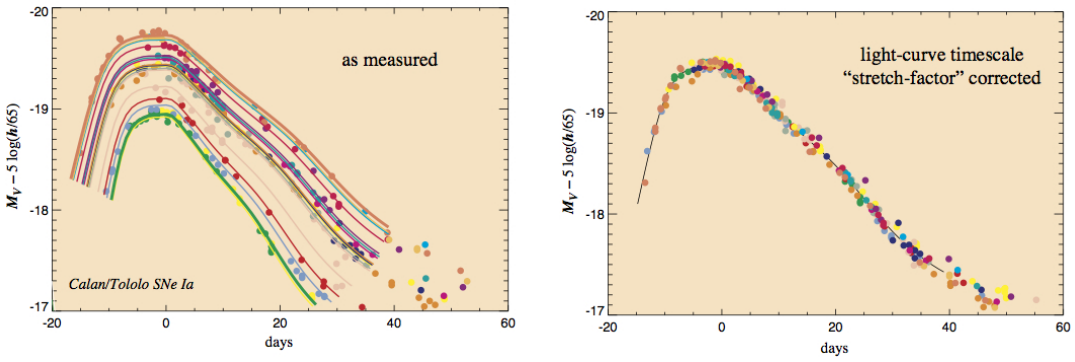

Figure 2.3: Left: light curves of Sn observed at low redshift. The peak magnitude correlates with the timescale. Right: the same light curves after calibrating. Figures from ref. [14]

magnitude and a "stretch factor" multiplying the lightcurve timescale fits the data quite well until over 45 rest frame days past peak, see [14]. The second important correction to to be made is known as K-correction, consisting in transforming the light curves in the Sn rest frame and to take into account cosmic time dilation. The effect of the correction is shown in figure 2.3.

2.2.2 Observations

The direct evidence for the current acceleration of the Universe was first reported in 1998 by two independent teams, the High-redshift Supernova Search Team (HSST) [16] and the Supernova Cosmology Project (SCP) [15].
Since the corrected absolute magnitude $\mathcal{M}$ is the same for every SnIa, the luminosity distance $d_L(z)$ is obtained from equation 2.2.3 measuring the apparent magnitude m. The correspondent redshift is measured from the wavelength of light, so observational data for $m(d_L(z))$ can be compared with the theoretical, model-dependent prediction 1.4.5.

The SCP discovered 42 SnIa in the redshift range $0.18 < z < 0.83$ while the HSST found 14 SnIa in the range $0.16 < z < 0.62$ and 34 nearby SnIa. Having sufficient statistics available, Perlmutter *et al.* were able to show that a cosmological constant is present at the 99% confidence level with the non-relativistic matter contained to a density $\Omega_M = 0.28^{+0.09}_{-0.08}$, and that an open Universe with no cosmological constant does not fit the data.
In figure 2.4 we show the Hubble diagram obtained by the SCP, while in figure 2.5 the space of parameters Ω_M-Ω_Λ is shown with the best-fit regions.

Subsequent observations have confirmed and improved these results. In 2003, Tonry *et al.* confirmed the previous works and gave the constraint for the EOS parameter w_{DE} to be $-1.48 < w_{DE} < -0.72$ at 95% confidence level. In 2004, Riess *et al.* constructed a large and robust dataset consisting of 157 points (known as the "Gold dataset ") and were able to identify the transition from a decelerated to an accelerated phase at $z = 0.46 \pm 0.13$ and found $w_{DE} = -1.02^{+0.13}_{-0.19}$ for an assumed static EOS [17]. Their ability to extend previous analyses to higher redshifts ($z > 1$) was decisive to provide the possibility to discriminate between a static and evolving dark energy equation of state. The standard parametrisation is $w_{DE}(z) = w_0 + w_a(1-a)$ where $a = 1/(1+z)$ is customary and it has been shown to hold for a large range of DE models [18].

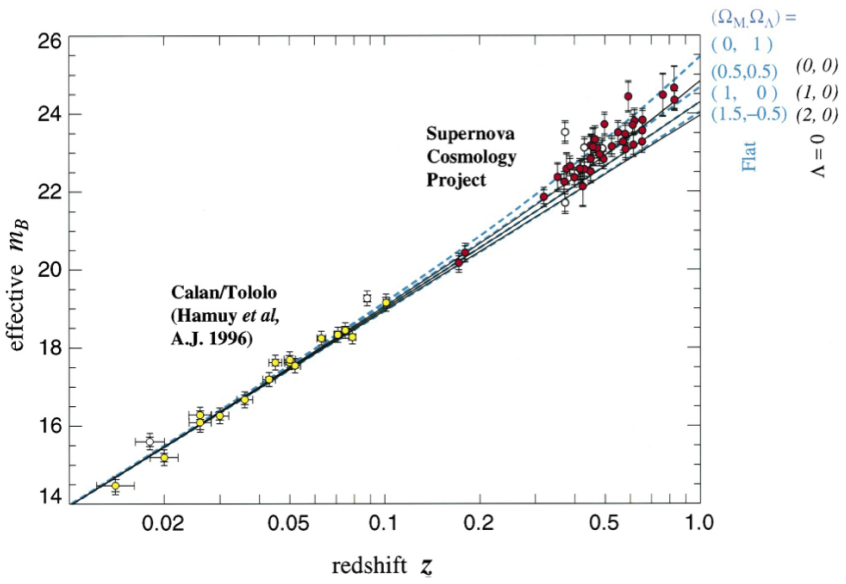

Figure 2.4: Hubble diagram for 42 SnIa from the Supernova Cosmology Project and 18 low-redshift supernovae from the Calan-Tonolo Supernova Survey. The solid curves show the theoretical $m_{EFF}(z)$ for different cosmological models without a cosmological constant. The dashed curves are for different flat models with a cosmological constant. Figure from reference [15]

Moreover, if cosmic acceleration is the reason why SnIa are dimmer at $z \sim 0.5$, then we expect cosmic deceleration at $z > 1$ to reverse the sign of the observed effect [19]. The observation of such effect made also possible to rule out the possible alternative explanation for the dimming to be due to the effect of intergalactic dust.

To conclude, we should mention other significant recent surveys, such as SuperNova Legacy Survey (SNLS) [20], Hubble Space Telescope (HST) [21], "Equation of State: SupErNovae trace Cosmic Expansion " (ESSENCE) [22]. Currently, the largest sample is the "Union2.1" SN Ia compilation by the SCP, now bringing together data for 833 Sn [23], while recently (2013) a sample of 146 SnIa has been analysed from the first 1.5 years of the Pan-STARRS1 Medium Deep Survey [24].

2.3 Cosmic Microwave Background

The Cosmic Microwave Background (CMB) is the relic radiation we receive from the epoch when photons decoupled from baryons. It represents the most precise black-body spectrum currently known, with temperature $T_0 \simeq 2.7$ K. Density fluctuations present at the time, though, cause fluctuations in such temperature of order $\delta T/T_0 \sim 10^{-5}$ (through their coupling to the radiation as well as through metric perturbations) that represent a crucial source of information about cosmological parameters.

As we describe in the appendix, an earlier period of inflation can be described by a minimally coupled scalar field rolling down a potential. Quantum fluctuations of the field cause inflation

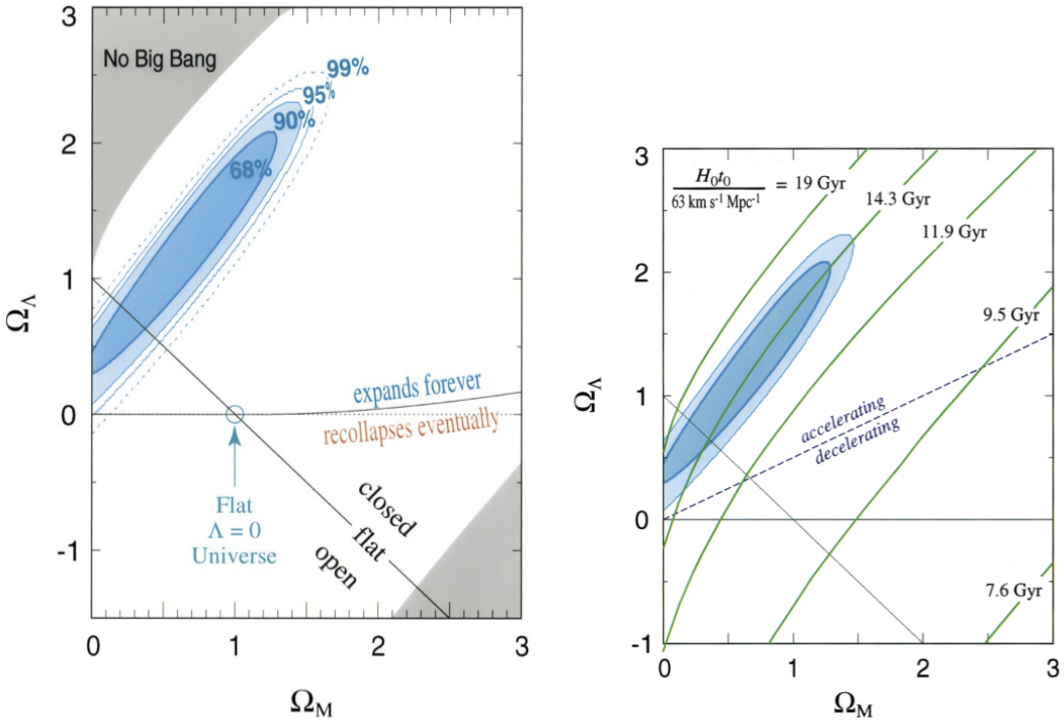

Figure 2.5: Left: best-fit confidence regions in the Ω_M-Ω_Λ plane. Right: isochrones of constant $H_0\, t_0$ (assuming $H_0 = 63\, km\, s^{-1}\, Mpc$) with the best-fit 68% and 90% confidence regions in the Ω_M-Ω_Λ plane.Figures from reference [15]

to end at slightly different times, hence giving rise to over(under)-dense regions through its coupling to the scalar sector of the background metric perturbations. The inhomogeneities do not have preferred physical scales, i.e. the power spectrum is spread continuously over the Fourier modes. Hence, the baryon-photon fluid ("tight coupling approximation": see appendix B.2) is attracted by the gravitational potential of the inhomogeneities and becomes compressed in the denser regions, while the pressure of the fluid opposes the compression and causes in turn an expansion that ends only when the originally over dense region has become slightly under dense, and so on. Thus a process of periodic expansion and contraction of the fluid is triggered, giving rise to standing sound waves of all wavelengths. These oscillations begin everywhere in phase. At the time of decoupling, the cool (rarified) and hot (compressed) regions of the mode is frozen and leaves imprints into the radiation field, that appears as spots in the CMB with temperatures different from the mean.

2.3.1 Temperature Anisotropies

The CMB fluctuations are well-measured by recent and ongoing experiments [10],[11]; a map of the measured fluctuations is shown in figure 2.6. We can quantify the power expanding in harmonics

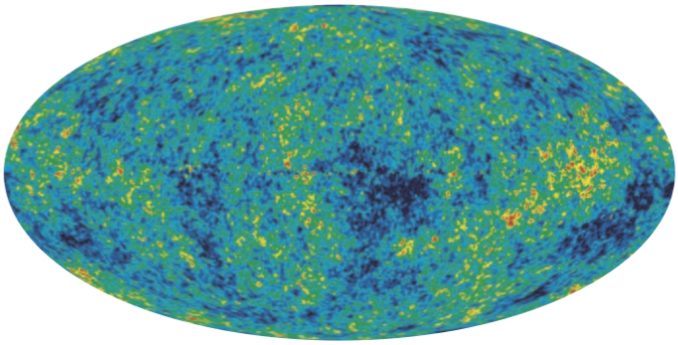

Figure 2.6: Temperature fluctuations in the CMB. Blue regions represent directions on the sky where the temperature is $\sim 10^{-5}$ below the mean, while yellow and red represent hotter (underdense) regions. Figure from reference [10].

$$\frac{\delta T}{T_0}(\hat{n}) = \frac{T(\hat{n}) - T_0}{T_0} = \sum_{\ell,m} a_{\ell m}\, Y_{\ell m}(\hat{n}) \tag{2.3.1}$$

where

$$a_{\ell m} = \int d\Omega_{(\hat{n})}\, Y^*_{\ell m}(\hat{n})\, \frac{\delta T}{T_0}(\hat{n}) \tag{2.3.2}$$

The rotationally-invariant angular power spectrum is defined as

$$C_\ell = \frac{1}{2\ell+1} \sum_m \langle a^*_{\ell m}\, a_{\ell m} \rangle \tag{2.3.3}$$

In appendix *B* we show that this can be expressed as

$$C_\ell = \frac{2}{\pi} \int d\log k \;\; \Theta^2_{\mathbf{k}}(\eta_{rec})\, j^2_\ell(k(\eta_0 - \eta_{rec}))\, k^3\, \mathcal{P}_\zeta(k) \tag{2.3.4}$$

Where $\mathcal{P}_\zeta(k)$ is the spectrum of primordial fluctuations at the end of inflation, described in detail in appendix *A*, $\Theta_{\mathbf{k}}(\eta_{rec})$ is the Fourier transform of the temperature fluctuation at recombination, $j_\ell(k(\eta_0 - \eta_{rec}))$ are Bessel functions depending on the position in the sky, and η_0 and η_{rec} are the values of the conformal time at present epoch and recombination respectively.

The computation of the "transfer function" $\Delta_{T\ell}(k) = \Theta_{\mathbf{k}}(\eta_{rec}) \times j_\ell(k(\eta_0 - \eta_{rec}))$ is performed using specifical codes such as CMBFAST [25] or CAMB [26].
In appendix *B* we provide some computational details which are useful to semi-quantitavely understand the main features of the measured angular power spectrum, while here we shall concentrate on the physics of the C_ℓ and on the dependence on cosmological parameters.

Basing on the results of appendix appendix *B*, we shall comment on the most important regions of the angular power spectrum of the CMB:

- **The Sachs-Wolfe plateau,** $\ell \lesssim 100$

  Anisotropies at scales larger than the horizon at recombination reflect directly the "initial conditions". For adiabatic initial conditions (i.e. entropy is conserved for each species),

temperature fluctuations can be expressed as $\delta T/T_0 \simeq (1/3)\Phi$ where Φ is the perturbation to the gravitational potential. This is due to an intrinsic fluctuation in the density of the photons at last scattering ($\rho_\gamma \propto T^4 \Rightarrow \delta T/T = \delta\rho_\gamma/(4\rho_\gamma)$), as well as to fluctuations in the gravitational potential which photons will have to climb out from (or roll down).

The transfer function is simply a Bessel function

$$\Delta_{T\ell}(k) = -\frac{1}{5}\, j_\ell(k(\eta_0 - \eta_{rec})) \tag{2.3.5}$$

leading to an angular power spectrum that is nearly constant in case of quasi-scale invariant initial conditions ($n_s \simeq 1$), see appendix *A*:

$$C_\ell \approx \frac{8\pi A_s}{25\,\ell\,(\ell+1)} \left(\frac{\ell}{\ell_*}\right)^{n_s-1} \tag{2.3.6}$$

This is usually referred to as *Sachs-Wolfe effect* [27].

- **The acoustic peaks,** $\ell \gtrsim 100$

  At higher multipoles, the structure in the anisotropy spectrum becomes rich and exhibits peaks and troughs.
  The underlying physics is that of gravity-driven acoustic oscillations before recombination, when the universe can be thought as a "baryon-photon plasma" with linearly growing perturbations in the underlying gravitational potential. Pressure gradients, mostly provided by photons, acted as restoring forces to such perturbations (equation *B*.2.10 of appendix *B*.2), driving oscillations of the fluid at the speed of sound (equation *B*.2.19 of appendix *B*.2); physically, the temperature oscillations corresponds to the heating and cooling of the fluid that is compressed or rarefied by the wave. This behaviour continues until recombination, when modes that are caught at maxima or minima of their oscillations leave peaks in the power.
  The spectrum in this approximation has the expression *B*.3.6:

$$C_\ell \approx \frac{8\pi A_s}{25\,\ell\,(\ell+1)}\, \cos^2\left(c_s \frac{\ell\,\eta_{rec}}{(\eta_0 - \eta_{rec})}\right) \left(\frac{\ell}{\ell_*}\right)^{n_s-1} \tag{2.3.7}$$

  The spectrum exhibits peaks at

$$\ell_n \simeq \frac{n\,\pi}{c_s\,\eta_{rec}}\,\eta_0 \tag{2.3.8}$$

  where $c_s = 1/\sqrt{3(1+R)}$ is the sound speed and $R = 3\rho_B/4\rho_\gamma$. The first peak corresponds to the mode that is caught at its first compression at recombination, the second to the one that underwent a full cycle of compression and rarefaction, and so on.

The above discussion suffices for an understanding of the existence of acoustic peaks in the power spectrum. The exact results needed to fit the CMB data should remove the approximations we discussed and consider other effects, such as dissipation (responsible for the damping at high multipoles), the contribution of radiation during matter domination, and the evolution of perturbations after photons began to stream freely, see e.g. [28] for a discussion.

2.3.2 Effects of a Dark Energy component

The most important effect of a Dark Energy is the change of the position of acoustic peaks coming from the modification of the angular diameter distance. We can generalise the result for the position of peaks as follows.
The angle measured in the sky is related to the multipole by $\theta = \pi/\ell$, while a spatial inhomogeneity in the CMB temperature of wavelength λ appears as an angular anisotropy of size $\theta \sim \lambda/D_A$ where D_A is the comoving angular diameter distance, $D_A = (1+z)\, d_A = d_L\, a = d_L/(1+z)$. We can define a characteristic angle for the location of the first peak [4]:

$$\theta_* = \frac{r_*}{D_{A*}} \tag{2.3.9}$$

where the $*$ indicates that the quantity is evaluated at recombination, r_* is the sound horizon, $r_* = \eta_{rec}\, c_s$ for a constant c_s as in our approximation or, more generally, $r_* = \int_0^{\eta_{rec}} c_s(\eta')\, d\eta'$. Then

$$\ell = \frac{\pi}{\theta_*} = \pi \frac{D_{A*}}{r_*} \tag{2.3.10}$$

so that in a flat universe with $c_s = $ const. we recover the result 2.3.8, since $D_{A*} = \eta_0 = \int dz (H_0\, E(z))^{-1}$.
The sound-crossing horizon at recombination provides a "standard ruler", i.e. an object whose intrinsic size is known, as a SnIa provides a "standard candle" in the sense that its intrinsic luminosity is known. In turn, the angle subtended in the sky can be evaluated for every geometry through D_A.
The expression for ℓ can be put in the convenient form [4]

$$\ell = \frac{3\pi}{4} \sqrt{\frac{\Omega_b h^2}{\Omega_\gamma h^2}}\, \mathcal{R} \left[\log \left(\frac{\sqrt{(R\,a)_{dec}} + \sqrt{1 + (R\,a)_{dec}}}{1 + \sqrt{(R\,a)_{eq}}} \right) \right]^{-1} \tag{2.3.11}$$

where we have introduced the *CMB shift parameter*

$$\mathcal{R} = \sqrt{\frac{\Omega_M}{\Omega_k}}\, \sinh \left(\sqrt{\Omega_k} \int_0^{z_{dec}} \frac{dz}{E(z)} \right) \tag{2.3.12}$$

The presence of a Dark Energy leads to a shift of $\mathcal{R}$, so the observed position of the acoustic peaks imposes constraints on Ω_{DE}.
The general relation for all peaks is usually written as

$$\ell_n = \ell(n - \phi_n) \tag{2.3.13}$$

where the factor ϕ_n takes into account the shift of multipoles due to other effects such as free streaming of photons.

In figure 2.7 we show the dependence of the position and height of the acoustic peaks on the cosmological parameters, while in figure 2.8 the angular power spectrum as measured by Planck [11] is shown together with the best-fit base ΛCDM cosmology.

The *Planck* results are well-described by a flat ΛCDM cosmology with a power-law spectrum of scalar perturbations. For this cosmology, the best-fit value for the Dark Energy density is $\Omega_\Lambda = 0.686 \pm 0.020$. We shall comment more extensively on the results below in section 2.5.

We conclude mentioning a second process that could affect the CMB anisotropies, the so-called *integrated Sachs-Wolfe effect* (ISW). This is a contribution from redshifting along the

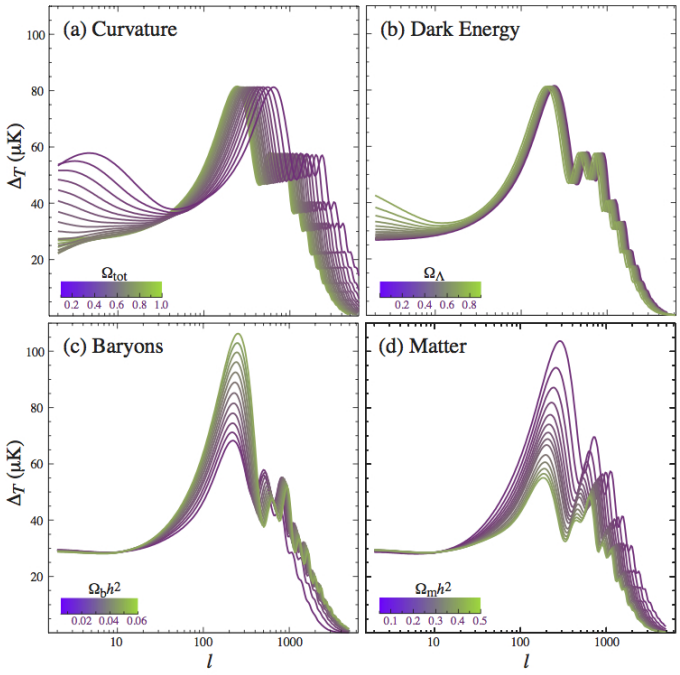

Figure 2.7: Sensitivity of the angular power spectrum to the cosmological parameters. Figure from reference [28].

photon path coming from considering the time-variation of the gravitational potential. In the approximation that lead to equation 2.3.7, see appendix *B*, we considered a matter-dominated epoch, which lead us to $\Phi = \Psi = \text{const.}$. Actually, a small component of radiation is always present, so a more complete treatment should include this effect. This leads to an additional term in *B*.2.8 [29],

$$\frac{\delta T}{T_0}(\hat{\mathbf{n}}) \propto \int_{\eta_{rec}}^{\eta_0} d\eta (\Psi' - \Phi') \tag{2.3.14}$$

This is a line-of-sight term affecting the photon propagation and could provide information on the recent Universe, when Dark Energy begins to dominate: since the gravitational potential is constant for a matter-dominated Universe - and therefore yields no ISW signal - the ISW effect is a direct diagnostic of something which is not ordinary pressureless matter. In the presence of dark energy, decaying potentials due to the accelerated expansion rate, result in a net ISW effect which is positive when the CMB photons cross over- dense regions and negative when the CMB photons cross under- dense regions. Therefore, the ISW effect is a potential indicator of either non-zero curvature, any form of dark energy, such as a cosmological constant, or modified gravity.
The projected effect of the ISW would give a contribution to the transfer function

$$\Delta_{T\,\ell}^{(ISW)} \propto \int_{\eta_{rec}}^{\eta_0} d\eta (\Psi' - \Phi')\, j_\ell(k(\eta_0 - \eta_{rec})) \tag{2.3.15}$$

Since the Bessel function peaks at $k(\eta_0 - \eta_{rec}) \sim \ell$ and since potential evolution is important only for modes within the horizon, the effect is typically relevant for modes with $\ell \sim (\eta_0 - \eta_c)/\eta_c$

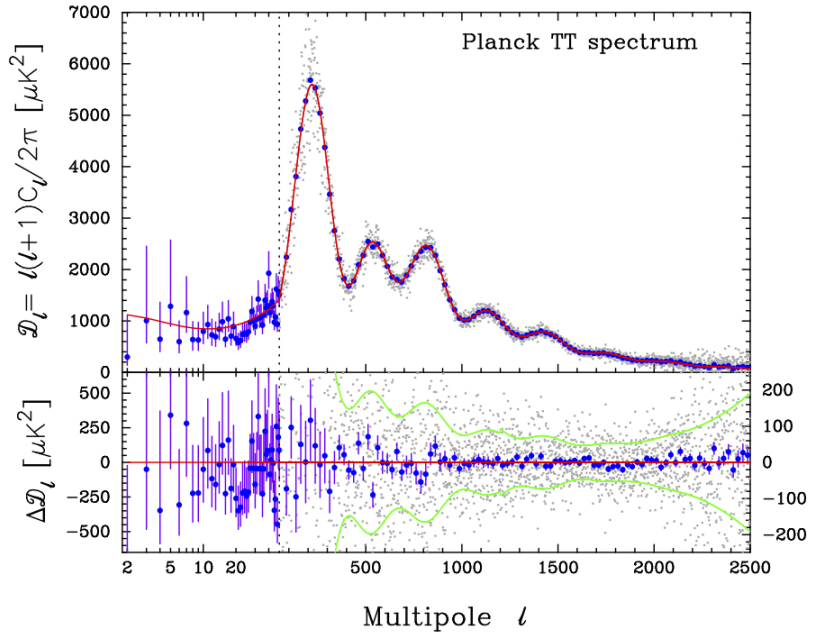

Figure 2.8: Planck temperature power spectrum. The asymmetric error bars show 68% confidence limits. At multipoles $50 \leq \ell \leq 2500$ (plotted on a linear multipole scale) we show the best-fit CMB spectrum. The light grey points show the power spectrum multipole-by-multipole. The blue points show averages in bands of width $\Delta\ell \simeq 31$ together with 1σ errors. The red line shows the temperature spectrum for the best-fit base ΛCDM cosmology. The lower panel shows the power spectrum residuals with respect to this theoretical model. Note the change in vertical scale in the lower panel at $\ell = 50$. Figure from reference [11].

where η_c is the time when the potential starts to evolve significantly. Since the Dark Energy starts to dominate quite recently over matter, the ISW is expected to peak at very low ℓ, or large angles.

Unfortunately, since we have a single sky, there are just a few "independent"large angle patches we can use to constrain the model: the fact that there are only $2\ell+1$ m-samples in each multipole moment leads to the inevitable error ("*cosmic variance*")

$$\Delta C_\ell \sim \frac{1}{\sqrt{2\ell+1}} C_\ell \tag{2.3.16}$$

Therefore, only rather extreme models can be convincingly ruled out by the ISW effect. The current determination of the Dark Energy dimensionless density Ω_{DE} from the detection of the ISW has an error of about 20% [30].

2.4 Baryon Acoustic Oscillations

Before recombination and decoupling, baryons are tightly coupled to photons, so we expect that the oscillations driven by sound waves, described in the previous section and appendix *B* should be imprinted in baryon perturbations as well. After recombination, photons are allowed

to free stream and form the CMB, while the baryon wave stalls with a characteristic radius imprinted in it, namely the radius of the spherical shell formed at recombination. Each over-density of the original perturbation evolves to become a central peak surrounded by a spherical shell, so the probability for a galaxy to form in such higher density shell is increased.
The radius of this shells is the already encountered sound horizon r_*. Then, if a statistic quantifying clustering on different scales is available, this should exhibit a preferred separation scale marked by the sound horizon; at recombination, this shell is roughly $150\,Mpc$ in radius, so the acoustic feature is manifested as a small single spike at $150\,Mpc$ separation.

2.4.1 Correlation functions

The simplest statistic of the galaxy distribution is provided by the *two-point correlation function* $\xi(r)$ (see e.g. [31]), which describes the excess probability of finding a galaxy at distance r from a galaxy randomly selected over that expected in a uniform, random distribution:

$$dP(r) = N_0\,[1 + \xi(r)]\,dV \tag{2.4.1}$$

where N_0 is the mean number of objects and $P(r)$ the probability of finding a second galaxy at distance r from a given object within the volume dV . An equivalent definition is that in terms of the density fluctuations $\delta(\mathbf{r})$:

$$\xi(r) = \langle \delta(\mathbf{x})\,\delta(\mathbf{x}+\mathbf{r})\rangle \tag{2.4.2}$$

Finally, the correlation function is related to the observed power spectrum $P(k)$ by a Fourier transform,

$$\xi(r) = \frac{1}{2\pi^2}\int d\log k\; j_0(kr)\,k^3 P(k) \tag{2.4.3}$$

A number of estimators has been presented in the literature, among which the most used is the Landy and Szalay estimator [32], based on the use of data and a random catalogue generated with the same survey geometry as the original catalogue:

$$\xi(s) = 1 + \frac{DD(s)}{RR(s)}\left(\frac{n_r}{n_d}\right)^2 - 2\frac{DR(s)}{RR(s)}\left(\frac{n_r}{n_d}\right) \tag{2.4.4}$$

where $s = c(z_1 - z_2)$ is the redshift-space distance between two galaxies at redshifts z_1 and z_2, DD, DR and RR are data-data, data-random and random-random pair counts in bins centered in s and and n_d, n_r are the mean number densities of galaxies in the data and random samples.

2.4.2 Cosmological implications

What we actually measure is a combination of two angular measurements (R.A. and Dec.) and one line-of-sight measurement (redshift). It is common [4, 33, 34] to report the distance constraints as

$$D_V(z) = \left[(1+z)^2\,d_A^2(z)\,\frac{cz}{H_0\,E(z)}\right]^{1/3} \tag{2.4.5}$$

where d_A is the angular diameter distance. (Note that, in contrast, the CMB measures a purely transverse quantity). A useful parameter is also

$$A(z_{eff}) = 100\,D_V(z_{eff})\frac{\sqrt{\Omega_M H_0^2}}{c\,z_{eff}} \tag{2.4.6}$$

which is independent from H_0 since $D_V \propto H_0^{-1}$. The parameter z_{eff} is the effective redshift of the sample,

$$z_{eff} = \sum_i^{N_b} \sum_j^{N_b} \frac{w_i w_j}{2\, N_b^2} (z_i + z_j) \tag{2.4.7}$$

where N_b is the number of galaxies in a given bin and w_i is the density weighting factor used in the random catalogue.

The fit is actually performed through a distortion parameter α

$$\xi_{model}(s) = \xi'_{model}(\alpha s) \tag{2.4.8}$$

where

$$\alpha = \frac{D_V(z_{eff})}{D_V^{(fid)}(z_{eff})} \tag{2.4.9}$$

and $D_V^{(fid)}(z_{eff})$ is the parameter computed from the available codes such as CMBFAST. This avoids to re-calculate the correlation function for each different set of cosmological parameters [33]. α measures the relative position of the acoustic peak in the data versus the model, thereby characterising any observed shift. Parameter constraints are then obtained by computing χ^2 with cosmological parameters $\Omega_M h^2$, $\Omega_b h^2$, n_s and D_V (note that the last contains h, Ω_M, Ω_k and $w(z)$).

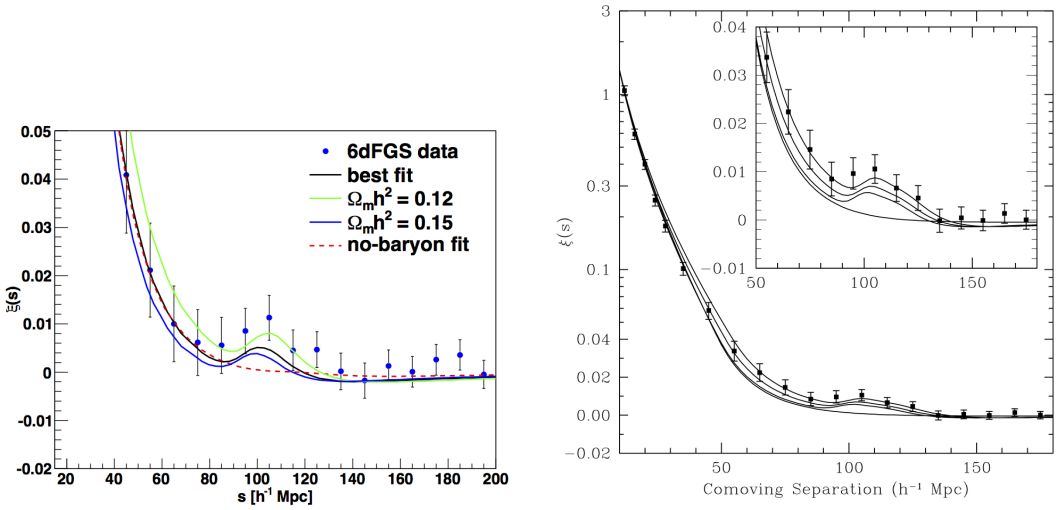

Figure 2.9: Left: The correlation function of 6dFGS with different fits. The best-fit value is $\Omega_M\, h^2 = 0.138 \pm 0.020$.Figure from reference [33]. Right: The correlation function of SDSS. Figure from reference [34]

In figure 2.9 we show the detection of the BAO peak in the correlation function obtained by two different galaxy surveys, the 6dF Galaxy Survey (6dFGS) [35] and the Sloan Digital Sky Survey (SDSS) [36].

Further implications on cosmological parameters and Dark Energy are discussed in section 2.5.

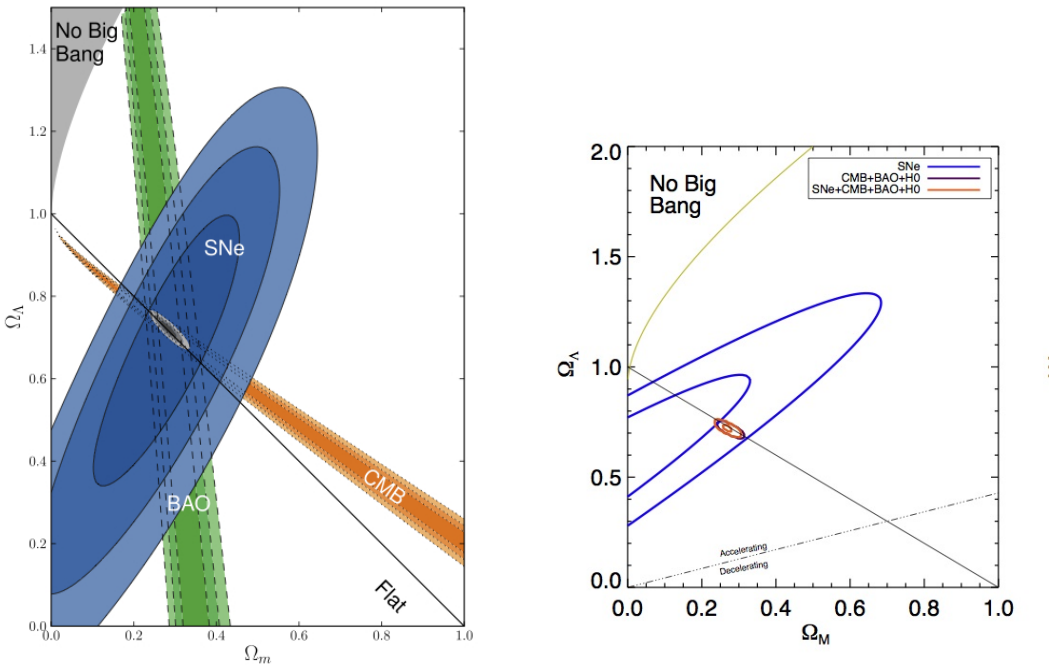

Figure 2.10: Left: Constraints in the $\Omega_M - \Omega_\Lambda$ plane with 68.3%, 95.4% and 99.7 % confidence regions from SnIa of the Union 2.1 compilation combined with CMB and BAO. Figure from reference [23]. Right: Constraints in the $\Omega_M - \Omega_\Lambda$ plane with 68.3% and 95.4% confidence regions from SnIa of the Pan-STARRS1 data combined with CMB, BAO and H_0. Figure from reference [24].

2.5 Putting it all together

A number of observables sensitive to the presence of a Dark Energy component has been presented. In this section we shall try to give a picture of the state-of-the-art including the most recent measurements and discussing their combination and agreement (or tension, if any), concentrating on the parameters relevant for our discussion, i.e. on the Dark Energy equation of state.

2.5.1 Cosmological parameters: flat and dominated by Dark Energy

The available data agree on a spatially-flat model, since fitting with $k = 0$ matches observations very well [10, 11, 23]. In principle, one could have a so-called "geometric degeneracy", since in equations such as 2.3.12 one could trade Ω_k and Ω_M off one another through h to give the same observed result. However, if an additional curvature parameter is included, one finds tight constraints on it, e.g. $|\Omega_k| < 0.0094$ at 95% C.L. was found by WMAP [10], and $\Omega_k = 0.002^{+0.005}_{0.005}$ by the Supernova Cosmology Project [23]. Alternatively the degeneracy is broken by combining different measurements, e.g. adding BAO data to *Planck* (see below) gives $100\Omega_k = -0.05^{+0.65}_{-0.66}$ [11]. Observations then suggest that our Universe is spatially flat to an accuracy of better than percent.

Standard fits hence assume a flat geometry, $k = 0$, and explore a variety of models, from the standard, ΛCDM models to Dark Energy models with constant, unknown w (referred to as "wCDM"), or models with varying w, parametrized by $w = w_0 + w_a(1 - a)$ (referred to as "w_0w_aCDM"). Broadly speaking, different measurements (SnIa, BAO, CMB) of the cosmological parameters relevant for our discussion seem to agree on the values $\Omega_\Lambda \simeq 0.7$, $\Omega_M \simeq 0.3$, $w_0 \simeq -1$, $w_a \simeq 0$. Despite this and an increasing precision in the determination of such parameters, though, recent discussion [11] showed that the results on dynamical dark energy are dependent on the supplementary data we use in addition to *Planck*. We shall comment on the differences shortly.

The most precise data are currently those of *Planck*.
Its most robust precision measurement is that of the angular size θ_*, equation 2.3.9, that gives $\theta_* = (1.04148 \pm 0.00066) \times 10^{-2} = 0.596724^\circ \pm 0.00038^\circ$. If one assumes a flat cosmology with a cosmological constant, then the parameters obtained from the combination r_*/D_{A*} (equation 2.3.9 again) are tightly constrained: the sound horizon r_* depends on the physical matter density $\Omega_M h^2$ and D_A on the geometry. The dimensionless energy densities must sum to unity (equation 1.3.9 with $k = 0$), and H_0 is the fixed by the value of $\Omega_M h^2$, so the result constrains Ω_M, Ω_Λ and H_0. The corresponding values with 68% limits are [11]

$$\Omega_M h^2 = 0.1423 \pm 0.0029 \qquad (68\ \%;\ \textit{Planck}) \tag{2.5.1}$$
$$H_0 = (67.4 \pm 1.4)\ km\, s^{-1}\, Mpc^{-1} \qquad (68\ \%;\ \textit{Planck}) \tag{2.5.2}$$
$$\Omega_\Lambda = 0.686 \pm 0.020 \qquad (68\ \%;\ \textit{Planck}) \tag{2.5.3}$$
$$\tag{2.5.4}$$

For comparison, SnIa of the Union 2.1 compilation give [23]

$$\Omega_\Lambda = 0.705^{+0.040}_{-0.043} \qquad (\ \textit{Union 2.1}\ ) \tag{2.5.5}$$

The first evidence [16, 15] of the acceleration of the Universe is strongly confirmed by current observation: we live in a spatially-flat, Dark-Energy dominated accelerating Universe.

As for the nature of the Dark Energy, if one allows for larger parameter spaces, such as wCDM or w_0w_aCDM, then a parameter degeneracy opens in the CMB, which alone does not tightly constrain w. This degeneracy is broken by combining different measurements, see next section.

In general, better constraints also on the already mentioned parameters are obtained by the addition of more data sets. In figure 2.10 we show the confidence intervals on Ω_M and Ω_Λ from Sn, CMB and BAO [23] for a ΛCDM model. Both the individual and combined constraints are shown.

2.5.2 Dark Energy EOS parameters

A cosmological constant has equation of state $P = -\rho$, or $w = -1$. More general models can be allowed to have constant $w \neq -1$ or time-varying w parametrized by a simple linear relation $w(z) = w_0 + w_a(1 - a)$, $a = 1/(1 + z)$.

For a constant w, adding to *Planck* WMAP data and BAO signal gives [11]

$$w = -1.13^{+0.24}_{-0.25} \qquad (95\ \%;\ \textit{Planck}{+}\text{WP}{+}\text{BAO}) \tag{2.5.6}$$

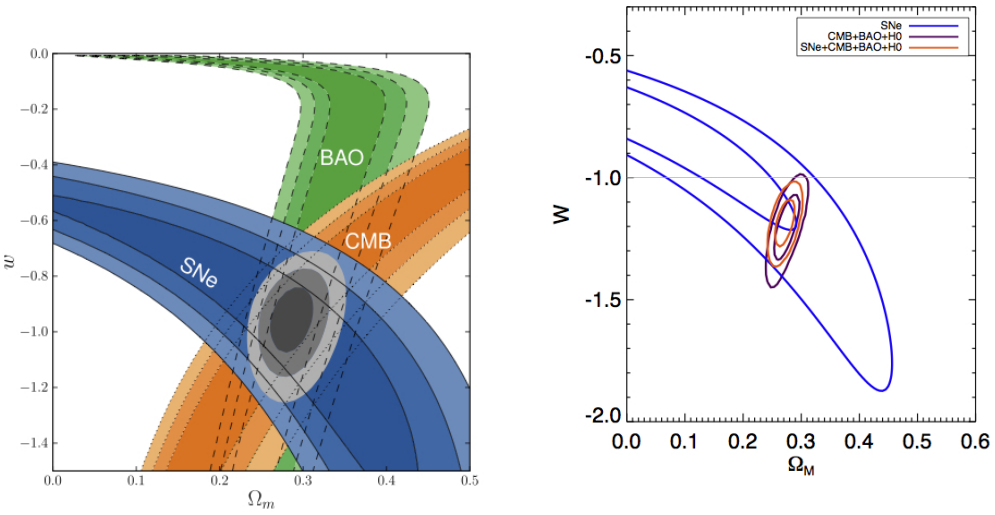

Figure 2.11: wCDM model. Left: 68.3%, 95.4%, and 99.7% confidence regions in the (Ω_M, w) plane from SnIa of Union 2.1 combined with CMB and BAO. Figure from reference [23]. Right: 68.3% and 95.4% confidence regions in the (Ω_M, w) plane from SnIa of Pan-STARRS1 combined with CMB, BAO and H_0. Figure from reference [24].

while using *Planck*, WMAP and Sn data gives [11]

$$w = -1.09 \pm 0.17 \qquad (95\ \%;\ \textit{Planck}{+}\text{WP}{+}\text{Union 2.1}), \tag{2.5.7}$$
$$w = -1.13^{+0.13}_{-0.14} \qquad (95\ \%;\ \textit{Planck}{+}\text{WP}{+}\text{SNLS}) \tag{2.5.8}$$

Otherwise one can use the CMB data alone adding an external measurement of H_0. Using the Riess *et al.* 2011 measurement [37] gives

$$w = -1.24^{+0.18}_{-0.19} \qquad (95\ \%;\ \textit{Planck}{+}\text{WP}{+}H_0) \tag{2.5.9}$$

On the other hand, by combining CMB, BAO and SnIa data, the SCP finds [23]

$$w = -1.013^{+0.068}_{-0.073} \qquad (\text{Union 2.1}{+}\text{CMB}{+}\text{BAO}) \tag{2.5.10}$$

Finally, the Pan-STARRS1 data [24], combined with BAO+*Planck*+H_0, give

$$w = -1.186^{+0.076}_{-0.065} \qquad (\text{Pan-STARRS1}{+}\text{BAO}{+}\textit{Planck}{+}H_0) \tag{2.5.11}$$

while when combined with WMAP9 give

$$w = -1.142^{+0.076}_{-0.087} \qquad (\text{Pan-STARRS1}{+}\text{BAO}{+}\text{WMAP9}{+}H_0) \tag{2.5.12}$$

In figure 2.11 we show the constraints in the (Ω_M, w) plane obtained by the SCP combined with CMB and BAO [23].

If instead we allow for a time-dependent EOS, we find a degeneracy in the $w_0 - w_a$ space. The *Planck* constraint becomes weaker,

$$w_0 = -1.04^{+0.72}_{-0.69} \qquad (95\ \%;\ \textit{Planck}{+}\text{WP}{+}\text{BAO}),$$
$$w_a < 1.32 \qquad (95\ \%;\ \textit{Planck}{+}\text{WP}{+}\text{SNLS}) \tag{2.5.13}$$

In figure 2.12 we show results from *Planck* [11], the SCP [23] and BAO in SDSS III [38].

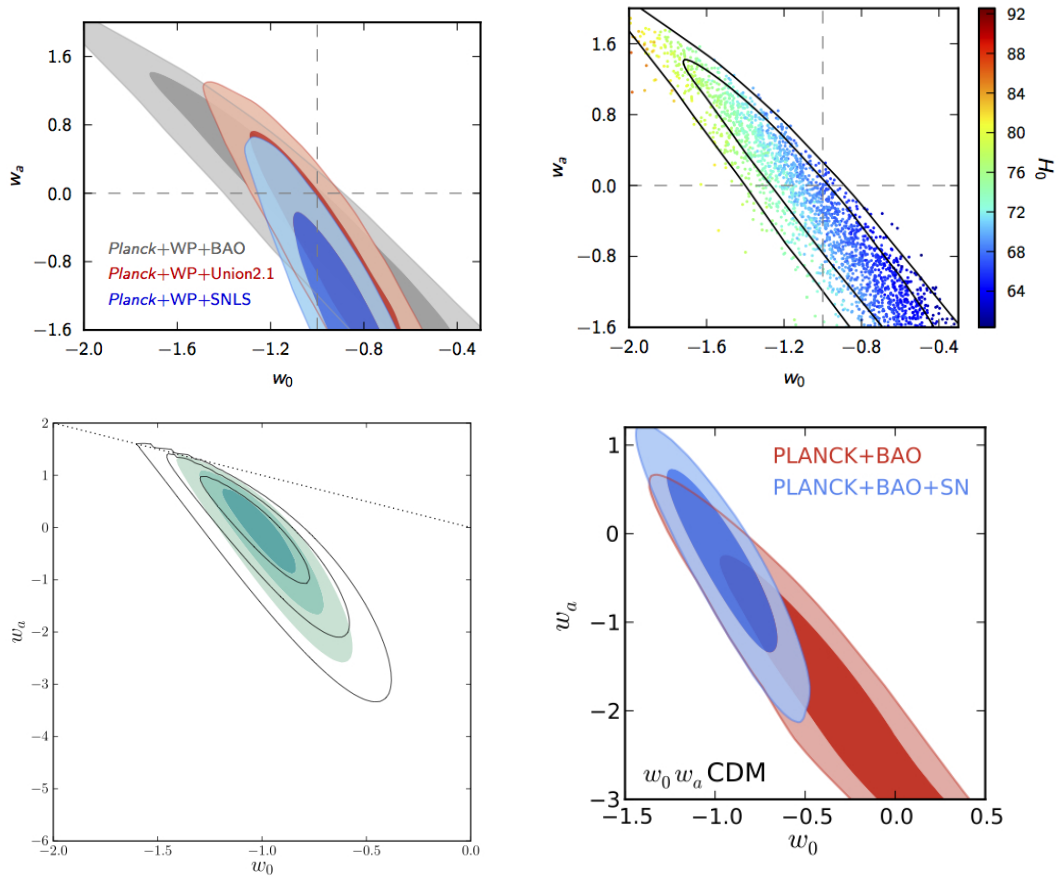

Figure 2.12: (w_0, w_a) plane. Top left: from *Planck*+WP+BAO (grey), *Planck*+WP+Union 2.1 (red), and *Planck*+WP+SNLS (blue). Top right: from *Planck*+WP+BAO. The points are coloured according to the corresponding value of H_0. In both, the contours are 68% and 95% and the dashed grey line shows the cosmological constant solution. Figures from reference [11]. Bottom left: from SNe+BAO+CMB+H0, both with (solid contours) and without (shaded contours) systematic errors, and 68.3%, 95.4%, and 99.7% confidence regions. Figure from reference [23]. Bottom right: from *Planck*+BAO (red) and *Planck*+BAO+Sn (blue). Figure from reference [38].

2.5.3 Any tension?

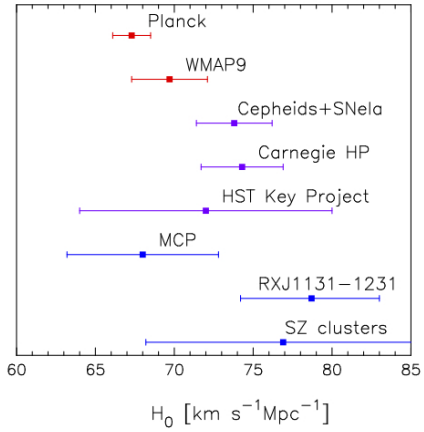

Figure 2.13: Comparison of H_0 measurements. Figure from reference [11]

The main outcome of the previous section is that the results for a non-cosmological constant Dark Energy, either $w = \text{const.} \neq -1$ or $w = w(z)$, are dependent on what supplementary data set is used in addition to CMB measurements.

In particular, the official Planck analysis points out that for a constant w the combination with SNLS (2.5.8) and Pan-STARRS1 favours the "phantom " ($w < -1$) side at $\sim 2\sigma$, while the Union 2.1 (2.5.7) is more compatible with a cosmological constant, a result confirmed by Shafer and Huterer (2013) [39]. The combination with an external measurement of H_0 is instead in tension with a cosmological constant at more than 2σ level (2.5.9).
The inclusion of a dynamical Dark Energy instead shows a 3-dimensional degeneracy in the $w_0 - w_a - H_0$ space, as one can see in the top-right panel of figure 2.12. The results of the Union 2.1 are in better agreement with a cosmological constant, while for the SNLS data the cosmological constant solution lies at the boundary of the 2σ region (top-right panel of figure 2.12). The SNLS sample seems then to favour a dynamical Dark Energy, while BAO data are more consistent with a cosmological constant.

A second striking outcome of the *Planck* results is the low value of the Hubble constant, equation 2.5.2. This is still compatible with the previous result from CMB experiments, i.e. the result of 9-year WMAP [10],

$$H_0 = (70.0 \pm 2.2)\ km\, s^{-1}\, Mpc^{-1} \qquad (68\ \%;\ \text{WMAP-9}) \tag{2.5.14}$$

but it is in tension with local measurements, as one can visually guess from figure 2.13. Actually, the most recent results are those of Riess *et al.* [37] with use of observation of Cepheids variables in the host galaxies of SnIa to calibrate the Sn redshift-magnitude relation,

$$H_0 = (73.8 \pm 2.4)\ km\, s^{-1}\, Mpc^{-1} \qquad (\text{Cepheids+SnIa}) \tag{2.5.15}$$

and Freedman *et al.*, [40] within the *Carnegie Hubble Program*

$$H_0 = [74.3 \pm 1.5(\text{statistical}) \pm 2.1(\text{systematic})]\ km\, s^{-1}\, Mpc^{-1} \qquad (\text{Carnegie HP}) \tag{2.5.16}$$

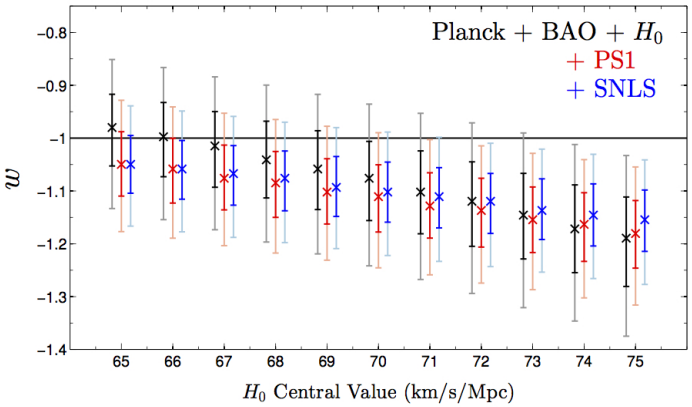

Figure 2.14: Effects of an external H_0 prior on the constant EOS parameter. Interesting evidence for the EOS to be on the phantom side appear when the prior is somewhat large $H_0 \gtrsim 71\ km/s/Mpc$. Figure from reference [39].

The above mentioned data include measurements of different nature, from the solar neighbourhood [8], to the local Universe [33, 34, 41], to the epoch of recombination, $z \simeq 1100$ [10, 11]). CMB measurements mostly probe the physics of the early Universe, and the interpretation of the results in terms of the cosmological parameters defined at $z = 0$ require extrapolation through a cosmological model, while local observables provide cosmology-independent measurements of cosmological parameters. On the other hand, the beauty of observables such as BAO and the CMB is that they use almost completely linear physics, while traditional astrophysical data set involve more complex physics and should rely on some internal calibration, such as the stretch-factor correction in SnIa measurements.

Being the CMB estimates on H_0 model-dependent, a comparison with astrophysical measurements is crucial. The tension could not be resolved by simply shifting the parameters of ΛCDM, which are tightly constrained by *Planck*, and this is a very good reason why one should explore the possibility of new physics.

Already from the publication of the official Planck analysis in 2013 [11] this tension has raised some interest in the community. Recently (2013), Shafer and Huterer [39] found that the constraint strongly depends on the prior on H_0 and a high prior $H_0 \gtrsim 71\ km/s/Mpc$ leads to a 2σ evidence for phantom Dark Energy. The dependence is understood since the CMB constraints the physical matter density $\Omega_m h^2$, so a change of H_0 produces a shift $\delta \log \Omega_m \simeq -2\delta \log h$ and a higher H_0 leads to a lower value of Ω_M; from the $\Omega_M - w$ degeneracy in figure 2.11 we see that a lower Ω_M leads to a more negative w. The effects are shown in fig. 2.14.
This shift towards $w < -1$ being uncorrelated with any known systematics related to SN observables, they therefore claim that either the SNLS and Pan-STARRS1 data have systematics that remain unaccounted for, or the Hubble constant is below 71 $km/s/Mpc$, or else the dark energy equation of state is indeed phantom.
The same conclusions have been reached independently by Nesseris and Tsujikawa in a recent work [42].

A quantitative estimate of the tension between local and high redshift measurements has

$\log \mathcal{T}$	interpretation	betting odds
<1	not significant	$< 3:1$
1-2.5	substantial	$\sim 3:1$
2.5-5	strong	$> 12:1$
>5	highly significant	$> 150:1$

Table 2.1: The scale to interpret the tension $\mathcal{T}$

been recently proposed by Verde *et al.* (2013) [43], which could be useful to understand whether ΛCDM is disfavoured, and in favour of what kind of extensions.

The estimator is defined as follows (we follow [43]).

If A,B are two different experiments to be compared, let $P_{A,B}(\theta|D_{A,B})$ be the probability of having a parameter set θ given the data $D_{A,B}$ from the experiments. We assume the same, uniform prior, $\pi_A = \pi_B = \pi$ with $\pi = 1$ or 0 and therefore $\pi_A \pi_B = \pi$. We define

$$\int P_A \, P_B \, dx = \lambda \int \pi_A \, \pi_B \, dx = \lambda \int \mathcal{L}_A \, \mathcal{L}_B \, \pi \, dx = \lambda \, E = \mathcal{E} \tag{2.5.17}$$

where $\mathcal{L}$ is the likelihood and $\lambda^{-1} = \int \mathcal{L}_A \pi_A dx \int \mathcal{L}_B \pi_B dx'$. E is the bayesian evidence for the joint distribution and $\mathcal{E}$ is then a sort of unnormalised Evidence.
If we were to perform a translation of the distributions in x, the new distribution $\bar{P}_A$ would have the same shape and different position of the maximum. If the null hypothesis is that the two experiments measure the same quantity, the models are correct and there are no unaccounted errors, then it would translate into the condition that the maxima of the old and shifted distribution coincide,

$$\int \bar{P}_A \, \bar{P}_B \, dx = \bar{\mathcal{E}}|_{maxA=maxB} \tag{2.5.18}$$

If the distance between the maxima increases, then

$$\int \bar{P}_A \, \bar{P}_B \, dx = e < \bar{\mathcal{E}} \tag{2.5.19}$$

Then the degree of tension is defined as

$$\mathcal{T} = \frac{\bar{\mathcal{E}}|_{maxA=maxB}}{\mathcal{E}} \tag{2.5.20}$$

The chances of the null hypothesis are $1:\mathcal{T}$, and a large tension $\mathcal{T}$ means that the null hypothesis is unlikey, while a small $\mathcal{T}$ means that the experiments can be combined. The empirical calibration of the scale $\mathcal{T}$ is shown in table 2.1.

In figure 2.15 we show the results of Verde *et al.* for the dependence of the tension on the EOS parameter. In particular, any extension of the ΛCDM with a slightly phantom value for w could be able to bring the tension to "*not significant*", while the ΛCDM value $w = -1$ indicates a "*strong*" tension between the data.

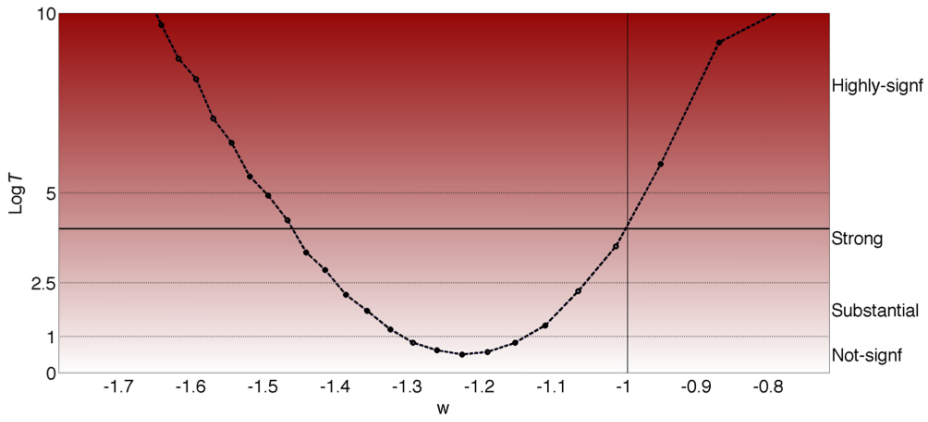

Figure 2.15: $\log \mathcal{T}$ as a function of w. The black solid line corresponds to the ΛCDM value. A value of $w < -1$ brings the tension down to a less significant value. Figure from reference [43].

Chapter 3

Phantom Dark Energy from non-local gravity

The observation of the accelerated expansion of the Universe raised an intense activity around the nature of the so-called Dark Energy.
As we have seen in the previous chapter, adding a "cosmological constant " term with EOS $P = -\rho$ fits a large number of observations, but at the same time the origin of this term is still mysterious. A plausible possibility is that the cosmological constant actually vanishes (a number of mechanisms has been put forward in the literature), and that the acceleration of the Universe is caused by an alternative model of Dark Energy.

Recent and planned observations open the possibility to measure the relevant Dark Energy parameters with increasing precision, hence a direct comparison between ΛCDM and any viable alternative model is very likely to be at our disposal in the near future.

In this chapter we introduce a non-local modification of General Relativity (section 3.2), that represents an original result of this work and has been recently published (2014) [1]. The most significant results of the present work are presented in section 3.3, where we show that tuning the only free parameter we are able to predict the value of the Dark Energy density today as well as the EOS parameter. In the rest of the chapter, we concentrate on some conceptual issues that could arise from the introduction of non-local operators, that have been extensively discussed in recent literature [44, 45, 46, 1, 47].

3.1 The road towards non-locality

The most studied possibility to obtain a dynamical Dark Energy is adding some scalar minimally coupled to gravity with an arbitrary potential, provided that one puts suitable constraints on the potential so to fit observations. Such mechanism is known in the literature as "quintessence". As discussed by Woodard, the issue becomes then one of plausibility, since one could reconstruct any expansion history [48]. Moreover, a general feature of these models is that they generally lead to equations of state $w \geq -1$ [3], which seems to be disfavoured by recent observations.

The other obvious possibility is that of modifying General Relativity on cosmological scales.

Modifications of the form "$f(R)$" obtained by replacing the Ricci scalar in the Einstein-Hilbert action with an arbitrary function suffer the same problems as scalars models (indeed, they can be turned into GR plus a minimally coupled scalar).

In recent years, a few authors explored the possibility of using non-local terms to produce modifications of General Relativity in the infrared with different motivations.
Deser and Woodard [49, 50] observed that non-local additions to GR can naturally arise as quantum loop corrections, and therefore introduced the phenomenological modification to the Einstein-Hilbert Lagrangian

$$\Delta\mathcal{L} = \frac{1}{16\pi G}\sqrt{-g}\,R\,f\left(\frac{1}{\Box}R\right) \tag{3.1.1}$$

The potential relevance of non-local cosmological effects due to quantum effects in loops have been investigated independently in very recent work by Donoghue and El-Menoufi [51].

An independent introduction of the inverse d'Alembertian is due to Barvinsky [52]. He observed that, expanding the Ricci tensor over flat-space background,

$$R_{\mu\nu} = -\frac{1}{2}\Box h_{\mu\nu} + \frac{1}{2}\boldsymbol{\nabla}_\mu\left(\boldsymbol{\nabla}^\lambda h_{\nu\lambda} - \frac{1}{2}\boldsymbol{\nabla}_\nu h\right) + \frac{1}{2}\boldsymbol{\nabla}_\nu\left(\boldsymbol{\nabla}^\lambda h_{\mu\lambda} - \frac{1}{2}\boldsymbol{\nabla}_\mu h\right) + \mathcal{O}(h^2_{\mu\nu}) \tag{3.1.2}$$

one can invert for h and get a non-local expansion in powers of the curvature. Plugging back into the Einstein-Hilbert action and upon use of the Bianchi identities one finds

$$S_{EH} = \frac{1}{16\pi G}\int d^4x\,\sqrt{-g}\,\left[-G_{\mu\nu}\frac{1}{\Box}R^{\mu\nu} + \mathcal{O}(R^3_{\mu\nu})\right] \tag{3.1.3}$$

His first suggestion for a non-local extension of GR is then

$$S = \frac{M^2}{2}\int d^4x\,\sqrt{-g}\,\left[-R + \alpha\,G_{\mu\nu}\frac{1}{\Box}R^{\mu\nu}\right] \tag{3.1.4}$$

we shall comment more extensively later on this kind of tensor non-localities, showing that they lead to instabilities in the cosmological evolution.

Finally, non-local operators can be very useful in cosmology through the degravitation mechanism [53].
The basic idea is that the vacuum energy is not small itself, but simply gravitates little. A phenomenological description can be given promoting Newton's constant G to an operator acting like a filter, $G = G(L^2\Box)$ where L is the scale of the filter. Sources with wavelength $\lambda >> L$ should be screened or "degravitated". At the linearized level, introducing a mass scale $m \sim 1/L$, this is achieved by $G(L^2\Box) = G \times (1 - m^2/\Box)$, so Einstein's equations become

$$\left(1 - \frac{m^2}{\Box}\right)\mathcal{E}^{\mu\nu}_{\rho\sigma}h^{\rho\sigma} = -16\pi G T^{\mu\nu} \tag{3.1.5}$$

The source is then screened and appears weakened at energies $E << m$. The cosmological constant would then appear very tiny.

Another natural way to extend GR in which a mass scale shows up, in particular from a particle physicist's point of view, is trying to give a mass to the graviton. "Massive gravity" has recently received a growth of attention, since, besides its intrinsic theoretical interest, a tiny

graviton mass could lead to late-time cosmic acceleration and possibly to a degravitation mechanism.
The subject has a long history and a series of very well-known issues. The original linear theory of Fierz and Pauli (1939) [54] has a so-called van Dam-Veltman-Zacharov (vDVZ) discontinuity such that GR is not recovered in the $m \to 0$ limit [55], while ghost-like modes - the "Boulware-Deser " (BD) ghost - arise as soon as one includes non-linearities [56].
In the context of non-local extensions of GR, the inverse d'Alembertian shows up again in massive theories since it provides a way to write a mass term without breaking the gauge invariance of the massless theory [57].

A promising approach to massive gravity has recently been introduced by Jaccard *et al.* [58], who provided a fully non-linear, covariant theory of massive gravity very close to the degravitation proposal 3.1.5, defined by the field equations

$$G_{\mu\nu} - m^2(\Box^{-1}G_{\mu\nu})^T = 8\pi G T_{\mu\nu} \tag{3.1.6}$$

where the superscript T denotes the extraction of the transverse part to preserve energy-momentum covariant conservation. The resulting theory respects causality and smoothly reduces to GR in the $m \to 0$ limit, but turns out to be cosmologically unstable [44, 59, 60, 61]. Subsequently, Maggiore [45] suggested that one can consider a more general class of models,

$$G_{\mu\nu} - m^2[\Box^{-1}(a_1\, R_{\mu\nu} + a_2\, g_{\mu\nu}R)]^T = 8\pi G T_{\mu\nu} \tag{3.1.7}$$

the most promising one being defined by $a_1 = 0$, $a_2 = 1/3$ (the latter choice of a_2 is a convenient normalization of the mass parameter). A correct understanding of the meaning of the non-local operators appearing in the above models, and a discussion of the promising cosmological implications, has been provided in [44] and [46] and will be discussed in detail below.

3.2 A new non-local model

A modification of gravity in the far infrared at scales $\ell \sim H_0^{-1}$ naturally leads to introduce some scale $m \sim H_0$, as we have seen for the degravitation mechanism and in theories of massive gravity.
We propose a model in which again the $\Box^{-1}$ operator acts on the Ricci scalar and a mass scale appears, but which is defined by the action

$$S_{\rm NL} = \frac{1}{16\pi G}\int d^{d+1}x\sqrt{-g}\,\left[R - \frac{d-1}{4d}m^2 R\frac{1}{\Box^2}R\right]\,, \tag{3.2.1}$$

where d is the number of spatial dimensions and the factor $(d-1)/4d$ is a convenient normalisation of the mass parameter m. We will see that, among the non-local models examined, such a model seems the most convincing one, both at the theoretical level and for its potentially very interesting cosmological consequences. The model has been introduced in [1] which we will follow throughout the rest of the section if not otherwise specified.

The equations of motion of the theory can be obtained introducing two scalar fields

$$U = -\Box^{-1}R\,, \tag{3.2.2}$$

and

$$S = -\Box^{-1}U = \Box^{-2}R\,, \tag{3.2.3}$$

and rewriting eq. (3.2.1) as

$$S_{\rm NL} = (16\pi G)^{-1} \int d^{d+1}x\sqrt{-g}\,\left[R(1-\mu S) - \xi_1(\Box U + R) - \xi_2(\Box S + U)\right]\,, \tag{3.2.4}$$

where we introduced $\mu = [(d-1)/(4d)]m^2$, and ξ_1, ξ_2 are two Lagrange multipliers. The variation is then straightforward: varying the action (3.2.4) with respect to the four scalar fields one obtains the equations of motion

$$\begin{aligned} \Box U &= -R \\ \Box S &= -U \\ \Box \xi_1 &= -\xi_2 \\ \Box \xi_2 &= -\mu\, R\,. \end{aligned} \tag{3.2.5}$$

Then, using the identities

$$\begin{aligned} \delta\sqrt{-g}(y) &= -\frac{1}{2}\sqrt{-g}\, g_{\mu\nu}\delta^4(x-y)\,\delta g^{\mu\nu}(x) \\ \delta R(y) &= [R_{\mu\nu} - \boldsymbol{\nabla}_\mu\boldsymbol{\nabla}_\nu + g_{\mu\nu}\Box]\,\delta^4(x-y)\delta g^{\mu\nu}(x) \end{aligned} \tag{3.2.6}$$

we get from the variation of (3.2.4) with respect to the metric - adding also the matter action S_M -

$$\begin{aligned} \delta_g(S_{NL}+S_M) \;=\; & \int \sqrt{-g}\,\delta g^{\mu\nu}\,\{[R_{\mu\nu} - \boldsymbol{\nabla}_\mu\boldsymbol{\nabla}_\nu + g_{\mu\nu}\Box]\,(1-\mu S - \xi_1) + \\ & -\frac{1}{2}g_{\mu\nu}\,[R\,(1-\mu S-\xi_1) + \partial_\alpha\xi_1\,\partial_\alpha U + \partial_\alpha\xi_2\,\partial^\alpha S - \xi_2\,U] + \\ & +\frac{1}{2}\,[\partial_\mu\xi_1\,\partial_\nu U + \partial_\nu\xi_2\,\partial_\mu S + \mu\leftrightarrow\nu] + \frac{1}{\sqrt{-g}}\frac{\delta S_M}{\delta g^{\mu\nu}}\Big\} = 0 \end{aligned} \tag{3.2.7}$$

We use the EOM 3.2.5 to eliminate ξ_1 and ξ_2 in favour of U, S:

$$\begin{aligned} \xi_2 &= -\mu\frac{1}{\Box}R = \mu\, U \\ \xi_1 &= \frac{1}{\Box}\xi_2 = -\mu\, S \end{aligned} \tag{3.2.8}$$

Thus, from 3.2.7 we get

$$G_{\mu\nu} - \mu K_{\mu\nu} \;=\; 8\pi G T_{\mu\nu}\,, \tag{3.2.9}$$

$$\Box U \;=\; -R\,, \qquad \Box S = -U\,. \tag{3.2.10}$$

where

$$K_{\mu\nu} = 2SG_{\mu\nu} - 2\boldsymbol{\nabla}_\mu\partial_\nu S - 2U g_{\mu\nu} + g_{\mu\nu}\partial_\rho S\partial^\rho U - (1/2)g_{\mu\nu}U^2 - (\partial_\mu S\partial_\nu U + \partial_\nu S\partial_\mu U)\,. \tag{3.2.11}$$

It is straightforward to check explicitly that $\boldsymbol{\nabla}^\mu K_{\mu\nu} = 0$, as it should, since it has been derived from a diff-invariant action.

We emphasise immediately that a crucial point (already discussed in detail in [62, 50, 44, 45, 46, 1]) is that, despite the appearance of the a Klein-Gordon operator, eq. (3.2.10) do not describe radiative degrees of freedom.
Indeed, to define our original non-local theory we must first specify what we mean exactly by $\Box^{-1}$. In general, an equation such as $\Box U = -R$ is solved by $U = -\Box^{-1}R$, where

$$\Box^{-1}R = U_{\rm hom}(x) - \int d^{d+1}x' \sqrt{-g(x')}\, G(x;x')R(x')\,, \tag{3.2.12}$$

and $U_{\rm hom}(x)$ is any solution of $\Box U_{\rm hom} = 0$. The choice of the homogeneous solution and of the Green's function is part of the definition of the $\Box^{-1}$ operator and therefore of the original non-local theory. To ensure causality, we shall define $\Box^{-1}$ with the choice of the retarded Green's function. As for the homogeneous solution, $U_{\rm hom}(x)$ is not a free field that can be expanded in plane waves which, at the quantum level, would corresponds to creation and annihilation operators of some particle. Neglecting this simple but important point leads to misinterpreting U as an extra propagating degree of freedom. Similar consideration holds for the equation $\Box S = -U$. We shall illustrate the situation in more detail in the following.

Our exposition will have to follow two paths: first, we should clarify some conceptual issues, namely, the correct interpretation of the theory 3.2.1 as a classical effective theory, the definition of the operator $\Box^{-1}$, the form of spherically symmetric static solutions and the absence of a vDVZ discontinuity. Second, we should discuss the cosmological properties of the model.

Actually, we choose to start with the cosmology, in order to display immediately the potential interest of the model.

3.3 Cosmological evolution and dark energy

We proceed straight to the cosmological consequences of the model, at the level of background evolution. We consider a flat FRW metric

$$ds^2 = -dt^2 + a^2(t)d\mathbf{x}^2\,, \tag{3.3.1}$$

in $d = 3$ and in presence of an energy-momentum tensor $T_{\mu\nu} = (\rho, a^2(t)\, p\, \delta_{ij})$. Our goal is to see whether a viable Dark Energy model emerges from the term proportional to μ, so we do not include a cosmological constant term: $\rho = \rho_M + \rho_R$.

From the $(0,0)$ component of 3.2.9 and from 3.2.10 we get the system

$$\begin{aligned} &H^2 + \frac{m^2}{d^2}\left(-dH\dot{S} - \frac{d(d-1)}{2}\, S\, H^2 - \frac{1}{2}\dot{S}\,\dot{U} - \frac{U^2}{4}\right) = \frac{16\pi G}{d\,(d-1)}\,\rho \\ &-\ddot{U} - dH\dot{U} = 2d\dot{H} + d(d+1)H^2 \\ &-\ddot{S} - dH\dot{S} = U \end{aligned} \tag{3.3.2}$$

for the three functions $H(t), S(t), U(t)$.

We introduce $W(t) = H^2(t)S(t)$ and $h(t) = H(t)/H_0$, where $H(t) = \dot{a}/a$ and H_0 is the present value of the Hubble parameter. We use $x = \ln a$ to parametrize the temporal evolution, and henceforth $f' \equiv df/dx$. Trading the equation for S for an equation for W, 3.3.2 becomes

$$h^2(x) = \Omega_M e^{-3x} + \Omega_R e^{-4x} + \gamma Y \tag{3.3.3}$$
$$U'' + (3+\zeta)U' = 6(2+\zeta)\,, \tag{3.3.4}$$
$$W'' + 3(1-\zeta)W' - 2(\zeta' + 3\zeta - \zeta^2)W = U\,, \tag{3.3.5}$$

where $\gamma = m^2/(9H_0^2)$, $\zeta = h'/h$ and

$$Y \equiv \frac{1}{2}W'(6-U') + W(3-6\zeta+\zeta U') + \frac{1}{4}U^2\,. \tag{3.3.6}$$

and we used $\rho_0 = 3H_0^2/(8\pi G)$, $\rho_M(x)/\rho_0 = \Omega_M a^{-3} = \Omega_M e^{-3x}$ and $\rho_R(x)/\rho_0 = \Omega_R e^{-4x}$. From the right hand side of 4.2.19 we see that we can consider the term $\gamma Y(x)$ as an effective dark energy density $\rho_{\rm DE}(x) = \rho_0 \gamma Y(x)$.

3.3.1 Perturbative solutions

The system of equations 3.3.3-3.3.5 is a coupled system of non-linear differential equations, since $Y(x)$ and its derivative appear also in $\zeta(x)$. Before integrating numerically, it is convenient to understand analytically the behaviour of the evolution. In particular, we can work perturbatively in γ, assuming that the contribution of the function $Y(x)$ to $\zeta(x)$ is negligible at early times - so that we recover the standard cosmology - and checking a posteriori the self-consistency of the procedure.
Then, as $x \to -\infty$,

$$\zeta(x) \simeq -\frac{3\Omega_M e^{-3x} + 4\Omega_R e^{-4x}}{\Omega_M e^{-3x} + \Omega_R e^{-4x}} \tag{3.3.7}$$

Under this assumption, in each given era $\zeta(x)$ can be approximated by a constant ζ_0, with $\zeta_0 = \{-2, -3/2, 0\}$ in RD, MD and a De Sitter inflationary epoch, respectively. Then, equation 3.3.4 can be integrated analytically,

$$U_{pert}(x) = \frac{6(2+\zeta_0)}{3+\zeta_0}\,x + u_0 + u_1\, e^{-(3+\zeta_0)x} \tag{3.3.8}$$

The coefficients u_0, u_1 parametrize the general solution of the homogeneous equation $U'' + (3+\zeta)U' = 0$. Plugging equation 3.3.8 into 3.3.5 we get

$$\begin{aligned} W_{pert}(x) &= w_1 e^{-(3-\zeta_0)x} + w_2 e^{2\zeta_0 x} + \frac{u_1}{6\zeta_0(1+\zeta_0)} e^{-(3+\zeta_0)x} + \\ &+ \frac{-18 + 9\,\zeta_0\,(1+\zeta_0) + u_0\,\zeta_0\,(-9+\zeta_0^2)}{2\,\zeta_0^2\,(\zeta_0-3)^2\,(3+\zeta_0)} - \frac{3\,(2+\zeta_0)}{(9-\zeta_0^2)\,\zeta_0}\,x \end{aligned} \tag{3.3.9}$$

where again w_1 and w_2 parametrize the homogeneous solution.

Observe that in RD $\zeta_0 = -2$ and the inhomogeneous solution for both U and W vanish. This is a consequence of the fact that in RD the Ricci scalar vanishes, so $\Box U = 0$ and the only contributions come from the solutions of the homogeneous equations. Moreover, in a generic epoch, as $x \to -\infty$ the inhomogeneous solutions go as $U(x) \propto x$ and $W(x) \propto x$, so $Y(x)$ goes at most as $Y(x) \propto x^2$ and its contribution to $h^2(x)$ is negligible with respect to the exponentially growing terms $\Omega_M e^{-3x}$ and $\Omega_R e^{-4x}$ in 3.3.3. As for the homogeneous solutions, we note that all the terms in equations 3.3.8, 3.3.9 proportional to u_0, u_1, w_1, w_2 are either constant or decaying

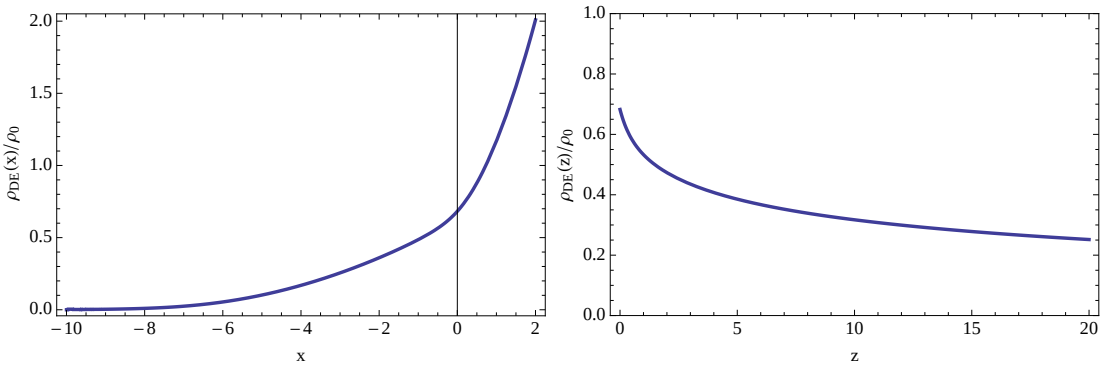

Figure 3.1: Left panel: the function $\gamma Y(x) = \rho_{\rm DE}(x)/\rho_0$, against $x = \ln a$. Right panel: the function $\gamma Y(z) = \rho_{\rm DE}(z)/\rho_0$, against the redshift $z = e^{-x} - 1$.

with x, since in the Early Universe we have $-2 \leq \zeta_0 \leq 0$, which means that the solutions are stable in MD, RD, as well as in a previous inflationary stage, and that, apart for a constant mode, in the perturbative regime the homogeneous solution is an attractor: starting the evolution in RD with initial conditions such that the exponential modes are excited, we will be quickly driven towards the inhomogeneous term of the perturbative solution. This shows that the perturbative approach is self-consistent.

Since the homogeneous solution vanishes in RD, starting the evolution deep in RD and imposing the initial conditions $U(x_{in}) = W(x_{in}) = 0$ (since in RD the Ricci scalar vanishes) amounts to set

$$U(x_{in}) = u_0 + u_1 e^{-x_{in}} = 0 \tag{3.3.10}$$

$$W(x_{in}) = w_1 e^{-5x_{in}} + w_2 e^{-4x_{in}} + \frac{u_0}{20} + \frac{u_1}{12} e^{-x_{in}} = 0 \tag{3.3.11}$$

i.e.

$$u_0 = u_1 = w_1 = w_2 = 0\,. \tag{3.3.12}$$

3.3.2 Numerical solutions

We can now integrate the full equations 3.3.3-3.3.5 numerically. We can eliminate the variable $h(x)$ (and hence $\zeta(x)$) through 3.3.3, so that equations 3.3.4 and 3.3.5 form a closed system for the variables $U(x)$, $W(x)$. We choose the initial conditions so that at early times we sit on the inhomogeneous analytical solution found above with the condition 3.3.12 - we shall set $\zeta_0 = -2 + \epsilon$ with $\epsilon = \Omega_M e^{x_{in}}/2\Omega_R$. We make use of the Planck best-fit values, $\Omega_M = 0.3175$, $\Omega_R = 4.15 \times 10^{-5}\, h_0^{-2}$, $h_0 = 0.6711$ [11], and we set $\Omega_\Lambda = 0$. The model has a single free parameter, γ, that has to be tuned by trial and error in such a way that today we have $\Omega_{DE} = 1 - \Omega_M - \Omega_R \simeq 0.6825$. This is of course the only consistent solution, since we have adopted a spatially flat metric. Choosing $\gamma \simeq 0.00891$ (corresponding to $m \simeq 0.283 H_0$) we reproduce the observed value $\Omega_{\rm DE} \simeq 0.68$. It is already quite significant that a DE is dynamically generated and that the observed value can be reproduced.

Furthermore, having fixed this, we are left with no more free parameters. In particular, we

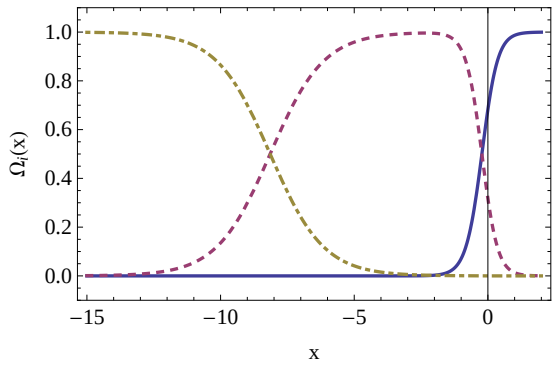

Figure 3.2: The quantities $\Omega_R(x)$ (brown, dot-dashed) , $\Omega_M(x)$ (red, dashed) and $\Omega_{\rm DE}(x)$ (blue, solid line).

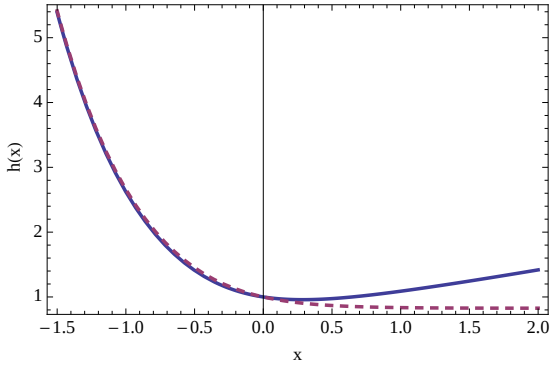

Figure 3.3: The normalized Hubble parameter $h(x) = H(x)/H_0$ in our model (blue, solid line) and in ΛCDM (red, dashed line)

obtain a pure prediction for the dark energy equation of state parameter $w_{\rm DE}$, defined from

$$\rho'_{\rm DE} + 3(1 + w_{\rm DE})\rho_{\rm DE} = 0\,. \tag{3.3.13}$$

Hence, since $\rho_{DE}(x) \propto Y(x)$,

$$w_{DE}(x) = -1 - \frac{Y'(x)}{3Y(x)} \tag{3.3.14}$$

The result of the numerical integration of eqs. (3.3.3)–(3.3.5) is shown in Figs. 3.1-3.3. In Fig. 1 we show the effective dark energy fraction $\Omega_{DE} = \rho_{\rm DE}/\rho_0 = \gamma Y$ as a function of $x = \log a$ (left panel) and of the redshift z (right panel). We see that it starts from zero in RD and then grows during MD. The quantities $\Omega_R(x) = \rho_R(x)/\rho_{\rm tot}(x)$, $\Omega_M(x) = \rho_M(x)/\rho_{\rm tot}(x)$ and $\Omega_{\rm DE}(x) = \rho_{\rm DE}(x)/\rho_{\rm tot}(x)$ are shown in figure 3.2.
In Fig. 3.3 we see that the normalised Hubble parameter $h(x)$ becomes a growing function when the DE density begins to dominate, while for comparison we have included the result of ΛCDM (red dashed line), which continues to decrease.

The result for $w_{DE}(x)$ is shown Fig. 3.4 as a function of x (left panel) and of the redshift

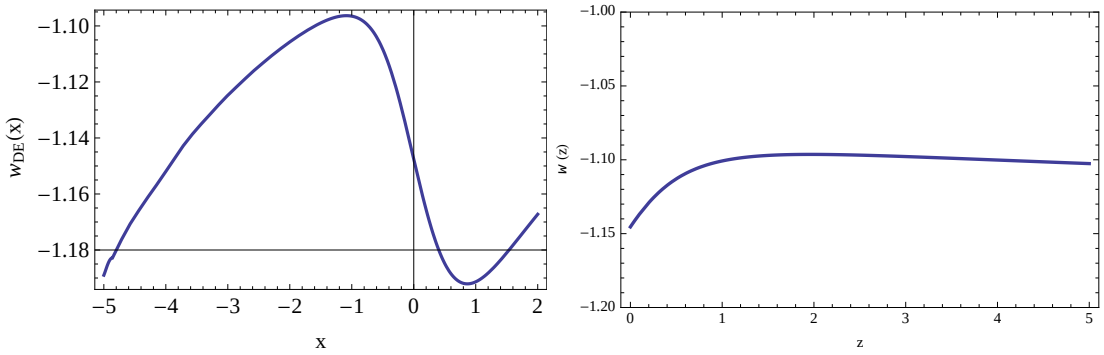

Figure 3.4: Left panel: the EOS parameter $w_{\rm DE}(x)$. Right panel: the EOS parameter $w_{\rm DE}(z)$.

(right panel).

3.3.3 A first look to experimental data

In principle, once the parameter m is fixed so to reproduce the DE density today, the model contains all the necessary information to fix the DE evolution, as well as its equation of state - and hence the whole background evolution (actually, it has been shown in recent work [63] that also the perturbations are fully characterised, a result that significantly strengthens the predictive power of the model). On the other hand, the value of Ω_M quoted above and used to derive our results, as well as the other cosmological parameters, has been obtained from the *Planck* data *assuming* ΛCDM. On the contrary, the correct values in the non-local model should be determined in a self-consistent way by a global fit to the CMB, BAO and Sn data taking into account the specific form of the perturbations.

However, in practise we can obtain some preliminary encouraging (or discouraging) hints by a "coarse graining" of the information in terms of a few parameters that can be directly compared to available observations, although in principle the model contains all the information necessary to a direct comparison. The most relevant region is the recent past, where the DE density starts to become important. In the region $-1 \leq x \leq 0$, corresponding to redshifts $0 \leq z \leq 1.72$, we use the standard fitting function

$$w_{\rm DE}(a) = w_0 + (1-a)w_a\,, \tag{3.3.15}$$

(where $a(x) = e^x$). We define Δw as the difference between the numerical expression and the fitting function, and we minimise with respect to the parameters w_0, w_a the quantity

$$\chi^2 = \int_{-1}^{0} dx\ (\Delta w)^2(x) \tag{3.3.16}$$

We find the best-fit values

$$w_0 = -1.144\,, \qquad w_a = 0.084\,. \tag{3.3.17}$$

In figure 3.5 (left panel) we show the numerical solution for $w_{DE}(x)$ (blue solid line) compared to the best-fit function (red, dashed line) and the value of $\Delta w/w$ (right panel). We see that the relative error is at the level $|\Delta w/w| \leq 5 \times 10^{-3}$ in this region.

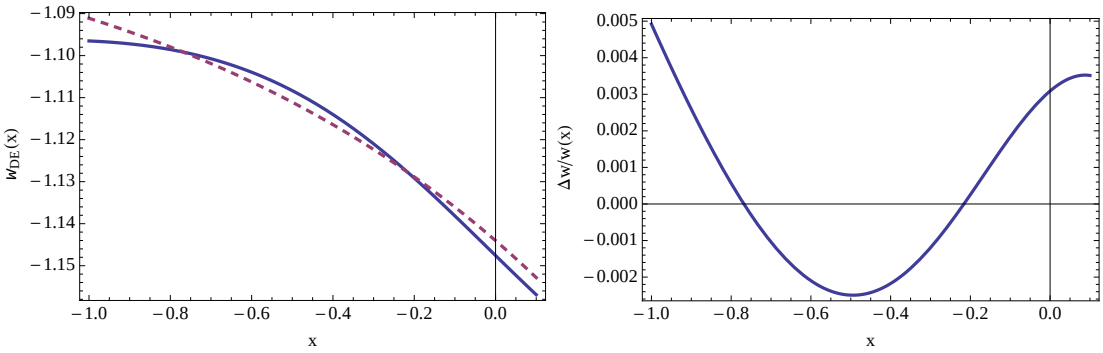

Figure 3.5: Left panel: the numerical solution for $w_{DE}(x)$ (blue solid line) compared to the best-fit function $w_{\rm DE}(a) = w_0 + (1-a)w_a$ with $w_0 = -1.144$, $w_a = 0.084$ (red, dashed line). Right panel: The value of $\Delta w/w$ in the region $-1 \leq x \leq 0$.

We can also compare to a more general fit of the form

$$w_{\rm DE}(a) = w_0 + (1-a^q)w_a\,, \tag{3.3.18}$$

with q another free fitting parameter. We get

$$w_0 = -1.149\,, \qquad w_a = 0.062\,, \qquad q = 2.129, \tag{3.3.19}$$

but the improvement in the minimisation of χ^2 is not relevant, so the introduction of q as a free parameter is not justified.

The fact that the EOS turns out to be on the phantom side is a general property of these non-local models, due to the fact the DE density starts from zero in RD and then grows during MD. Thus, in this regime $\rho_{\rm DE} > 0$ and $\rho'_{\rm DE} > 0$, and then eq. (3.3.13) gives $(1 + w_{\rm DE}) < 0$.

The numerical values in (3.3.17) are quite interesting, considering that the result from Planck+WP+BAO in the (w_0, w_a) plane is the one given in 2.5.13, $w_0 = -1.04^{+0.72}_{-0.69}$, $w_a < 1.36$ at 95% c.l.. Since our prediction for w_a is such that $|w_a| \ll 1$, it makes sense to compare directly with the fit for a constant w_{DE}, which gives more tight constraints. The result of Planck+WP+SNLS for a constant $w_{\rm DE}$ is the one given in 2.5.8

$$w_{\rm DE} = -1.13^{+0.13}_{-0.14}\,, \tag{3.3.20}$$

at 95% c.l. [11], while the Pan-STARRS1 data, combined with BAO+Planck+H_0, give 2.5.11

$$w_{\rm DE} = -1.186^{+0.076}_{-0.065}\,, \tag{3.3.21}$$

while, when combined with WMAP9 instead of Planck, give 2.5.12

$$w_{\rm DE} = -1.142^{+0.076}_{-0.087}\,. \tag{3.3.22}$$

As discussed in the previous chapter, in the framework of ΛCDM there is a tension between the value of H_0 derived from the Planck measurement and that derived from direct measurements in the local Universe. Ref. [43] has studied the impact of various extensions of ΛCDM on such a discrepancy. It has been found that the only parameter that can reduce the tension to a

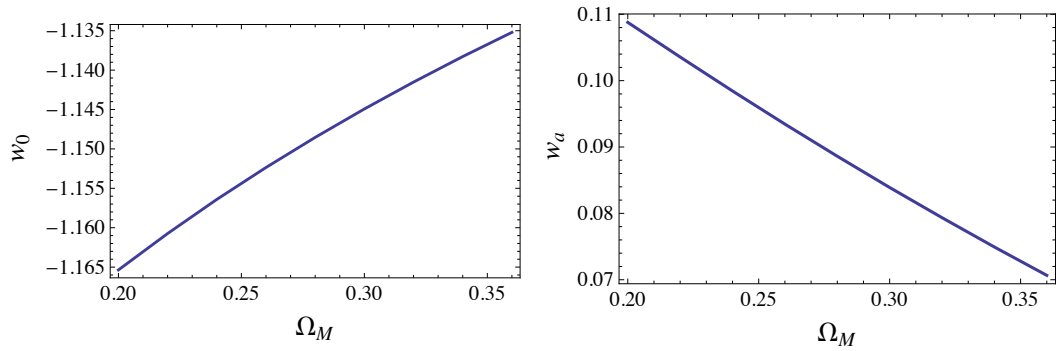

Figure 3.6: Left panel: w_0 as a function of Ω_M. Right panel: w_a as a function of Ω_M.

statistically non-significant value is indeed $w_{\rm DE}$, and this requires a value of $w_{\rm DE}$ approximately in the range $-1.3 < w_{\rm DE} < -1.1$. Our prediction (3.3.17) is therefore able to bring this discrepancy down to a statistically not significant value, even if the indicators should only be taken as a first suggestion that needs more accurate data to assess the real significance of such "tension". In any case, it is quite remarkable that such a value of $w_{\rm DE}$ is predicted by a relatively simple and theoretically consistent modification of GR. This should be compared with models that involve an arbitrary function such as $f(R)$ or $f(\Box^{-1}R)$, which can be chosen to reproduce any expansion history. For instance, the function $f(\Box^{-1}R)$ of the Deser-Woodard model 3.1.1 can be reconstructed to fit any expansion history, and Deffayet and Woodard [64] showed that the numerical form needed to fit observation can be analytically approximated by a rather artificial expression,

$$f(X) = 0.245[\tanh\left(0.350Y + 0.032Y^2 + 0.003Y^3\right) - 1] \tag{3.3.23}$$

where $Y = 16.5 + X$.

The model 3.2.1 is therefore much more predictive, and gives an equation of state consistent with present limits without the need of a fine-tuning. Moreover, in the next few years planned surveys should measure w_0 and w_a to an accuracy that will allow for direct comparison between this non-local model and ΛCDM, making our proposal highly testable and well distinguishable from ΛCDM. Of course, given what we said at the beginning of this paragraph, the final sentence will be given only once a global fit to the data assuming this nonlocal model will become available: strictly speaking, one could not claim that this model is falsified even if a tension with fits performed assuming ΛCDM emerged, since the only logically consistent option is to test its predictivity through a *direct* fit of the data. On the other hand, if one had found a result already in strong tension with the observed value of w as fitted assuming ΛCDM, this would be a significant indication that the model is unable to predict a viable evolution either of the background (e.g. if $w > -0.5$ we would not have an accelerating solution) or of the perturbations. Then, the results obtained above are highly non-trivial and promising, and motivate further (ongoing) investigations.

Given this discussion, a final important observation concerns the robustness of our prediction with respect to a change in the measured values of the cosmological parameters. If we change the value of Ω_M, we should contemporarily adjust the value of Ω_{DE} so to maintain the flatness condition, $\Omega_M + \Omega_R + \Omega_{DE} = 1$, and hence the value of γ should be changed to a new value $\tilde{\gamma}$. Since $\Omega_{DE} = \gamma\, Y(0)$, we get the new value $\tilde{\Omega}_{DE} \simeq \Omega_{DE} \times (\tilde{\gamma}/\gamma)$, while $\tilde{w_0} \simeq w_0 + \gamma\, \partial_\gamma w_0 \times (\tilde{\gamma} - \gamma)/\gamma$.

Hence, even a revision of the value of Ω_M at the 10% level would produce a change in our prediction only at a level $\Delta w_0/w_0 \simeq 10^{-3}(\partial_\gamma w_0/w_0)$. In recent work, Dirian *et al.* [63] repeated the analysis for different values of Ω_M in the broad range $[0.20, 0.35]$, adjusting each time γ so to reproduce the desired value of Ω_M. The results for w_0 and w_a are shown in figure 3.6. They find that the w_0 remains within the relatively narrow range $[-1.165, -1.135]$, while w_a varies between $[0.07, 0.11]$.

3.4 Conceptual issues

As already mentioned, the presence of the $\Box^{-1}$ operator raises a number of potential problems of theoretical consistency that have to be clarified. In particular, the theory should be considered as a classical effective one, as we shall discuss in this section. In this framework, it is shown that it is fully consistent at the theoretical level.

3.4.1 Classical effective equations vs non-local QFT

The crucial feature of the non-local terms introduced in our theory is that they come explicitly with a *retarded* propagator, since this choice is forced by causality. The difference with the usual appearance of such prescription with respect to, say, the solution of some classical equation, is that here the retarded propagator already appears in the *definition* of the theory, and not just in the solution of its equations.

Consider what happens if we study the classical matter-matter interaction in the classical theory defined by equation 3.2.9, linearizing it over Minkowski space. Writing $g_{\mu\nu} = \eta_{\mu\nu} + h_{\mu\nu}$ we get from 3.2.9

$$\mathcal{E}^{\mu\nu,\rho\sigma} h_{\rho\sigma} - \frac{d-1}{d}\, m^2 P^{\mu\nu} P^{\rho\sigma} h_{\rho\sigma} = -16\pi G T^{\mu\nu}\,, \tag{3.4.1}$$

where $\mathcal{E}^{\mu\nu,\rho\sigma}$ is the Lichnerowicz operator,

$$\begin{aligned} \mathcal{E}^{\mu\nu,\rho\sigma} \;\equiv\; & \frac{1}{2}\left(\eta^{\mu\rho}\eta^{\nu\sigma} + \eta^{\nu\rho}\eta^{\mu\sigma} - 2\eta^{\mu\nu}\eta^{\rho\sigma}\right)\Box + \left(\eta^{\rho\sigma}\partial^\mu\partial^\nu + \eta^{\mu\nu}\partial^\rho\partial^\sigma\right) + \\ - \;& \frac{1}{2}\left(\eta^{\mu\rho}\partial^\sigma\partial^\nu + \eta^{\nu\rho}\partial^\sigma\partial^\mu + \eta^{\mu\sigma}\partial^\rho\partial^\nu + \eta^{\nu\sigma}\partial^\rho\partial^\mu\right)\,, \end{aligned} \tag{3.4.2}$$

so

$$\mathcal{E}^{\mu\nu,\rho\sigma} h_{\rho\sigma} = \Box h^{\mu\nu} - \eta^{\mu\nu}\Box h + \eta^{\mu\nu}\partial_\rho\partial_\sigma h^{\rho\sigma} + \partial^\mu\partial^\nu h - \partial_\rho\partial^\nu h^{\mu\rho} - \partial_\rho\partial^\mu h^{\nu\rho}\,. \tag{3.4.3}$$

We have also defined

$$P^{\mu\nu} = \eta^{\mu\nu} - \frac{\partial^\mu\partial^\nu}{\Box}\,, \tag{3.4.4}$$

and $\Box$ is now the flat-space d'Alembertian. We solve equation 3.4.1 for $h_{\mu\nu}$ fixing the gauge $\partial^\mu \bar{h}_{\mu\nu} = 0$, where $\bar{h}_{\mu\nu} = h_{\mu\nu} - (1/2)\,\eta_{\mu\nu}\,h$, $\bar{h} = -(d-1)\,h/2$. Equation 3.4.1 becomes

$$\Box \bar{h}_{\mu\nu} + \frac{m^2}{d} P^{\mu\nu}\bar{h} = -16\pi G T_{\mu\nu} \tag{3.4.5}$$

Taking the trace in momentum space we can invert for $\bar{h}$, $\bar{h}(k) = 16\pi G T(k)/(k^2 - m^2)$ and plug back into 3.4.5. We get

$$-\,k^2\,\bar{h}_{\mu\nu} = -16\pi G T_{\mu\nu} - \frac{m^2\; P_{\mu\nu}(k)}{d\,(k^2 - m^2)}\; 16\pi G\, T \tag{3.4.6}$$

We then solve for $h_{\mu\nu}(k)$. We get, as in [45],

$$\begin{aligned} h_{\mu\nu}(k) &= \Delta^{\rho\sigma}_{\mu\nu}\, T_{\rho\sigma} = \\ &= \frac{16\pi G}{k^2}\left[T_{\mu\nu} - \frac{1}{d-1}\eta_{\mu\nu}T - \frac{1}{d(d-1)}\frac{m^2}{(k^2-m^2)}\eta_{\mu\nu}\,T\right] \end{aligned} \tag{3.4.7}$$

where we have neglected terms proportional to $k_\mu k_\nu$ that do not contribute when saturated with a conserved EM tensor.

The first two terms correspond to the usual GR propagator, while the third corresponds to the non-local modification, and for $m \to 0$ it smoothly goes to zero, so the theory smoothly reduces to GR.

The above computation of the matter-matter interaction stresses the purely classical nature of the derivation. If one were instead so ambitious to consider the theory 3.2.1 as a fundamental non-local quantum field theory, he would try to read the propagating degrees of freedom from the saturated propagator, $-i\,T_{\mu\nu}\,\Delta^{\mu\nu\rho\sigma}\,T_{\rho\sigma}$. In the language of QFT, the first two terms in 3.4.7 describe the exchange of a massless graviton, while the non-local modification gives extra terms in the scalar sector, that read

$$\frac{-i}{d(d-1)}T(-k)\left[\frac{1}{k^2} - \frac{1}{k^2-m^2}\right]T(k) \tag{3.4.8}$$

In a quantum framework, the above term would describe the exchange of a healthy massless scalar plus a ghostlike massive scalar (remember we are working in the "mostly $+$" signature $\eta_{\mu\nu} = (-1,1,1,1)$). In general, a ghost has two distinct effects: (1) at the classical level, it can give rise to runaway solutions. In the cosmological context, with a ghost of mass $m = \mathcal{O}(H_0)$, this is an IR issue, since the instability shows up on cosmological scales. This can then even be a virtue of the theory, since a phase of accelerated expansion can be considered in a sense as an instability of the classical background evolution. (2) At the quantum level, a ghost corresponds to a particle with negative energy and induces a vacuum decay rate Γ rendering the theory inconsistent. This is clearly a UV problem, since the rate is determined by the UV cutoff of the theory and one could circumvent it appealing to a suitable UV completion of the theory.

However, there is no such problem in our theory, since the $\Box^{-1}$ operator in the equations of motion automatically comes with a retarded prescription. Since it is this term that gives rise to the scalar sector contribution in eq. 3.4.8, these propagators inherit the retarded prescription and cannot be promoted to Feynman propagators. They describe classical radiation effects from already existing degrees of freedom, and not new propagating degrees of freedom.

A related points concerns the Lagrangian giving the linearised equations 3.4.1, that is,

$$\mathcal{L} = \frac{1}{2}h_{\mu\nu}\,\mathcal{E}^{\mu\nu,\rho\sigma}h_{\rho\sigma} - \frac{d-1}{2d}\,m^2 h_{\mu\nu}\,P^{\mu\nu}P^{\rho\sigma}h_{\rho\sigma} \tag{3.4.9}$$

Since we stressed that the equations of the theory already contain themselves a retarded propagator, the question is if it is possible to obtain them from a variational principle. The answer is crucially no: the variation of the above Lagrangian never gives a retarded $\Box^{-1}$ in the equations of motion, whatever definition of the Green's function we use, as extensively discussed in the existing literature about non-local extensions of GR [45, 58, 52, 49, 44, 65, 51]. Consider for example a scalar field with a non-local term in the action of the form

$$\int d^4x\,\phi\,\Box^{-1}\phi \tag{3.4.10}$$

Taking the variation with respect to $\phi(x)$ we get

$$\frac{\delta}{\delta\phi(x)}\int d^4x'\phi(x')(\Box^{-1}\phi)(x') = \frac{\delta}{\delta\phi(x)}\int d^4x'\, d^4x''\ \phi(x')G(x';x'')\phi(x'') = \\ = \int d^4x'\,[G(x;x') + G(x';x)]\phi(x') \tag{3.4.11}$$

In other words, the variational derivative automatically symmetrizes the Green's function, and we cannot obtain equations of motions in which a retarded propagator appears from a variational principle, since $G_{ret}(x;x')$ is not symmetric under $x \leftrightarrow x'$ (actually, $G_{ret}(x;x') = G_{adv}(x';x)$). The correct point of view is then that the action is used as a "formal trick" to obtain the classical equations of motions from a variational principle, as extensively recognised in the literature after the original proposal by Barvinsky and Velkovisky [66, 65, 51]. After taking the variation, one should adopt the rule of replacing $\Box^{-1}_{sym} \mapsto \Box^{-1}_{ret}$. This way we loose any connection with a fundamental *quantum* field theory. The model 3.2.1 should rather be considered as a *classical* effective one. The "QFT" that one would obtain taking the propagators in 3.4.8 as Feynman propagators has nothing to do with our classical equations, and those degrees of freedom are simply not degrees of freedom of our theory. In particular, this shows that any discussion on "ghostlike" and "propagating" degrees of freedom, that one is inevitably tempted to address, simply makes no sense in this framework, but it could consistently addressed only in the fundamental (and local) theory giving rise to such classical effective equations.
Thus, equation 3.4.1 is not the classical equation of motion of a non-local QFT. On the contrary, non-local classical equations emerge in other context in physics, and are never fundamental.
A related situation comes from the classical post Newtonian formalism for GW production ([44], [67]). In the linearised theory, the GW amplitude is $\Box\bar{h}_{\mu\nu} = -16\pi G T_{\mu\nu}$, so this is a classical radiation problem and is solved by $\bar{h}_{\mu\nu} = -16\pi G\Box^{-1}_{ret}T_{\mu\nu}$. Considering higher order corrections, the radiation generated at the linear order becomes itself source for GW production at next perturbative order. In the far-wave zone, then, one has an effect described by effective equations containing $\Box^{-1}_{ret}$. Any issue of quantization, however, should address the underlying fundamental theory and not such effective equations. This is what happens in our theory.

3.4.2 Spurious degrees of freedom from auxiliary fields

The issue of the extra degrees of freedom in non-local theories can be understood considering the "localisation" obtained by the introduction of auxiliary fields, as we did in passing from 3.2.1 to 3.2.4. The point is that such localisation procedure can introduce spurious degrees of freedom, and in particular spurious "ghosts" if one adopts the wrong point of view of considering the theory a fundamental QFT.
As we have pointed out from the beginning, to define our original non-local theory we must specify what we mean exactly by $\Box^{-1}$. In general, an equation such as $\Box U = -R$ is solved by $U = -\Box^{-1}R$, where

$$\Box^{-1}R = U_{\rm hom}(x) - \int d^{d+1}x'\,\sqrt{-g(x')}\,G(x;x')R(x')\,, \tag{3.4.12}$$

The choice of both $U_{\rm hom}(x)$ and $G(x;x')$ are then part of the *definition* of the theory, and as such remain fixed from the very beginning. Introducing the auxiliary field $U(x)$, the assignment of the homogeneous solution translates into the assignment of given initial conditions on the field $U(x)$: there exists one, and only one, choice that gives back the original model. Our model is defined by the choice of the retarded Green's function and by the requirement that $U = 0$ in

RD, that translates into the initial conditions 3.3.12. Different choices of the homogeneous solution would therefore define different theories, and since the choice of U_{hom} amounts to impose different initial conditions on the fields U, W as those given in 3.3.12, the space of such theories can be parametrized by the space of the coefficients u_0, u_1, w_1, w_2.

As far as the issue of quantisation is concerned, the homogeneous solution of an equation such as $\Box\phi = 0$ for a scalar theory in flat space is just a superposition of plane waves,

$$\phi_{hom}(x) = \int \frac{d^3k}{(2\pi)^3} \left[a_{\mathbf{k}} e^{ikx} + a^*_{\mathbf{k}} e^{-ikx}\right] \tag{3.4.13}$$

where the coefficients $a_{\mathbf{k}}$, $a^*_{\mathbf{k}}$ are subsequently promoted to creation and annihilation operators during the quantization procedure. In our case, the coefficients are instead uniquely fixed once the initial conditions are specified, hence they cannot be promoted to operators and there is no quantum degree of freedom associated to them.

The case of the Deser-Woodard model 3.1.1 is interesting. We recall the action 3.1.1,

$$S = \frac{1}{16\pi G} \int d^4x\sqrt{-g}\, R \left[1 + f\left(\frac{1}{\Box} R\right)\right] \tag{3.4.14}$$

Rewriting the action 3.4.14 in local form with two fields $\phi \equiv \Box^{-1}R$ and a Lagrange multiplier ξ that enforces $\Box\phi = R$. We get

$$S = \frac{1}{16\pi G} \int d^4x\sqrt{-g}\, \{R[1 + f(\phi)] + \xi(\Box\phi - R)\} \tag{3.4.15}$$

The kinetic term can be diagonalised setting $\xi = \varphi_1 + \varphi_2$, $\phi = \varphi_1 - \varphi_2$, so

$$S = \frac{1}{16\pi G} \int d^4x\sqrt{-g}\, \left\{R[1 + f(\varphi_1 - \varphi_2) - \varphi_1 - \varphi_2] - (\partial\varphi_1)^2 + (\partial\varphi_2)^2\right\} \tag{3.4.16}$$

The field φ_2 in our signature is then a ghost, and this is true even in the case $f = 0$, i.e. General Relativity! Again, the point is that 3.4.16 is equivalent to 3.4.14 only if we discard the homogeneous solution of $\Box\phi = R$, and therefor neither ϕ nor ξ are propagating degrees of freedom.

Vacuum (in)stability in classical General Relativity

A very instructive example of how spurious degrees of freedom arise if one uses non-local variables has been provided in [44] and [68] and comes from GR itself. We shall illustrate it here following in particular reference [44]. Consider the quadratic Einstein-Hilbert action,

$$S = \frac{1}{2} \int d^4x\, h_{\mu\nu}\, \mathcal{E}^{\mu\nu,\rho\sigma} h_{\rho\sigma} + 16\pi G \int d^4x\, h_{\mu\nu} T^{\mu\nu} \tag{3.4.17}$$

We can decompose the metric as

$$h_{\mu\nu} = h^{TT}_{\mu\nu} + \frac{1}{2}\left(\partial_\mu\epsilon_\nu + \partial_\nu\epsilon_\mu\right) + \frac{1}{3}\eta_{\mu\nu}\, s \tag{3.4.18}$$

where $h^{TT}_{\mu\nu}$ is the transverse-traceless part. This part and the scalar s are gauge invariant under linearised diffeomorphism. Plugging 3.4.18 into 3.4.17, the "pure gauge" mode ϵ_μ cancels and we are left with

$$S = \frac{1}{2} \int d^4x \left[h^{TT}_{\mu\nu} \Box h^{TT}_{\mu\nu} - \frac{2}{3} s\Box s\right] + 16\pi G \int d^4x \left[h^{TT}_{\mu\nu} (T^{\mu\nu})^{TT} + \frac{1}{3} s\, T\right] \tag{3.4.19}$$

Then, it seems that we have an additional scalar propagating degree of freedom with respect to what we would expect in GR, i.e. the two radiative degrees of freedom corresponding to the ± 2 helicities of the massless graviton. Moreover, the additional degree of freedom s is ghost-like. Of course, this conclusion is wrong, and all degrees of freedom different from the latter are physical (i.e. gauge invariant) but non-radiative.
The spurious radiative degree of freedom is in fact nothing but an artefact of the decomposition 3.4.18. The crucial point is that $h^{TT}_{\mu\nu}$ and s are obtained from $h_{\mu\nu}$ through a non-local operator. In particular, inverting 3.4.18 for s one finds

$$s = \left(\eta_{\mu\nu} - \frac{1}{\Box}\partial_\mu\partial_\nu\right) h_{\mu\nu} = P^{\mu\nu} h_{\mu\nu} \tag{3.4.20}$$

Being s a non-local function of $h_{\mu\nu}$, an ordinary counting of the degrees of freedom in 3.4.19 leads to a wrong result, since the initial data assigned on $h_{\mu\nu}$ are not sufficient to evolve s. This is better understood [44] in the case of a scalar field ϕ that satisfies the Poisson's equation, $\boldsymbol{\nabla}^2\phi = \rho$. If we define a new field $\tilde{\phi}$ as $\tilde{\phi} = \Box^{-1}\phi$, the original equation can be written as

$$\Box\tilde{\phi} = \boldsymbol{\nabla}^{-2}\rho \equiv \tilde{\rho} \tag{3.4.21}$$

so that now $\tilde{\phi}$ looks like a propagating field. The point is that for $\rho = 0$ our original equation has the unique solution $\phi = 0$, so equation 3.4.21 must be solved with the condition that $\tilde{\phi} = 0$ if $\rho = 0$. The homogeneous plane-wave solution would read

$$\tilde{\phi}_{hom}(x) = \int \frac{d^3k}{(2\pi)^3} \left[a_{\mathbf{k}} e^{ikx} + a^*_{\mathbf{k}} e^{-ikx}\right] \tag{3.4.22}$$

with $a_{\mathbf{k}}$, $a^*_{\mathbf{k}}$ becoming creation and annihilation operators upon quantization. Here however such solution is fixed uniquely by the condition $\tilde{\phi} = 0$ if $\rho = 0$, and they cannot be considered as free parameters.

The situation in GR is exactly the same, since s can be related to a non-radiative degree of freedom via a non-local transformation using the $3+1$ decomposition of the metric. In terms of the Bardeen's variables Φ, Ψ one has

$$s = 6\Phi - 2\Box^{-1}\boldsymbol{\nabla}^2(\Phi + \Psi) \tag{3.4.23}$$

As in the simple example given above, this potentially introduces a spurious degree of freedom. Considering the equation of motion for s,

$$\Box s = 8\pi G\, T \tag{3.4.24}$$

we see that the correct solution corresponding to GR is the one that satisfies the condition $s = 0$ when $T = 0$, i.e. the homogeneous solution must be discarded, and there are no annihilation and creation operators associated to s.

3.4.3 Radiative and non-radiative degrees of freedom

Another way to study what radiative and non-radiative degrees of freedom are described by eq. (3.4.1) is proceeding as in GR. We henceforth restrict to $d = 3$, we consider first the scalar sector, and we use the diff-invariance of the non-local theory to fix the Newtonian gauge

$$h_{00} = 2\Psi\,, \qquad h_{0i} = 0\,, \qquad h_{ij} = 2\Phi\delta_{ij}\,. \tag{3.4.25}$$

We also write the energy-momentum tensor in the scalar sector as

$$T_{00} = \rho\,, \qquad T_{0i} = \partial_i \Sigma\,, \qquad T_{ij} = P\delta_{ij} + [\partial_i\partial_j - (1/3)\delta_{ij}\boldsymbol{\nabla}^2]\sigma\,. \tag{3.4.26}$$

The field equations 3.2.9 in this gauge are obtained by a straightforward generalization of the standard computation performed in GR (see e.g. [68]). The linearization of the $(0,0)$ component gives

$$\boldsymbol{\nabla}^2\left[\Phi - (m^2/6)S\right] = -4\pi G\rho\,, \tag{3.4.27}$$

while from the (i,j) component we get

$$-\delta_{ij}\boldsymbol{\nabla}^2(\Phi+\Psi) + \partial_i\partial_j(\Phi+\Psi) - 2\delta_{ij}\partial_0^2\Psi - \frac{m^2}{3}(U\delta_{ij} + \partial_i\partial_j S) = 8\pi G T_{ij} \tag{3.4.28}$$

where we have written all spatial indices as lower indices since we are linearising over Minkowsky. We apply the projector $(\boldsymbol{\nabla}^{-2}\partial_i\partial_j - \frac{1}{3}\delta_{ij})$ to extract the traceless part, and we get

$$\boldsymbol{\nabla}^2\left(\Phi + \Psi - \frac{m^2}{3}S\right) = 8\pi G\,\boldsymbol{\nabla}^2\sigma \tag{3.4.29}$$

Since this holds over all space and we impose the boundary condition that the potentials vanish at infinity, this has the solution $\Phi + \Psi - \frac{m^2}{3}S - 8\pi G\sigma = 0$. Finally, from the trace of the field equations we get

$$2\boldsymbol{\nabla}^2\Phi + 4\boldsymbol{\nabla}^2\Psi - 6\,\partial_0^2\,\Psi + m^2 U = -8\pi G(\rho - 3P) \tag{3.4.30}$$

Hence, since the Ricci scalar is

$$R = -\Box U = -\boldsymbol{\nabla}^2\Phi + 3\,\partial_0^2\,\Psi - \boldsymbol{\nabla}^2(\Phi+\Psi) - 3\Box\Psi = -(2\boldsymbol{\nabla}^2\Phi + 4\boldsymbol{\nabla}^2\Psi - 6\,\partial_0^2\,\Psi)\,, \tag{3.4.31}$$

we have

$$(\Box + m^2)U = -8\pi G(\rho - 3P) \tag{3.4.32}$$

To summarise, we have four independent equations for the four scalar variables Φ, Ψ, U and S,

$$\begin{aligned}
\boldsymbol{\nabla}^2\left[\Phi - (m^2/6)S\right] &= -4\pi G\rho\,, && (3.4.33)\\
\Phi - \Psi - (m^2/3)S &= 8\pi G\sigma\,, && (3.4.34)\\
(\Box + m^2)U &= -8\pi G(\rho - 3P)\,, && (3.4.35)
\end{aligned}$$

together with $\Box S = -U$.

Eqs. (3.4.33) and (3.4.34) show that Φ and Ψ remain non-radiative, just as in GR. This should be contrasted with what happens when one linearizes massive gravity with a Fierz-Pauli mass term, in which case Φ becomes a radiative field that satisfies $(\Box - m^2)\Phi = 0$ [68]. Furthermore, in local massive gravity with a mass term that does not satisfies the Fierz-Pauli tuning, in the Lagrangian also appears a term $(\Box\Phi)^2$ [68], signaling the presence of a dynamical ghost. In our non-local model, in contrast, Φ and Ψ satisfy Poisson equations and therefore remain non-radiative. The equations for U and S might fool us to believe that we have two radiative scalars. However, eq. (3.4.35) is just the linearization of $\Box U = -R$ where, as we have discussed, the radiative solution is a spurious one, introduced when the original non-local model is written in a local form using the auxiliary fields U and S. In a quantum treatment, there are no

annihilation and creation operators associated to them, and they do not represent radiative degrees of freedom of the original non-local theory (see also the discussion in [44]). Observe that the argument on the absence of radiative ghost-like degrees of freedom is not restricted to the linearized approximation. The full non-linear equations (3.2.10) by definition must be supplemented with a given fixed choice of the homogeneous solutions, so they never describe propagating fields.

3.5 Absence of a vDVZ discontinuity and of a Vainsthein mechanism

A general feature of theories of massive gravity is that they become strongly coupled at distances smaller than a critical distance which is larger than the Schwarzschild radius r_S. For example, adding a Fierz-Pauli term to the Einstein-Hilbert action one finds that the classical non-linearities become large below a "Vainshtein radius" $r_V = (GM/m^4)^{1/5}$. At the classical level, this is due to the so-called "Vainshtein mechanism" [69], and it it necessary to cure the vDVZ discontinuity that would otherwise rule out the theory through the usual Solar System tests. In appendix *C* we illustrate these classical results.

In the case of our non-local model, eq. (3.4.8) shows that, in the limit $m \to 0$, the contribution of the scalar sector to the matter-matter interaction vanishes, and the result reduces smoothly to that of GR. Therefore there is no vDVZ discontinuity, and no Vainshtein mechanism is needed. Of course, by itself this does not necessarily mean that non-linearities will remain small down to the Schwarzschild radius r_S, where also the classical non-linearities of GR get large. However, this can be checked computing the metric generated by static sources in the non-local theory. This computation has been performed in detail in [47] for the model defined adding a term $m^2(g_{\mu\nu}\Box^{-1}R)^{\rm T}$ to the Einstein equations, and can be simply adapted to our case. Thus, we will follow very close the computations illustrated in [47] and adapted to our model in [1] throughout the rest of the section.

In our theory, for a static source we have two independent lenght-scales, the Schwarzschild radius r_S of the source and $m^{-1} = \mathcal{O}(H_0^{-1}) >> r_S$. Since between the two there is a huge separation, we should explicitly check if in the intermediate region $r_S << r << m^{-1}$ the theory remains linear and close to GR, in contrast to usual massive gravity theories.

We write the most general static spherically symmetric metric in the form

$$ds^2 = -e^{2\alpha(r)}dt^2 + e^{2\beta(r)}dr^2 + r^2(d\theta^2 + \sin^2\theta\, d\phi^2)\,. \tag{3.5.1}$$

Since the theory is diff-invariant, we can use the invariance to set to one a function $e^{2\mu(r)}$ that in the most general solution would multiply the term $r^2 d\Omega^2$. We use the labels $(0,1,2,3)$ for the coordinate system (t, r, θ, ϕ) and we denote $f' \equiv df/dr$. The Christoffel symbols are those of GR and can be found e.g. in [2].
In GR two independent equations for α and β are usually obtained taking the combinations $e^{2(\mp\alpha)}R_{00}+R_{11}$ and R_{22} (see e.g. [2]). In our non-local theory, using eq. (3.2.9) we get, respectively

$$(1-2\mu S)(\alpha'+\beta') = -\mu r[S'' - (\alpha'+\beta'-U')S']\,, \tag{3.5.2}$$

and

$$(1-2\mu S)\left\{1+e^{-2\beta}[r(\beta'-\alpha')-1]\right\} = \mu r^2(U+U^2/2) - 2\mu r e^{-2\beta}S'\,, \tag{3.5.3}$$

which reduce to their GR counterparts for $\mu = 0$. Finally, in the metric (3.5.1) eq. (3.2.10) becomes

$$r^2U'' + [2r + (\alpha' - \beta')r^2]U' = -2e^{2\beta} + 2[1 + 2r(\alpha' - \beta') + r^2(\alpha'' + \alpha'^2 - \alpha'\beta')]\,, \quad (3.5.4)$$

$$S'' + (\alpha' - \beta' + 2/r)S' = -e^{2\beta}U\,. \quad (3.5.5)$$

Eqs. (3.5.2)–(3.5.5) provide four independent equations for the four functions α, β, U, S. As discussed in [47], we can study these equations with two different expansions: in the region $r \ll m^{-1}$ we can perform a low-m expansion, in which we solve the equation iteratively taking m as a small expansion parameter. The solution in the region $r \gg r_S$, with no limitation of the parameter mr, can instead be obtained considering the effect of the source as a perturbation of Minkowski space, adapting the standard analysis performed in GR to recover the Newtonian limit. The low-m expansion is valid for $mr \ll 1$ while the Newtonian analysis is valid for $r \gg r_S$. The two expansions therefore have an overlapping domain of validity $r_S \ll r \ll m^{-1}$, where they can be matched, and this allows us to fix uniquely all the coefficients that appears in the solutions, see the discussion in [47].

3.5.1 Solution for $r << m^{-1}$

We perform a low-m expansion, summing that in the limit $mr \to 0$ the terms $\propto \mu$ are negligible and checking a posteriori the del-consistency of the procedure. We shall consider the equations in the external region, $T_{\mu\nu} = 0$. Hence, to lowest order equations 3.5.2-3.5.3 reduce to their GR counterparts, whose solution is given by

$$\alpha(r) = \frac{1}{2}\log\left(1 - \frac{r_S}{r}\right), \qquad \beta(r) = -\alpha(r) \quad (3.5.6)$$

We plug into 3.5.4 and we get

$$U(r) = u_0 - u_1 \log\left(1 - \frac{r_S}{r}\right) \quad (3.5.7)$$

with u_0, u_1 are some constants that parametrize the solution of the associated homogeneous equation. The choice of the homogeneous solutions is a point extensively discussed above in the context of the definition of the inverse d'Alembertian and of or non-local theory. Each choice of the coefficients u_0, u_1 defines a different theory. Since the choice of u_1 could be subtle in this context, we shall keep it generic, while we set to zero the constant u_0. Equation 3.5.5 reads

$$S'' + (\alpha' - \beta' + 2/r)S' = -e^{2\beta}U \quad (3.5.8)$$

The computation could be done in principle for every $r << m^{-1}$, but the full solutions involve polylog functions and are not very interesting to write down here. Hence, we expand for $r >> r_S$ with the above solution for U and we get

$$S'' + \left[2/r + \mathcal{O}\left(\frac{r_S^2}{r^2}\right)\right] S' = u_1\frac{r_S}{r} + \mathcal{O}\left(\frac{r_S^2}{r^2}\right) \quad (3.5.9)$$

with solution

$$S(r) = \frac{1}{2}r_S^2 u_1 \frac{r}{r_S} \quad (3.5.10)$$

This completes the zeroth-order solution of the system Eqs. (3.5.2)–(3.5.5) in the regime $r_S \lesssim r << m^{-1}$. To get the first-order correction to α and β we plug these solutions back into

the equations.

From 3.5.2, to leading order in r_s/r we still find

$$\alpha' + \beta' = 0 \tag{3.5.11}$$

while plugging into 3.5.3 we find

$$2r\beta' \simeq -e^{2\beta} + 2u_1\,\mu\, r_s\, r \tag{3.5.12}$$

In the limit $r >> r_S$ we can further approximate $e^{2\beta} \simeq 1$, and the solution can be written as

$$\alpha(r) = \beta(r) = \frac{1}{2}\log\left(1 - \frac{r_S}{r} - u_1 \mu r_s r\right) \tag{3.5.13}$$

Thus, in the region $r_S << r << m^{-1}$ we have, using $\mu = m^2/6$ in $d = 3$,

$$A(r) \equiv e^{2\alpha(r)} \simeq 1 - \frac{r_S}{r}\left(1 + \frac{u_1 m^2 r^2}{6}\right), \qquad B(r) \equiv e^{2\beta(r)} = 1/A(r) \tag{3.5.14}$$

Observe that, since $\mu = m^2/6$ in $d = 3$, to first order in the low-m expansion and for $r \gg r_S$, the result for α and β is the same as that found in [47]. The corrections to linearised theory are very small for $mr << 1$, so the perturbative procedure is self-consistent.

3.5.2 The Newtonian limit

We can obtain the solution in the regime $r >> r_S$ without limitation on the product mr following the standard analysis of GR to recover the Newtonian limit, i.e., considering the effects of the source as perturbations of Minkowsky space. For a static non-relativistic source, we have the Newtonian gauge 3.4.25 and for a static non-relativistic source the energy-momentum tensor perturbations 3.4.26 read $\delta T_{00} = \rho$,$\delta T_{0i} = \delta T_{ij} = 0$. We start from a background where $U_{back} = S_{back} = 0$, so we shall write the perturbations simply as U, S keeping in mind that they are first order quantities as Φ and Ψ. since the source is static, we set to zero all time dependencies. Equations 3.2.10 become

$$\boldsymbol{\nabla}^2 U = \boldsymbol{\nabla}^2(2\Psi + 4\Phi) \tag{3.5.15}$$

$$U = -\boldsymbol{\nabla}^2 S \tag{3.5.16}$$

while equation 3.4.33 with $\sigma = 0$ is

$$\boldsymbol{\nabla}^2\left(\Phi + \Psi - \frac{m^2}{3}S\right) = 0 \tag{3.5.17}$$

However, in this section we are considering equations valid in the regime $r >> r_S$, so we cannot conclude that $\Phi + \Psi - \frac{m^2}{3}S = 0$. Any function that at large r reduce to the form $f(r) = a_1 r_S/r$ satisfies $\boldsymbol{\nabla}^2 f = 0$ at large r and vanishes at infinity. Hence, the solution of equation 3.5.17 reads

$$\Phi + \Psi = \frac{m^2}{3}S + a_1\frac{r_S}{r} \tag{3.5.18}$$

From the same reasoning we conclude that equation 3.5.15 has solution

$$U = 2\Psi + 4\Phi + a_2\frac{r_S}{r} \tag{3.5.19}$$

Finally, from equation 3.4.35 with $P = 0$ and $\Box \mapsto \boldsymbol{\nabla}^2$ we get the inhomogeneous Helmoltz equation

$$(\boldsymbol{\nabla}^2 + m^2)U = -8\pi G\rho \tag{3.5.20}$$

The solution is written in terms of the Green's function $G(\mathbf{x} - \mathbf{x}')$,

$$U(\mathbf{x}) = -8\pi G \int_V d^3x'\, G(\mathbf{x} - \mathbf{x}')\rho(\mathbf{x}') \tag{3.5.21}$$

where

$$(\boldsymbol{\nabla}^2 + m^2)G(\mathbf{x}) = \delta^{(3)}(\mathbf{x}) \tag{3.5.22}$$

Writing $G = G(r) = -(1/4\pi r)f(r)$ one has

$$(\boldsymbol{\nabla}^2 + m^2)G(\mathbf{x}) = \delta^{(3)}(\mathbf{x})f(0) - \frac{1}{4\pi r}(f'' + m^2 f) \tag{3.5.23}$$

Therefore $f(0) = 1$ and $f'' + m^2 f = 0$. The most general solution is

$$f(r) = \cos(mr) + \beta \sin(mr) \tag{3.5.24}$$

hence 3.5.21 becomes

$$U(\mathbf{x}) = 2G \int_V d^3x'\, \frac{\rho(\mathbf{x}')}{|(\mathbf{x} - \mathbf{x}'|} \left[\cos(m|(\mathbf{x} - \mathbf{x}'|) + \beta \sin(m|(\mathbf{x} - \mathbf{x}'|)\right] \tag{3.5.25}$$

to leading order in $r >> r_S$,

$$U(\mathbf{x}) \simeq \frac{2G}{r} \int_V d^3x'\, \rho(\mathbf{x}') \left[\cos(m|(\mathbf{x} - \mathbf{x}'|) + \beta \sin(m|(\mathbf{x} - \mathbf{x}'|)\right] \tag{3.5.26}$$

For a point like source, $\rho(\mathbf{x}) = M\delta^{(3)}(\mathbf{x})$ we finally find

$$U(r) = \frac{r_S}{r} \left[\cos(mr) + \beta \sin(mr)\right] \tag{3.5.27}$$

The coefficient β has to be determined by matching this solution with the solution in the region $mr << 1$ found above. Plugging this solution in 3.4.33 and using $U = -\boldsymbol{\nabla}^2 S$, $\rho(\mathbf{x}) = M\delta^{(3)}(\mathbf{x})$ we get

$$\boldsymbol{\nabla}^2\Phi = -2\pi r_S \delta^{(3)}(\mathbf{x}) - \frac{m^2 r_S}{6r} \left[\cos(mr) + \beta \sin(mr)\right] \tag{3.5.28}$$

The solution can be put in the form

$$\Phi = \frac{r_S}{2r} \left\{ c_\Phi + \frac{1}{3} \left[\cos(mr) + \beta \sin(mr)\right] \right\} \tag{3.5.29}$$

then, plugging the solutions for U and Φ into equation 3.5.19 we get

$$\Psi = \frac{r_S}{2r} \left\{ c_\Psi + \frac{1}{3} \left[\cos(mr) + \beta \sin(mr)\right] \right\} \tag{3.5.30}$$

with $c_\Phi = -(a_2 + 2c_\Psi)$.

We are now ready to perform the matching with the functions $A(r)$ and $B(r)$ found in the previous section. In the region $r >> r_S$,

$$A(r) \simeq 1 + 2\alpha(r)\,, \qquad B(r) \simeq 1 + 2\beta(r)\,. \tag{3.5.31}$$

On the other hand, we must perform the matching considering the fact that the radial coordinate used in the previous section is different from that used here, since we are in a different gauge. This is clear from the fact that the linearised metric 3.5.1 is

$$ds^2 = -(1+2\alpha)dt^2 + (1+2\beta)dr^2 + r^2 d\Omega^2 \tag{3.5.32}$$

while in the Newtonian gauge the factor $1+2\Psi$ multiplies the while factor $d\mathbf{x}^2$: denoting by r_N the radial coordinate in the Newtonian gauge,

$$ds^2 = -(1+2\Psi)dt^2 + (1+2\Phi)[dr_N^2 + r_N^2 d\Omega^2] \tag{3.5.33}$$

Thus we need a relation between α, β, Φ, Ψ, r, r_N. This is obtained rewriting 3.5.33 as

$$ds^2 = -(1+2\Psi)dt^2 + (1+2\Phi)\left(\frac{dr_N}{dr}\right)dr^2 + (1+2\Phi)r_N^2 d\Omega^2 \tag{3.5.34}$$

Comparing with 3.5.32 we find

$$r = (1+2\Phi)r_N\,, \qquad 1+\beta = (1+\Phi)\frac{dr_N}{dr} \tag{3.5.35}$$

Combining the two we get $\beta = -r\Phi'/(1+\Phi)$ which at linearised order is equivalent to $\beta = r\Phi'$. In summary,

$$r = (1+2\Phi)r_N\,, \qquad \beta = -\Phi'\,, \qquad \alpha = \Psi\,. \tag{3.5.36}$$

Using the latter and 3.5.31 we find $A(r) = 1+2\Psi$, $B(r) = 1-2r\Phi'$, so

$$A(r) = 1 + \frac{r_S}{r}\left\{c_\Psi + \frac{1}{3}\left[\cos(mr) + \beta\sin(mr)\right]\right\} \tag{3.5.37}$$

$$B(r) = 1 + \frac{r_S}{r}\left\{c_\Phi + \frac{1}{3}\left[\cos(mr) + \beta\sin(mr)\right] + \frac{mr}{3}\left[\sin(mr) - \beta\cos(mr)\right]\right\} \tag{3.5.38}$$

In the limit $mr << 1$ we get

$$A(r) = 1 + \frac{r_S}{r}\left(c_\Psi + \frac{1}{3} + \beta mr - \frac{m^2r^2}{6}\right) \tag{3.5.39}$$

$$B(r) = 1 + \frac{r_S}{r}\left(c_\Phi + \frac{1}{3} + \frac{m^2r^2}{6}\right) \tag{3.5.40}$$

Matching these with the solution found in the regime $mr << 1$, equation 3.5.14, we get $\beta = 0$, $c_\Psi = -4/3$ and $c_{Phi} = 2/3$. Comparing the terms $\propto m^2r^2$ also allows us to fix $u_1 = 1$.

In conclusion, the solution for $r \gg r_S$ (and mr generic) is

$$A(r) = 1 - \frac{r_S}{r}\left[1 + \frac{1}{3}(1-\cos mr)\right]\,, \tag{3.5.41}$$

$$B(r) = 1 + \frac{r_S}{r}\left[1 - \frac{1}{3}(1 - \cos mr - mr\sin mr)\right]. \tag{3.5.42}$$

In particular, for $r_S \ll r \ll m^{-1}$ we have

$$A(r) \simeq 1 - \frac{r_S}{r}\left(1 + \frac{m^2r^2}{6}\right)\,, \tag{3.5.43}$$

and $B(r) \simeq 1/A(r)$.

This should be compared with the analogous result obtained in massive gravity, when one considers the Einstein-Hilbert action plus a Fierz-Pauli mass term, which reads [69, 57]

$$A(r) = 1 - \frac{4}{3}\frac{r_S}{r}\left(1 - \frac{r_S}{12m^4r^5}\right) . \tag{3.5.44}$$

The factor 4/3 in front of r_S/r gives rise to the vDVZ discontinuity, see appendix C. In contrast, no vDVZ discontinuity is present in eq. (3.5.43). Furthermore, in eq. (3.5.44) the linearized expansions breaks down for r below the Vainshtein radius $r_V = (GM/m^4)^{1/5}$, while in eq. (3.5.43) the correction becomes smaller and smaller as r decreases. Thus the theory (3.2.1) (as well as the theory defined adding a term $m^2(g_{\mu\nu}\Box^{-1}R)^{\rm T}$ to the Einstein equations) remain linear down to $r \sim r_S$, where eventually also GR becomes non-linear. This means that, taking $m \sim H_0$, these non-local theory pass with flying colors all solar system tests. We have found that, for $r \ll m^{-1}$, the corrections to the GR result are $1 + \mathcal{O}(m^2r^2)$. For $m \sim H_0$ and $r \sim 1$ a.u. we have $m^2r^2 \sim 10^{-30}$, and the predictions of these non-local theories are indistinguishable from that of GR.

Chapter 4

Possible extensions

In the previous chapter we have proposed a non-local extension of GR in which the fundamental ingredients are a mass parameter $m^2 = \mathcal{O}(H_0)$ and the inverse d'Alembertian acting on the Ricci scalar.
Despite the fact that if one aims to modify GR on cosmological scale it is not surprising that a mass scale $m = \mathcal{O}(H_0)$ shows up, it would be interesting to check if such scale can be obtained dynamically from existing degrees of freedom. The most obvious choice one has is trying to exploit the curvature terms, since in FRW those can be expressed as functions of H and its derivatives; for instance, $R(t) \sim H^2(t)$, hence its value today sets a scale $R_0 = \mathcal{O}(H_0) \sim m^2$. Then, one could try to replace the scale m with a dynamical term R.
On the other hand, it would be interesting to see if, keeping a mass parameter in the theory, a viable Dark Energy model emerges from the inverse d'Alembertian applied to other terms involving the curvature, e.g. $R_{\mu\nu}\Box^{-1}R^{\mu\nu}$, though the instability of such kind of terms has recently emerged in the literature [58, 61].

4.1 Additional curvature terms

4.1.1 An immediate extension

The first action one could try to get rid of the mass parameter is obtained by replacing directly the term m^2 in 3.2.1 with αR, where α is an dimensional parameter. Then

$$S_{\rm NL} = \frac{1}{16\pi G}\int d^{d+1}x\sqrt{-g}\left[R + \alpha R^2\frac{1}{\Box^2}R\right], \tag{4.1.1}$$

Introducing the usual auxiliary fields $U = -\Box^{-1}R$, $S = -\Box^{-1}U$ with the aid of two Lagrange multipliers we get

$$\begin{aligned} S_{\rm NL} &= \frac{1}{16\pi G}\int d^{d+1}x\sqrt{-g}\left[R + \alpha\, R^2\, S - \alpha\xi_1(\Box U + R) - \alpha\xi_2(\Box S + U)\right] \\ &= \frac{1}{16\pi G}\int d^{d+1}x\sqrt{-g}\left[R(1 - \alpha\,\xi_1 + \alpha\, R\, S) + \alpha\partial\xi_1\cdot\partial U + \alpha\partial\xi_2\cdot\partial S - \alpha\,\xi_2\, U\right] \end{aligned} \tag{4.1.2}$$

The equations of motion of the four scalar fields are

$$\begin{aligned}
&\Box U + R = 0 \\
&\Box S + U = 0 \\
&\Box \xi_1 = -\xi_2 \\
&\Box \xi_2 = R^2
\end{aligned} \tag{4.1.3}$$

while the equations for the metric read

$$\begin{aligned}
&G_{\mu\nu} + (R_{\mu\nu} - \boldsymbol{\nabla}_\mu \boldsymbol{\nabla}_\nu + g_{\mu\nu}\Box)\,(2\alpha\, R\, S - \alpha\, \xi_1) + \\
&-\frac{\alpha}{2} g_{\mu\nu}\,[\,R\,(R\,S - \xi_1) + \partial\xi_1 \cdot \partial U + \partial\xi_2 \cdot \partial S - \,\xi_2\, U] + \\
&+\frac{\alpha}{2}\,(\partial_\mu \xi_1\, \partial_\nu U + \partial_\mu \xi_2\, \partial_\nu S + \mu \leftrightarrow \nu) = 8\pi G T_{\mu\nu}
\end{aligned} \tag{4.1.4}$$

The $(0,0)$ component in FRW gives, after a little manipulation,

$$\begin{aligned}
&H^2 - \alpha \left[H^2\, \xi_1 + 6\, S \left(H\, \ddot{H} + 2H^2 \dot{H} - \dot{H}^2 \right) - H\dot{\xi}_1 + \right. \\
&\left. + \,12\dot{S}(H\dot{H} + 2H^3) + \frac{1}{6}\left(\dot{\xi}_1 \dot{U} + \dot{\xi}_2 \dot{S} - U\xi_2 \right) \right] = \frac{8\pi G}{3}\rho
\end{aligned} \tag{4.1.5}$$

Passing to $x = \log a$, $V = H_0^2\, S$, $\chi_2 = \xi_2 / H_0^2$, $\zeta = h'/h$ and $h = H/H_0$ we get

$$\begin{aligned}
&h^2 + \alpha \left\{ h^2 \left(-\xi_1 - \xi_1' + \frac{1}{6}\xi_1' U' + \frac{1}{6}\chi_2' V' \right) \right. \\
&\left. + \,h^4 \left[12V'(2+\zeta) + 6\, V\,(\zeta^2 + \zeta' + \zeta) \right] - \frac{1}{6}\chi_2 U \right\} = \Omega_M e^{-3x} + \Omega_R e^{-4x}
\end{aligned} \tag{4.1.6}$$

The EOM 4.1.3 give instead

$$\begin{aligned}
&U'' + U'(3+\zeta) = 6(2+\zeta) \\
&V'' + V'(3+\zeta) = \frac{U}{h^2} \\
&\chi_2'' + \chi_2'(3+\zeta) = -36\,(2+\zeta)^2 \\
&\xi_1'' + \xi_1'(3+\zeta) = \frac{\chi_2}{h^2}
\end{aligned} \tag{4.1.7}$$

We perform the change of variables $\chi_2 = h^2\, X$, $W = h^2 V$ and replace the equations for χ_2 and V with those for W and X:

$$U'' + U'(3+\zeta) = 6(2+\zeta) \tag{4.1.8}$$

$$W'' + 3\,W'(1-\zeta) - 2\,W(\zeta' + 3\zeta - \zeta^2) = U \tag{4.1.9}$$

$$X'' + X'(3+5\zeta) + 2X(\zeta' + 3\zeta + 3\zeta^2) = -36\,(2+\zeta)^2 \tag{4.1.10}$$

$$\xi_1'' + \xi_1'(3+\zeta) = X \tag{4.1.11}$$

The effective DE density is then, from 4.1.6,

$$\begin{aligned}
\rho_{DE}(x) \quad = \quad & \rho_0 \alpha\, h^2(x) \left[-\xi_1 - \xi_1' + \frac{1}{6}\left(\xi_1' U' + 2\zeta\, XW' - 4W\, X\, \zeta^2 + \right. \right. \\
& X'W' - 2WX'\zeta - UX) + W' - 2W\zeta + \frac{1}{2}W'\zeta - W\zeta^2 + \\
& \left. +6W(\zeta^2 + \zeta + \zeta') \right]
\end{aligned} \tag{4.1.12}$$

The equations for U and W, 4.1.8 and 4.1.9, are the same as in section 3.3 and in [1] and they have been proven to be perturbatively stable.

On the other hand, the equation for X in the perturbative approximation $\zeta = \text{const.} = \zeta_0$ has the homogeneous solution

$$X_{hom} = a_1 e^{-3(1+\zeta_0)x} + a_2 e^{-2\zeta_0 x} \tag{4.1.13}$$

Since $-2 \leq \zeta_0 \leq 0$, the homogeneous solution blows up in the early Universe. The divergence affects the whole evolution, since X enters in the evolution of other fields and in the effective Dark Energy density. Then, this model is unable to give a convincing background evolution in RD and MD.

4.1.2 Deser-Woodard models

The extension of 3.2.1 to 4.1.1 by promoting m^2 to a curvature term is not unique, since we have the inequivalent possibility

$$S_{\rm NL} = \frac{1}{16\pi G}\int d^{d+1}x\sqrt{-g}\left[R + \alpha R\left(\frac{1}{\Box}R\right)^2\right], \tag{4.1.14}$$

This is indeed a model of the Deser type 3.1.1 with $f(X) = \alpha X^2$. It is then convenient to start with an arbitrary function $f(X)$.

The action is

$$S = \frac{1}{16\pi G}\int \sqrt{-g}\, R\left[1 + f\left(\frac{1}{\Box}R\right)\right] \tag{4.1.15}$$

With the usual procedure of localisation, the field equations can be written in the form $G_{\mu\nu} + \Delta G_{\mu\nu} = 8\pi G T_{\mu\nu}$ where

$$\begin{aligned}\Delta G_{\mu\nu} &= \left[G_{\mu\nu} + g_{\mu\nu}\Box - \boldsymbol{\nabla}_\mu\boldsymbol{\nabla}_\nu\right]\{f(X) + U\} + \\ &+ \left[\delta^{(\rho}\delta^{\sigma)}_{\nu} - \frac{1}{2}g_{\mu\nu}g^{\rho\sigma}\right]\partial_\rho X\,\partial_\sigma U\end{aligned} \tag{4.1.16}$$

where $f_X \equiv df(X)/dX$ and

$$\begin{aligned}X &= \frac{1}{\Box}R \\ U &= \frac{1}{\Box}\left[R f_X(X)\right]\end{aligned} \tag{4.1.17}$$

The $\{0,0\}$ component in FRW gives

$$H^2 + \left[H^2 f(X) + H\dot{X}f_X + H^2 U + H\dot{U} + \frac{1}{6}\dot{X}\dot{U}\right] = \frac{8\pi G}{3}\rho \tag{4.1.18}$$

Passing to $x = \log a$ and setting $h = H/H_0$ we get

$$\begin{aligned}&h^2 = \Omega_M e^{-3x} + \Omega_R e^{-4x} - h^2\left[f + f' + U + U' + \frac{1}{6}X'U'\right] \\ &X'' + X'\left(3 + \frac{h'}{h}\right) = -6\left(2 + \frac{h'}{h}\right) \\ &U'' + U'\left(3 + \frac{h'}{h}\right) = -6 f_X\left(2 + \frac{h'}{h}\right)\end{aligned} \tag{4.1.19}$$

so we can define a Dark Energy density $\rho_{DE}(x) = -\rho_0 h^2(x) Z(x)$ where

$$Z = f + f' + U + U' + \frac{1}{6} X' U' \tag{4.1.20}$$

Consider a power law of the form $f(X) = \gamma\, X^k$, $k > 0$.

We shall adopt the usual perturbative approach, according to which $Y \equiv \rho_{DE}/(\gamma\,\rho_0)$ contributes negligibly to h at early times, so $h'/h = \zeta_0 \sim const.$ in every epoch. Under this assumption, the variable X has the perturbative solution

$$X_{pert}(x) = -\frac{6(2+\zeta_0)}{3+\zeta_0}\, x + x_0 + x_1\, e^{-(3+\zeta_0)x} \tag{4.1.21}$$

The perturbative equation for U becomes

$$U'' + U'(3+\zeta_0) = (-)^k\, 6\,\gamma k\,(2+\zeta_0)\, X^{k-1} \tag{4.1.22}$$

Since $X_{pert} = -A_0 x$, where $A_0 = 6(2+\zeta_0)/3 + \zeta_0$, the perturbative solution for U is a polynomial of degree k in x. Plugging a solution of the form $U_{pert} = \sum_{n=1}^{k} a_n\, x^n$ one finds

$$a_n = (n+1)\,(n+2)...(k-1)\,(-)^{2k-n}\frac{\gamma\, k\, A_0^k}{(3+\zeta_0)^{k-n}} \tag{4.1.23}$$

Then the largest contribution to the dynamical Dark Energy goes as $Y \sim h^2\, x^{2(k-1)}$ if $k > 1$, or $Y \sim h^2\, x^x$ if $k = 1$, as can be seen plugging the solutions for U and X in 4.1.20.

In particular, the case of the action 4.1.14 corresponds to $k = 2$, $f(X) = \gamma\, X(x)^2$.

We get the perturbative inhomogeneous solution for U

$$U_{pert}(x) = -\frac{72\,\gamma\,(2+\zeta_0)^2}{(3+\zeta_0)^3}\, x + \frac{36\,\gamma\,(2+\zeta_0)^2}{(3+\zeta_0)^2}\, x^2 \tag{4.1.24}$$

We then get the perturbative expression for the Dark Energy density

$$Y = -h^2 Z = -h^2\left[f + f' + U + U' + \frac{1}{6} X' U'\right] \propto h^2(ax^2 + bx)\,, \tag{4.1.25}$$

where a and b are constant coefficients depending on ζ_0 that can be obtained by direct substitution and which we shall not need below. Indeed, a problem of consistency immediately comes around. The assumption that Y contributes negligibly to h^2 is safe if and only is a and b are very small numbers. As discussed in section 3.3, in RD, $R = 0$, $\zeta_0 = -2$ and the non-local corrections vanish, and so do the perturbative inhomogeneous solutions 4.1.21 and 4.1.24. Actually, since we never have a "pure radiation" Universe, we can estimate the contribution of the matter component by writing $\zeta_0 \sim -2 + \epsilon$. In this case, $X_{pert} \sim (2+\zeta_0)x \sim \epsilon\, x$, $U_{pert} \sim (2+\zeta_0)^2 x^2 \sim \epsilon^2\, x^2$ and the perturbative assumption is safe. However, this in no more true as soon as we approach the MD epoch, since $\zeta_0 = -3/2$ in MD. In this epoch the Dark Energy can then dominate over matter, and we do not get back standard cosmology.

We have checked the above considerations integrating the equations numerically with initial conditions such that in RD we sit on the perturbative solution. We should fix the value of the free

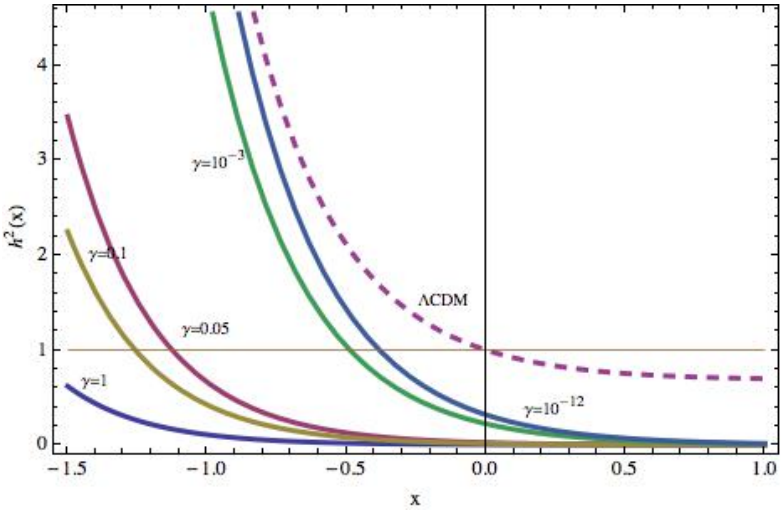

Figure 4.1: The function $h^2(x)$ for different values of the parameter γ, indicated in the figure.

parameter γ so that the observed value of the Hubble parameter today reproduces the observed value, i.e. $h(0) = 1$.

However, there exist no value for γ such that a solution exists. In figure 4.1 we show the function

$$h^2(x) = \frac{\Omega_M e^{-3x} + \Omega_R e^{-4x}}{1 + Z(x)} \tag{4.1.26}$$

for different values of γ. As γ decreases, we approach the asymptotic value $h^2(0) \simeq 0.32 < 1$. Since the function $Z(x)$ appears in the denominator and, as we just saw, the contribution of this function becomes non-perturbative already in MD, the value of $h(0)$ is driven towards small values.

The considerations of this section also apply to other powers of X in the choice of $f(X)$. The result is not particularly surprising, since, as we have mentioned in section 3.1, the functional form that gives the correct value of the Dark Energy today is the one provided by Deffayet and Woodard, 3.3.23 [64].

4.2 Keeping the mass parameter

It is clear from dimensional considerations that, if one sticks to a model in which two powers of the curvature and of the inverse d'Alembertian show up, then a mass parameters has to appear in the theory. The possible combinations of this type are

$$m^2 R \frac{1}{\Box^2} R \tag{4.2.1}$$

$$m^2 R_{\mu\nu} \frac{1}{\Box^2} R^{\mu\nu} \tag{4.2.2}$$

$$m^2 R_{\mu\nu\rho\sigma} \frac{1}{\Box^2} R^{\mu\nu\rho\sigma} \tag{4.2.3}$$

$$m^2 C_{\mu\nu\rho\sigma}\frac{1}{\Box^2}C^{\mu\nu\rho\sigma} \tag{4.2.4}$$

(4.2.5)

Where the Weyl tensor is given by

$$C_{\rho\sigma\mu\nu} = R_{\rho\sigma\mu\nu} - \frac{2}{d-1}\left(g_{\rho[\mu}R_{\nu]\sigma} - g_{\sigma[\mu}R_{\nu]\rho}\right) + \frac{2}{d(d-1)}g_{\rho[\mu}g_{\nu]\sigma}R \tag{4.2.6}$$

Another intriguing possibility could be to insert the $\Box^{-2}$ operator between the terms that appear in the Gauss-Bonnet invariant,

$$R\frac{1}{\Box^2}R - 4R_{\mu\nu}\frac{1}{\Box^2}R^{\mu\nu} + R_{\mu\nu\rho\sigma}\frac{1}{\Box^2}R^{\mu\nu\rho\sigma} \tag{4.2.7}$$

Other combinations such as $R_{\mu\nu}\Box^{-2}(g^{\mu\nu}R)$ reduce to the above due to metric compatibility. Moreover, also the above terms are not independent, due to the definition 4.2.6 of the Weyl tensor.

Being interested in the cosmological implications, we note that, as pointed out in [61], in particular, in FRW the Weyl tensor vanishes, hence 4.2.4 just vanishes, while from 4.2.6 we get:

$$R^{\mu\nu}_{\rho\sigma} = g^\mu_\rho R^{\nu\sigma} - g^\mu_\sigma R^{\nu\rho} - g^\nu_\rho R^{\mu\sigma} + g^\nu_\sigma R^{\mu\rho} - \frac{1}{3}\left(g^\mu_\rho g^\nu_\sigma - g^\mu_\sigma g^\nu_\rho\right) R \tag{4.2.8}$$

Moreover, the metric commutes with the inverse d'Alembertian, since it certainly commutes with $\boldsymbol{\nabla}$ for metric compatibility, so for any tensor $T_{\mu\nu}$ we have

$$g^{\mu\nu}T_{\mu\nu} = \Box(g^{\mu\nu}\Box^{-1}T_{\mu\nu}) \Rightarrow \Box^{-1}(g^{\mu\nu}T_{\mu\nu}) = g^{\mu\nu}\Box^{-1}T_{\mu\nu} \tag{4.2.9}$$

Hence, upon use of 4.2.8, the term 4.2.3 may be written as

$$R_{\mu\nu\rho\sigma}\frac{1}{\Box^2}R^{\mu\nu\rho\sigma} = -\frac{1}{3}R\frac{1}{\Box^2}R + 2R_{\mu\nu}\frac{1}{\Box^2}R^{\mu\nu} \tag{4.2.10}$$

while 4.2.7 becomes

$$R\frac{1}{\Box^2}R - 4R_{\mu\nu}\frac{1}{\Box^2}R^{\mu\nu} + R_{\mu\nu\rho\sigma}\frac{1}{\Box^2}R^{\mu\nu\rho\sigma} = \frac{2}{3}R\frac{1}{\Box^2}R - 2R_{\mu\nu}\frac{1}{\Box^2}R^{\mu\nu} \tag{4.2.11}$$

Then, the most general action we may write including two curvature terms just reduces to a combination of 4.2.2 and 4.2.1,

$$S_{NL} = \frac{1}{16\pi G}\int d^4x\,\sqrt{-g}\,\left[R - \mu\left(\alpha R\frac{1}{\Box^2}R + \beta R_{\mu\nu}\frac{1}{\Box^2}R^{\mu\nu}\right)\right] \tag{4.2.12}$$

where α and β are adimensional factors and we have introduced a normalisation of the mass term in agreement with [1], $\mu = [(d-1)/(4d)]\,m^2$. Note that the case $\alpha = 1$, $\beta = 0$ is just the action introduced in [1].

The corresponding equations of motion can be obtained localising the action through the introduction of two auxiliary scalar fields

$$U \equiv -\Box R\,, \qquad S \equiv -\Box U = \Box^{-2}\,R, \tag{4.2.13}$$

and two auxiliary tensor fields,

$$U_{\mu\nu} \equiv -\Box^{-1}\,R_{\mu\nu}\,, \qquad S_{\mu\nu} \equiv -\Box^{-1}U_{\mu\nu} = \Box^{-2}\,R_{\mu\nu} \tag{4.2.14}$$

The action can be rewritten as

$$\begin{aligned} S_{NL} &= \frac{1}{16\pi G}\int d^4x\,\sqrt{-g}\,\left\{R+\alpha\,\mu\left[-2S\,R-U^2+2g^{\mu\nu}\left(\boldsymbol{\nabla}_\mu S\boldsymbol{\nabla}_\nu U\right)\right]+\right. \\ &+ \left.\beta\,\mu\left[-2R_{\mu\nu}S^{\mu\nu}-\mu U_{\mu\nu}U^{\mu\nu}+2g^{\mu\nu}\left(\boldsymbol{\nabla}_\mu S_{\alpha\beta}\boldsymbol{\nabla}_\nu U^{\alpha\beta}\right)\right]\right\} \end{aligned} \tag{4.2.15}$$

The field equations obtained from 4.2.15 are

$$G_{\mu\nu}-\mu\,\alpha\,K_{\mu\nu}+\mu\,\beta\,I_{\mu\nu}=8\pi G T_{\mu\nu} \tag{4.2.16}$$

where

$$K_{\mu\nu}=2SG_{\mu\nu}-2\boldsymbol{\nabla}_\mu\partial_\nu S-2Ug_{\mu\nu}+g_{\mu\nu}\partial_\rho S\partial^\rho U-(1/2)g_{\mu\nu}U^2-(\partial_\mu S\partial_\nu U+\partial_\nu S\partial_\mu U) \tag{4.2.17}$$

is just the result found in [1], and

$$\begin{aligned} I_{\mu\nu} &= g_{\mu\nu}G^{\alpha\beta}S_{\alpha\beta}+\frac{1}{2}g_{\mu\nu}U_{\alpha\beta}U^{\alpha\beta}-2S_{\mu\alpha}G^\alpha_\nu-2G^\alpha_\mu S_{\nu\alpha}+\frac{1}{2}RS^\alpha_\alpha\,g_{\mu\nu}-2U^\alpha_\mu U_{\nu\alpha}-2RS_{\mu\nu}+ \\ &- g_{\mu\nu}\boldsymbol{\nabla}^\rho(S^{\alpha\beta})\boldsymbol{\nabla}_\rho(U_{\alpha\beta})-g_{\mu\nu}\boldsymbol{\nabla}_\beta(\boldsymbol{\nabla}_\alpha(S^{\alpha\beta}))+ \\ &+ \boldsymbol{\nabla}_\mu(U_{\alpha\beta})\boldsymbol{\nabla}_\nu(S^{\alpha\beta})+\boldsymbol{\nabla}_\mu(S^{\alpha\beta})\boldsymbol{\nabla}_\nu(U_{\alpha\beta})+\boldsymbol{\nabla}_\alpha(S^{\alpha\beta})\boldsymbol{\nabla}_\mu(U_{\nu\beta})+ \\ &+ \boldsymbol{\nabla}_\alpha(S^{\alpha\beta})\boldsymbol{\nabla}_\nu(U_{\mu\beta})-\boldsymbol{\nabla}_\beta(U^{\mu\alpha})\boldsymbol{\nabla}_\nu(S^{\alpha\beta})-\boldsymbol{\nabla}_\mu(S^{\alpha\beta})\boldsymbol{\nabla}_\beta(U_{\nu\alpha})+\boldsymbol{\nabla}_\beta(U^\beta_\alpha)\boldsymbol{\nabla}_\mu(S^\alpha_\nu)+ \\ &+ \boldsymbol{\nabla}_\beta(U^\beta_\alpha)\boldsymbol{\nabla}_\nu(S^\alpha_\mu)+U^{\alpha\beta}\boldsymbol{\nabla}_\beta(\boldsymbol{\nabla}_\mu(S_{\nu\alpha}))-U^\alpha_\nu\boldsymbol{\nabla}_\beta(\boldsymbol{\nabla}_\mu(S^\beta_\alpha))+S^{\alpha\beta}\boldsymbol{\nabla}_\beta(\boldsymbol{\nabla}_\mu(U_{\nu\alpha}))+ \\ &- S^\alpha_\nu\boldsymbol{\nabla}_\beta(\boldsymbol{\nabla}_\mu(U^\beta_\alpha))+U^{\alpha\beta}\boldsymbol{\nabla}_\beta(\boldsymbol{\nabla}_\nu(S_{\mu\alpha}))-U^\alpha_\mu\boldsymbol{\nabla}_\beta(\boldsymbol{\nabla}_\nu(S^\beta_\alpha))+S^{\alpha\beta}\boldsymbol{\nabla}_\beta(\boldsymbol{\nabla}_\nu(U_{\mu\alpha}))+ \\ &- S^\alpha_\mu\boldsymbol{\nabla}_\beta(\boldsymbol{\nabla}_\nu(U^\beta_\alpha))-U^\alpha_\nu\boldsymbol{\nabla}_\beta(\boldsymbol{\nabla}^\beta(S_{\mu\alpha}))-U^\alpha_\mu\boldsymbol{\nabla}_\beta(\boldsymbol{\nabla}^\beta(S_{\nu\alpha}))-S^\alpha_\nu\boldsymbol{\nabla}_\beta(\boldsymbol{\nabla}^\beta(U_{\mu\alpha}))+ \\ &- S^\alpha_\mu\boldsymbol{\nabla}_\beta(\boldsymbol{\nabla}^\beta(U_{\nu\alpha}))-\boldsymbol{\nabla}^\beta(S^\alpha_\mu)\boldsymbol{\nabla}_\nu(U_{\alpha\beta})-\boldsymbol{\nabla}_\mu(U_{\alpha\beta})\boldsymbol{\nabla}^\beta(S^\alpha_\nu)+ \\ &+ \boldsymbol{\nabla}_\alpha(\boldsymbol{\nabla}_\mu(S^\alpha_\nu))+\boldsymbol{\nabla}_\alpha(\boldsymbol{\nabla}_\nu(S^\alpha_\mu))-\boldsymbol{\nabla}_\alpha(\boldsymbol{\nabla}^\alpha(S_{\mu\nu})) \end{aligned} \tag{4.2.18}$$

We proceed with the cosmological consequences of the model, at the level of background evolution. We consider a flat FRW metric $ds^2=-dt^2+a^2(t)d\mathbf{x}^2$, in $d=3$ spatial dimensions and in presence of an energy-momentum tensor $T_{\mu\nu}=(\rho,a^2(t)\,p\,\delta_{ij})$. Our goal is to see whether a viable Dark Energy model emerges from the term proportional to μ, so we do not include a cosmological constant term: $\rho=\rho_M+\rho_R$.

Then, the $(0,0)$ component of 4.2.16 gives $G_{00}=8\pi G\rho(t)+\mu(\alpha K_{00}-\beta I_{00})$. Parametrizing the temporal evolution via $x\equiv\log a$ and defining $h(x)=H(x)/H_0$, $\Omega(x)=\rho(x)/\rho_c$ we get in $d=3$

$$h^2=\Omega(x)+\gamma\,(\alpha K_{00}-\beta I_{00}) \tag{4.2.19}$$

where $\gamma\equiv\mu/(9H_0^2)$. From the right hand side of 4.2.19 we see that we can consider the term $\gamma Y(x)\equiv\gamma(\alpha K_{00}-\beta I_{00})$ as an effective dark energy density, $\rho_{\rm DE}(x)=\rho_0\gamma Y(x)$.

In general, from the EOM for the scalars U, V, and of the tensor fields $U_{\mu\nu}, S_{\mu\nu}$ in addition to the $(0,0)$ component of the field equations, one can obtain a complete system of non-linear differential equations that can be integrated numerically and completely specifies the temporal evolution of the background once the free parameter m is fixed so to reproduce the Dark Energy density today, see [45, 58, 44, 1].

Here, we shall first concentrate on the equations of motion for the auxiliary tensor fields, equation 4.2.14. This can be also derived from the variation of the action 4.2.15 with respect to $U_{\mu\nu}$ and $S_{\mu\nu}$, as it should. The $\Box$ operator evaluated on a rank-(1,1) tensor gives for $\Box U^\mu_\nu=-R^\mu_\nu$

$$\begin{aligned}\Box U_0^0 &= -\ddot{U}_0^0 - dH\dot{U}_0^0 + 2dH^2U_0^0 - 2H^2U_i^i = -R_0^0\\ \Box U_i^i &= -\ddot{U}_i^i - dH\dot{U}_i^i - 2dH^2U_0^0 + 2H^2U_i^i = -R_i^i\end{aligned} \tag{4.2.20}$$

The system 4.2.20 can be diagonalised introducing $U = U_0^0 + U_i^i$, $V = U_0^0 - U_i^i/d$, so

$$\begin{aligned}\ddot{U} + dH\dot{U} &= 2d\dot{H} + d(1+d)\,H^2\\ \ddot{V} + dH\dot{V} - 2(d+1)H^2\,V &= (d-1)\,\dot{H}\end{aligned} \tag{4.2.21}$$

It is easy to show that the equation for V contains a growing mode. Passing again to $x \equiv \log a$, we get in $d = 3$

$$V'' + V'\,(3+\zeta) - 8\,V = 2\,\zeta \tag{4.2.22}$$

where we denote $f' \equiv df/dx$ and $\zeta(x) = h'(x)/h(x)$.

It is convenient to understand analytically the behaviour of the evolution. In the perturbative approximation, in each given era $\zeta(x) = h'(x)/h(x)$ can be approximated by a constant ζ_0, with $\zeta_0 = \{-2, -3/2, 0\}$ in RD, MD and a De Sitter inflationary epoch, respectively.

The homogeneous equation associated to 4.2.22 is the same encountered in the non-local model introduced in [58] and further analyzed in [44]. The solution in the perturbative approximation is

$$V(x) = \frac{\zeta_0}{4} + v_0\,e^{\beta_+ x} + v_1\,e^{\beta_- x} \tag{4.2.23}$$

with

$$\beta_\pm = -\frac{3+\zeta_0}{2} \pm \sqrt{\left(\frac{3+\zeta_0}{2}\right)^2 + 8} \tag{4.2.24}$$

We have $\beta_+ > 0$ both in MD and RD, which leads to a growing solution that affects the whole cosmological evolution, since the function V contributes to the time evolution of the dynamical Dark Energy, since the function V enters in the term I_{00} in 4.2.19. Then, it seems that the growing behaviour does not allow to recover standard cosmology at early times. One could hope that some "cancellation" between growing homogeneous modes occurs in the time evolution of the DE density, which in principle could be obtained by an appropriate choice of the coefficients α and β in 4.2.12. However, there isn't any growing mode in the part coming from the scalar auxiliary fields, since that part is nothing but the model introduced in the previous chapter, that has been proven to be perturbatively stable, and the two sets of auxiliary fields - scalars and tensors - do not mix between each other. Hence, each of the two non-local terms in 4.2.12 must be stable on its own to allow a feasible cosmological evolution.

In a model such as 4.2.12, the instability originates can be traced back to equation 4.2.21 - since U, V are just introduced to decouple such equations - and thus to the very definition of $U_{\alpha\beta} = \Box^{-1}R_{\alpha\beta}$. The presence of V in the form of equation 4.2.22 is then a feature of every tensorial model involving the operator $\Box^{-1}R_{\alpha\beta}$, or $\Box^{-1}G_{\alpha\beta}$, and is in general due to the presence of non-derivative terms of the form $\sim \Gamma\Gamma H$, as nicely illustrated in [61].

We thus conclude that tensor non-localities containing terms such as $\Box^{-1}R_{\mu\nu}$ or $\Box^{-1}G_{\mu\nu}$ are unstable due to the tensorial nature of this additional term, in agreement with [61] and [44], and that the only combination that allows for a feasible cosmology is that presented in the present work, containing just the Ricci scalar, equation 4.2.1.

Conclusions and Perspectives

The main result of this work is the introduction of a modification of General Relativity (GR) which is effective at cosmological scales. Any modification of GR is an extremely subtle and challenging task for a number of reasons: on the one hand, any extension should face with the impressive success of Einstein's theory at Solar System scales, thus leaving (almost) untouched predictions such as the deflection of light and the precession of perihelia. This aspect is at the base, for example, of the difficulties in constructing a viable theory of massive gravity, as discussed in the text, though one would expect that moving slightly away from the point $m = 0$ (where m is the graviton mass) could be one of the most natural paths to try. On the contrary, already from the works of Van Dam, Veltman and Zacharov it has been known that the $m \to 0$ limit is subtle and faces severe problems of theoretical consistency.
Besides Solar System scales, on the other hand, in recent years General Relativists have at their disposal an impressive progress in cosmological observations that, from the first discovery of the acceleration of the Universe in 1998, have increased their precision in a rapid and promising way. Such observations indeed concern the long-distance regime of the theory, and do open the possibility for any modification of ΛCDM to be tested directly against the data in the near future. A ΛCDM model fits a large number of observations, but any theoretical investigation on the nature of Dark Energy could provide interesting benchmarks against it. In particular, the most intriguing puzzle to be attacked remains the mysterious nature of the Cosmological Constant itself and the huge departure of its value from any known scale in particle physics.

We believe that, in light of these reasoning, the non-local model we propose opens a new and promising line of research for a variety of reasons. From a more theoretical point of view, as we explained in detail, it is fully consistent and does recover all GR successes at Solar System and lab scales. Indeed, the most important aspects are the absence of a vDVZ discontinuity, which one can see already from the propagator in the linearised theory, and which we showed by the explicit computation of the spherically symmetric, static solutions, and the absence of ghosts - which is ensured by the fact that the non-local terms automatically come with a retarded prescription, and hence do not describe propagating degrees of freedom. This last features comes at the price that one can't interpret the resulting equations as those of a fundamental QFT, but rather as effective classical equations. They will likely be obtained from some smoothing procedure of some more fundamental (and local) QFT.
As for the phenomenological side, we underlined repeatedly (and we believe that this is one of the most remarkable features of the work) that the model is highly predictive, since it has the same number of free parameters as ΛCDM and, after fixing the mass scale m so to reproduce the observed value of the matter density Ω_M, leads to a sharp prediction for the DE equation of state at any redshift. The value today is in very good agreement with the *Planck* results and on the phantom side, a feature that could help to solve the tension between existing measurements.

The nature of the model naturally opens two main lines of investigation.
First, since the theory is an effective classical one involving non-local terms, an obvious point is to understand if such equations can emerge from a fundamental quantum theory. At the same time, one should continue investigating the cosmological consequences. We stress that, at least in first approximation, the two problems are decoupled, even if the necessity to embed our equations in a more fundamental theory may lead to the introduction of a different nonlocal structure for the effective theory. At the same time, extra degrees of freedom may emerge at the quantum level, thus leading to a modified picture - e.g. of quantum fluctuations during inflation, and subsequently to a different spectral index n_s, or to non-standard polarisations in GW stochastic background to which future experiments may be sensible. This motivates our investigation in the last chapter of this work, in which we showed that a number of possible combinations in the effective equations, in particular those containing a tensorial structure, actually generate an unstable background evolution, thus providing a constraint on the spectrum of the possible terms. In any case, as already stressed in this thesis, a full analysis should be obtained evolving the perturbations with a Boltzmann code and comparing with the available data. The first issue in this direction is to understand whether the perturbations are well-behaved, a point that already allows a more direct comparison with CMB, BAO and SnIa data. This is the subject of a recent work by Dirian *et al.* [63] which is the natural prosecution of the results presented in this thesis as far as the cosmological consequences of the model are concerned. Their results are encouraging for two reasons. First, the predictive power of the model is confirmed and even enhanced by the fact that even the DE perturbations (energy, pressure, anisotropic stress and velocity divergence) are fully characterised as functions of redshift and momentum once the only free parameter m is fixed. Moreover, the cosmological perturbations are well-behaved, i.e. sufficiently close to those of ΛCDM to be consistent with observations. Second, even if such difference lies within the current experimental errors, they show that deviations from ΛCDM are still sufficiently significant to allow a clear distinction to be made with near-future surveys.

While the field-theoretical aspect indeed opens an interesting problem for a more theoretical mind, we believe that these last results indicate that our model deserves attention since it could provide a significant way to approach the DE problem that may lead to decisive results in the near future, either helping to solve the Cosmological Constant problem - if it will turn out that it behaves better then ΛCDM- or strengthening ΛCDM - if falsified by a direct comparison with future data.

Appendix A

Spectrum of inflationary scalar perturbations

The initial conditions of FRW cosmology are highly fine-tuned. Inflation - an earlier period of accelerated expansion - allows the observed Universe to arise from generic initial conditions. As we pointed out in section 1.3, for acceleration to happen in Einstein's gravity one should introduce a negative pressure source (equation 1.3.6). A way to model inflation is if the Universe is initially filled by a scalar field (the inflaton). The definition of the inflationary model amounts to the definition of its potential and its coupling to gravity. One of the simplest models is the single-field slow-roll inflation, where the scalar field is minimally coupled to gravity

$$S = \int d^4x \sqrt{-g} \left[\frac{1}{2}R + \frac{1}{2}g^{\mu\nu}\partial_\mu\phi\,\partial_\nu\phi - V(\phi) \right] \tag{A.0.1}$$

and the slow-roll conditions are satisfied:

$$\varepsilon_V = \frac{M_{PL}^2}{2}\left(\frac{V'}{V}\right)^2 << 1 \qquad \eta_V = M_{PL}^2\left(\frac{V''}{V}\right) << 1 \tag{A.0.2}$$

This will lead to the realization of the (equivalent) conditions for inflation,

$$\ddot{a} > 0 \quad \Rightarrow \quad \frac{d\,(aH)^{-1}}{dt} < 0 \quad \Rightarrow \quad p < \frac{\rho}{3} \tag{A.0.3}$$

Quantum fluctuations around the classical background evolution of the inflation will lead local delays of the instant at which inflation ends, so different parts of the Universe will undergo slightly different evolutions, acquiring relative density fluctuations $\delta\rho(t, \mathbf{x})$ that represent the seeds of large-scale structure formation.

We define perturbations around the background solutions in FRW,

$$\phi(t, \mathbf{x}) = \phi_0(t) + \varphi(t, \mathbf{x}) \qquad g_{\mu\nu}(t, \mathbf{x}) = \bar{g}_{\mu\nu}(t) + \delta g_{\mu\nu}(t, \mathbf{x}) \tag{A.0.4}$$

The symmetries of the flat FRW solution allow to decompose the metric perturbations as scalar, vector and tensor components,

$$ds^2 = -(1 + 2\Phi)\,dt^2 + 2\,a(t)\,B_i\,dx^i\,dt + a^2(t)\,[(1 - 2\Psi)\,\delta_{ij} + E_{ij}]\,dx^i dx^j \tag{A.0.5}$$

Our focus will be on scalar perturbations, that dominate the CMB temperature fluctuations [70]. It is convenient to introduce the gauge-independent variable ([71])

$$\zeta = -\Psi - H\,\frac{\varphi}{\dot{\phi}_0} \tag{A.0.6}$$

With a certain amount of labour (see [72] for the computation and [70] for a review) one can show that the action A.0.1 can be rewritten as an action for the sole field ζ, which we write in terms of the conformal time $d\eta = dt/a(t)$:

$$S = \frac{1}{2}\int d^3x\, d\eta \left(\frac{a\,\dot{\phi}_0}{H}\right)^2 \left[(\zeta')^2 - (\boldsymbol{\nabla}\zeta)^2\right] \tag{A.0.7}$$

in the gauge

$$h_{ij} = a^2(t)\left(e^{2\zeta}\,\delta_{ij} + \gamma_{ij}\right)\,, \qquad \phi(t,\mathbf{x}) = \phi_0(t)\,, \qquad \partial_i\gamma^{ij} = \gamma^i_i = 0 \tag{A.0.8}$$

In this gauge the inflation field is unperturbed and the scalar degrees of freedom are parametrized by the metric fluctuations.

An important property of ζ is that it remains constant outside the comoving Hubble horizon $(a\,H)^{-1}$, as can be seen from the action A.0.7, since the spatial derivative term gives $\partial_i\zeta/(a\,H) \sim 0$ at scales $k << a\,H$.

In a De Sitter background, $H = const.$ and the action A.0.7 is the action of a free field, so the quantization can proceed in the standard way (see [73]). It is convenient to define the *Mukhanov variable*

$$v \equiv z\,\zeta \qquad z^2 \equiv a^2\frac{\dot{\phi}_0^2}{H^2} \tag{A.0.9}$$

so the action becomes :

$$S = \frac{1}{2}\int d^3x\, d\eta \left[(v')^2 - (\boldsymbol{\nabla}v)^2 + \frac{z''}{z}v^2\right] \tag{A.0.10}$$

Expanding the field v in Fourier modes

$$v(\eta,\mathbf{x}) = \int \frac{d^3k}{(2\pi)^3}\, v_{\mathbf{k}}(\eta)\, e^{i\mathbf{k}\cdot\mathbf{x}} \tag{A.0.11}$$

The corresponding equations of motion are

$$v''_{\mathbf{k}} + \left(k^2 - \frac{z''}{z}\right) v_{\mathbf{k}} = 0 \tag{A.0.12}$$

We may write the general solution for $v_{\mathbf{k}}$ as

$$v_{\mathbf{k}} = v_k(\eta)\hat{a}_{\mathbf{k}} + v_k^*(\eta)\hat{a}^\dagger_{-\mathbf{k}} \tag{A.0.13}$$

Quantization is achieved promoting the coefficients $\hat{a}_{\mathbf{k}}$, $\hat{a}^\dagger_{-\mathbf{k}}$ to creation and annihilation operators satisfying the canonical commutation relations

$$\left[\hat{a}_{\mathbf{k}}, \hat{a}^\dagger_{\mathbf{p}}\right] = (2\pi)^3\delta(\mathbf{k}-\mathbf{p}) \tag{A.0.14}$$

which are realised if and only if the function v is normalised as

$$i\,W[v_k, v_k^*] \equiv i(v_k^*\,v_k' - v_k'^{\,*}\,v_k) = 1 \tag{A.0.15}$$

In this case the solution $v_k(\eta)$ is called a *mode function*.

Equation A.0.15 is the first boundary condition to solve A.0.12. The second comes from "vacuum selection", i.e. the requirement that the vacuum state for the fluctuations, $\hat{a}_{\mathbf{k}}|0\rangle = 0$, reduce to the Minkowski vacuum of a comoving observer in the far past. In this limit A.0.12 becomes the equation of a simple harmonic oscillator with time-independent frequency, which has a well-known, unique solution. Then, the second boundary condition we impose is

$$v_k(\eta) \overset{\eta\to-\infty}{\longrightarrow} \frac{e^{-ik\eta}}{\sqrt{2k}} \tag{A.0.16}$$

In a De Sitter universe with $H = const.$, $z''/z = a''/a = 2/\eta^2$, the solution for v with the above boundary conditions is

$$v_k = \frac{e^{-ik\eta}}{\sqrt{2k}}\left(1 - \frac{i}{k\eta}\right) \tag{A.0.17}$$

The resultant solution is known as *Bunch-Davies vacuum*

$$v(\eta, \mathbf{x}) = \int \frac{d^3k}{(2\pi)^3\sqrt{2k}}\left[\hat{a}_{\mathbf{k}}e^{-ik\eta}\left(1 - \frac{i}{k\eta}\right) + \hat{a}_{\mathbf{k}}^\dagger e^{ik\eta}\left(1 + \frac{i}{k\eta}\right)\right]e^{i\mathbf{k}\cdot\mathbf{x}} \tag{A.0.18}$$

An important propriety is that, after a mode exits the horizon, it can be described as a "classical" (in a sense to be specified) variable with a given probability distribution. In a De Sitter background, the field $\zeta = (H\,v)/(\dot{\phi}_0\,a)$, with $a = a_{DS} = -1/(\eta\,H)$ can be written using A.0.18 as

$$\zeta(\eta, \mathbf{x}) = \frac{i\,H^2}{\dot{\phi}_0}\int \frac{d^3k}{(2\pi)^3\sqrt{2k^3}}\left[\hat{a}_{\mathbf{k}}e^{-ik\eta}\,(1 + ik\eta) - \hat{a}_{\mathbf{k}}^\dagger e^{ik\eta}\,(1 - ik\eta)\right]e^{i\mathbf{k}\cdot\mathbf{x}} \tag{A.0.19}$$

For a mode outside the horizon, $k|\eta| << 1$ and we can expand $(1 - ik\eta)e^{ik\eta} \simeq 1 + k^2\eta^2/2 - ik^3\eta^3/3$, $(1 + ik\eta)e^{-ik\eta} \simeq 1 + k^2\eta^2/2 + ik^3\eta^3/3$, so

$$\zeta_{\mathbf{k}}(\eta) = \frac{i\,H^2}{\dot{\phi}_0\sqrt{2k^3}}\left[\left(1 + \frac{k^2\eta^2}{2}\right)\left(\hat{a}_{\mathbf{k}}^\dagger - \hat{a}_{\mathbf{k}}\right) + \frac{i}{3}(k\eta)^3\left(\hat{a}_{\mathbf{k}}^\dagger + \hat{a}_{\mathbf{k}}\right)\right] \tag{A.0.20}$$

On the other hand, the conjugate momentum obtained from A.0.7 is

$$\pi = \frac{\partial\mathcal{L}}{\partial\zeta'} = \left(\frac{a\,\dot{\phi}_0}{H}\right)^2\zeta' \tag{A.0.21}$$

Using A.0.20 we find for modes outside the horizon

$$\pi_{\mathbf{k}} = \left(\frac{\dot{\phi}_0}{H}\right)^2 a\,H\sqrt{\frac{k}{2}}\left[\left(\hat{a}_{\mathbf{k}}^\dagger - \hat{a}_{\mathbf{k}}\right) + ik\eta\left(\hat{a}_{\mathbf{k}}^\dagger + \hat{a}_{\mathbf{k}}\right)\right] \tag{A.0.22}$$

In De Sitter, $\eta = -1/(Ha) \sim e^{-Ht}$, so the terms proportional to $k\eta$ are decaying modes. For the remaining, "growing" part of the solution we have, from A.0.20 and A.0.22,

$$[\zeta_{\mathbf{k}}, \pi_{\mathbf{p}}] \sim \left[\left(\hat{a}_{\mathbf{k}}^\dagger - \hat{a}_{\mathbf{k}}\right), \left(\hat{a}_{\mathbf{p}}^\dagger - \hat{a}_{\mathbf{p}}\right)\right] = 0 \tag{A.0.23}$$

since we don't measure the decaying mode, the variable ζ appears then as a classical stochastic variable.

After a mode exits the horizon, then, it is described by a classical probability distribution with variance given by the power spectrum $\mathcal{P}_\zeta(k)$ evaluated at horizon crossing, defined as

$$\langle \zeta_{\mathbf{k}}(\eta)\, \zeta_{\mathbf{k}'}(\eta)\rangle = (2\pi)^3 \delta^3(\mathbf{k}-\mathbf{k}')\, \mathcal{P}_\zeta(k) \tag{A.0.24}$$

where $\mathcal{P}_\zeta(k) = \left|\zeta^{(cl)}_{\mathbf{k}}(\eta)\right|^2$ and $\zeta^{(cl)}_{\mathbf{k}}(\eta)$ is the Bunch-Davies solution. Since the field is a free field, we expect a Gaussian spectrum, so the two-point function is sufficient to characterise the probability distribution.
On super horizon scales, $|k\,\eta| << 1$ one finds [70]

$$\langle \zeta_{\mathbf{k}}(\eta)\, \zeta_{\mathbf{k}'}(\eta)\rangle = (2\pi)^3 \delta^3(\mathbf{k}-\mathbf{k}') \left[\frac{H_*^2}{2k^3}\, \frac{H_*^2}{\dot\phi_{0\,*}^2}\right] \tag{A.0.25}$$

where the $*$ denotes that the quantity should be evaluated at horizon-crossing, i.e. at $k = aH$. The standard parametrization is

$$\mathcal{P}_\zeta(k) = \frac{H_*^4}{2k^3\, \dot\phi_{0\,*}^2} = 2\pi^2\, A_s \left(\frac{k}{k_*}\right)^{n_s-1} k^{-3} \tag{A.0.26}$$

Hence, inflation predicts a *scale-invariant power spectrum*, $n_s = 1$. Observations give a quasi scale-invariant spectrum, $n_s \simeq 0.96$ [11].

Appendix B

CMB anisotropies

B.1 Angular Power Spectrum

The primordial fluctuations during inflation as described by $\mathcal{P}_\zeta(k)$ are related to cosmological observables such as the CMB as they represent the initial conditions for cosmic evolution.

The measured CMB shows fluctuations $\delta T/T_0 \sim 10^{-5}$ with respect to the background blackbody temperature $T_0 \simeq 2.7$ K that are well-measured by recent and ongoing experiments ([10],[11]). A map of the measured fluctuations is shown in figure 2.6. We can quantify the power expanding in harmonics

$$\frac{\delta T}{T_0}(\hat{n}) = \frac{T(\hat{n}) - T_0}{T_0} = \sum_{\ell,m} a_{\ell m}\, Y_{\ell m}(\hat{n}) \tag{B.1.1}$$

where

$$a_{\ell m} = \int d\Omega_{(\hat{n})}\; Y^*_{\ell m}(\hat{n})\, \frac{\delta T}{T_0}(\hat{n}) \tag{B.1.2}$$

The rotationally-invariant angular power spectrum is defined as

$$C_\ell = \frac{1}{2\ell+1} \sum_m \langle a^*_{\ell m}\, a_{\ell m} \rangle \tag{B.1.3}$$

For instantaneous recombination, the temperature fluctuations along the line-of-sight direction can be represented as

$$\frac{\delta T}{T_0}(\hat{n}) = \int \frac{d^3k}{(2\pi)^3}\, \Theta_{\mathbf{k}}(\eta_{rec})\, \zeta_{\mathbf{k}}\, e^{i\mathbf{k}\cdot\mathbf{x}_{rec}} \tag{B.1.4}$$

Plugging into *B.1.2* and using the expansion

$$e^{i\mathbf{k}\cdot\mathbf{r}} = 4\pi \sum_{\ell m} (i)^\ell\, j_\ell(kr)\, Y^*_{\ell m}(\hat{n})\, Y_{\ell m}(\hat{n}) \tag{B.1.5}$$

we get, after the integration over the solid angle,

$$a_{\ell m} = 4\pi (i)^\ell \int \frac{d^3k}{(2\pi)^3}\, Y^*_{\ell m}(\hat{n})\, \Theta_{\mathbf{k}}(\eta_{rec})\, \zeta_{\mathbf{k}}\, j_\ell(k(\eta_0 - \eta_{rec})) \tag{B.1.6}$$

where we have used $r_{rec} = \eta_0 - \eta_{rec}$ for the geodesic of the photon travelling from recombination until the present. Then

$$\begin{aligned}\langle a^*_{\ell m}\, a_{\ell' m'}\rangle &= (4\pi)^2 \int \frac{d^3k}{(2\pi)^3}\,\frac{d^3k'}{(2\pi)^3}\,\Theta_{\mathbf{k}}(\eta_{rec})\,\Theta_{\mathbf{k}'}(\eta_{rec})\; j_\ell(k(\eta_0-\eta_{rec}))\, j_{\ell'}(k'(\eta_0-\eta_{rec}))\times \\ &\quad \times\langle \zeta_{\mathbf{k}}\,\zeta_{\mathbf{k}'\,m'}\rangle\, Y^*_{\ell m}(\hat{n})\, Y_{\ell' m'}(\hat{n}) = \\ &= \frac{2}{\pi}\int k^2\, dk\;\Theta^2_{\mathbf{k}}(\eta_{rec})\, j^2_\ell(k(\eta_0-\eta_{rec}))\,\mathcal{P}_\zeta(k)\;\delta_{\ell\,\ell'}\delta_{m\,m'} \end{aligned} \tag{B.1.7}$$

where we have used the definition of power spectrum, equation A.0.24. Finally, we put the angular power spectrum in the standard form

$$C_\ell = \frac{2}{\pi}\int d\log k\;\;\Theta^2_{\mathbf{k}}(\eta_{rec})\, j^2_\ell(k(\eta_0-\eta_{rec}))\, k^3\,\mathcal{P}_\zeta(k) \tag{B.1.8}$$

The angular power spectrum contains then information about initial conditions - $\mathcal{P}_\zeta(k)$ -, plasma physics - $\Theta_{\mathbf{k}}(\eta_{rec})$ - and sky position - $j_\ell(k(\eta_0-\eta_{rec}))$.

B.2 Tight-coupling approximation and Sachs-Wolfe effect

The computation of the power spectrum B.1.8 requires the numerical integration of the Boltzmann equations to get the function $\Theta_{\mathbf{k}}(\eta_{rec})$. Here we shall show how the computation can be analytically performed under a few assumptions, and we shall give a qualitative understanding and an estimate of the acoustic peaks appearing in the angular power spectrum.

Since we are concentrated on scalar perturbations, we shall work in the *Newtonian gauge*,

$$ds^2 = -(1+2\Phi)\,dt^2 + a^2(t)\,(1-2\Psi)\,\delta_{ij}\,dx^i dx^j \tag{B.2.1}$$

The traceless part of Einstein's equations at first order gives, in absence of anisotropic stress,

$$0 = G^i_j - \frac{1}{3}\delta^i_j\, G^k_k \propto \Psi - \Phi \;\Rightarrow\; \Psi = \Phi \tag{B.2.2}$$

While the trace $G^k_k = 0$ gives in matter domination ($a \sim \eta^2$)

$$\Phi'' + 3\,\frac{2}{\eta^2}\Phi' = 0 \tag{B.2.3}$$

which has solutions $\Phi_+ = $ const. and $\Phi_- \sim 1/\eta^5$. The second is a decaying mode and can be neglected, so we obtain that in MD both Φ and Ψ are constant.

The first step to compute the transfer function is to take into account the redshift. Since after decoupling the distribution function of the photons is fixed, energy and temperature are related by

$$\frac{T_{obs}}{T_{rec}} = \frac{\omega_{obs}}{\omega_{rec}} \tag{B.2.4}$$

On the other hand, in the metric B.2.1 we have

$$\frac{\omega_{obs}}{\omega_{rec}} = \sqrt{\frac{g^{(rec)}_{00}}{g^{(obs)}_{00}}} \simeq \frac{a_{rec}}{a_{obs}}\,(1+\Phi_{rec}-\Phi_{obs}) \tag{B.2.5}$$

The term propertional to Φ_{obs} corresponds to $\ell = 0$ in the multipole expansion, and can be neglected.

The Doppler effect instead gives

$$\frac{\omega_{obs}}{\omega_{rec}} = \frac{1 + \hat{\mathbf{n}} \cdot \mathbf{v}_{obs}}{1 + \hat{\mathbf{n}} \cdot \mathbf{v}_{rec}} \simeq 1 + \hat{\mathbf{n}} \cdot (\mathbf{v}_{obs} - \mathbf{v}_{rec}) \tag{B.2.6}$$

Here, the term with $\mathbf{v}_{obs}$ is a multipole with $\ell = 1$ which can be subtracted. Combining the above expressions with the definition of δT, equation B.2.8, we end up with the expression

$$\frac{\delta T}{T_0}(\hat{n}) = \left(\frac{\delta T}{T} + \Phi - \hat{\mathbf{n}} \cdot \mathbf{v} \right) \Big|_{\eta = \eta_{rec}} \tag{B.2.7}$$

The first term in brackets on the right-hand side is the intrinsic temperature fluctuation at early times, while the second indicates the energy lost when the photon climbs out of a potential well. Furthermore, $\rho_\gamma \sim T^4$ so we can set $\delta T/T = \delta_\gamma/4$ where $\delta_\gamma = \delta\rho_\gamma/\rho_\gamma$:

$$\frac{\delta T}{T_0}(\hat{n}) = \left(\frac{1}{4}\delta_\gamma + \Phi - \hat{\mathbf{n}} \cdot \mathbf{v} \right) \Big|_{\eta = \eta_{rec}} \tag{B.2.8}$$

To make progress, we shall examine the behaviour of the system in the **tight coupling limit**, i.e. protons and electron are highly coupled to photons through Compton scattering. This condition is realised if the scattering rate is much larger than the expansion rate. Thus we have a "baryon-photon" perfect fluid, described by Euler's and continuity equations for the variables $\delta \equiv \delta\rho/\rho$ and $\mathbf{v}$. These can be obtained to the evaluation of $\boldsymbol{\nabla}^\mu T_{\mu\nu}$ at first order, see e.g. [31]

$$\delta' + (1 + w)\,(\theta - w\Psi') = \frac{3a'}{a}\,(w - c_s^2) \tag{B.2.9}$$

$$\theta' + \frac{a'}{a}(1 - 3w)\,\theta + \frac{w'}{1 + w}\,\theta + \frac{\boldsymbol{\nabla}^2[\delta P]}{(1 + w)} + \boldsymbol{\nabla}^2\Phi = 0 \tag{B.2.10}$$

where $\theta = \boldsymbol{\nabla} \cdot \mathbf{v}$ and $c_s^2 = \partial P/\partial\rho$ is the sound speed.

Let us make the further assumption that the baryons contribute negligibly to the energy of the fluid. For a relativistic perfect fluid with $P_\gamma = \rho_\gamma\, w$, $\delta P_\gamma = c_s^2\, \delta_\gamma$ we have thus $w = c_s^2 \simeq 1/3$. Taking the derivative of B.2.9 and using B.2.10 we get

$$\delta_\gamma'' = \frac{4}{3}\boldsymbol{\nabla}^2 \left(\frac{1}{4}\delta_\gamma + \Phi \right) \tag{B.2.11}$$

which in Fourier space has the solution

$$\frac{1}{4}\delta_\gamma + \Phi = A_{\mathbf{k}} \cos\left(\frac{1}{\sqrt{3}}\, k\eta \right) + B_{\mathbf{k}} \sin\left(\frac{1}{\sqrt{3}}\, k\eta \right) \tag{B.2.12}$$

The initial conditions are fixed by requiring adiabatic fluctuations in a MD universe. Following [74], we move from the rest frame of the fluid to the Newtonian gauge performing the shift of time coordinate

$$dt \mapsto \sqrt{1 + 2\Phi}\, dt \simeq (1 + \Phi) dt \tag{B.2.13}$$

If the equation of state is $P = w\,\rho$ then $a \sim t^{2/3(1+w)}$ and the temperature scales as $aT_0 =$ const., so with the aid of B.2.13 we get

$$\frac{\delta T}{T_0} = -\frac{\delta a}{a} = -\frac{2}{3(1+w)}\Phi \tag{B.2.14}$$

Furthermore, from equation B.2.10 we have $\mathbf{v}' \sim \boldsymbol{\nabla}\Phi \Rightarrow \mathbf{v} \sim k\eta\,\Phi << \Phi$ on super horizon scales, so we can neglect the Doppler shift term in B.2.8. Using B.2.14 we get the **Sachs-Wolfe formula**

$$\frac{\delta T}{T_0}(\hat{\mathbf{n}}) = \frac{1}{3}\Phi \tag{B.2.15}$$

Our initial conditions for the solution B.2.12 follow from equation B.2.8

$$\left(\frac{1}{4}\delta_\gamma + \Phi\right)_{in} = \left(\frac{\delta T}{T_0}(\hat{\mathbf{n}})\right)_{in} = \frac{1}{3}\Phi_{in} \tag{B.2.16}$$

This gives $A_{\mathbf{k}} = \Phi_{\mathbf{k}}/3$, $B_{\mathbf{k}} = 0$. Finally, the velocity is obtained from B.2.10 in Fourier space for a velocity field without vorticity, $\mathbf{v}_{\mathbf{k}} = -i\mathbf{k}\,v_{\mathbf{k}}$:

$$(i\mathbf{k}\cdot(-i\mathbf{k}\,v_{\mathbf{k}}))' = -k^2\left(\frac{1}{4}\delta_{\gamma\,\mathbf{k}} + \Phi_{\mathbf{k}}\right) = -\frac{k^2}{3}\Phi_{\mathbf{k}}\,\cos\left(\frac{1}{\sqrt{3}}\,k\eta\right) \tag{B.2.17}$$

So, using the fact that in MD $\Phi = -3\zeta/5$,

$$\mathbf{v}_{\mathbf{k}} = i\hat{\mathbf{k}}\,\frac{\sqrt{3}}{5}\,\zeta_{\mathbf{k}}\sin\left(\frac{1}{\sqrt{3}}\,k\eta\right) \tag{B.2.18}$$

Putting all the results together, we find

$$\begin{aligned}\frac{\delta T}{T_0}(\hat{\mathbf{n}}) &= \frac{1}{4}\delta_\gamma + \Phi - \hat{\mathbf{n}}\cdot\mathbf{v} = \\ &= -\frac{1}{5}\zeta_{\mathbf{k}}\left[\cos\left(\frac{1}{\sqrt{3}}\,k\eta\right) + i\hat{\mathbf{n}}\cdot\hat{\mathbf{k}}\,\sqrt{3}\,\sin\left(\frac{1}{\sqrt{3}}\,k\eta\right)\right]\end{aligned} \tag{B.2.19}$$

Note that the modes are in phase with each other. This is another characteristic prediction of inflation.

B.3 Acoustic peaks

Comparing equations B.2.19 and B.1.4 we find

$$\Theta_{\mathbf{k}}(\eta_{rec}) = -\frac{1}{5}\left[\cos\left(\frac{1}{\sqrt{3}}\,k\eta_{rec}\right) + i\hat{\mathbf{n}}\cdot\hat{\mathbf{k}}\,\sqrt{3}\,\sin\left(\frac{1}{\sqrt{3}}\,k\eta_{rec}\right)\right] \tag{B.3.1}$$

We shall examine two opposite regimes:

- $k\eta_{rec} << 1$ $(\ell \leq 90)$
  In this regime, we simply have $\Theta_{\mathbf{k}} \simeq 1/5$. Plugging into B.1.8 we have

$$C_\ell = \frac{2}{\pi}\int d\log k\,\left(-\frac{1}{5}\right)^2 j_\ell^2(k(\eta_0 - \eta_{rec}))\,k^3\,\mathcal{P}_\zeta(k) \tag{B.3.2}$$

The function $j_\ell(k(\eta_0 - \eta_{rec}))$ is oscillating with a sharped peak at $\ell \simeq k(\eta_0 - \eta_{rec})$. Hence, we can approximate

$$k^3 \mathcal{P}_\zeta(k) \simeq \left(\frac{\ell}{\eta_0 - \eta_{rec}}\right)^3 P_\zeta\left(\frac{\ell}{\eta_0 - \eta_{rec}}\right) \tag{B.3.3}$$

Using A.0.26 we get

$$\begin{aligned} C_\ell &= \frac{2}{\pi} 2\pi^2 A_s \left(\frac{\ell}{k_*(\eta_0 - \eta_{rec})}\right)^{n_s - 1} \frac{1}{25} \int d\log k \;\; j_\ell^2(k(\eta_0 - \eta_{rec})) \\ &= \frac{8\pi A_s}{25\,\ell\,(\ell+1)} \left(\frac{\ell}{\ell_*}\right)^{n_s - 1} \end{aligned} \tag{B.3.4}$$

Hence, for a quasi-scale invariant spectrum $n_s \sim 1$ the spectrum exhibits a plateau at low multipoles.

- $k\eta_{rec} >> 1$

Using again the fact that $j_\ell(k(\eta_0 - \eta_{rec}))$ is sharply peaked at $\ell \simeq k(\eta_0 - \eta_{rec})$, we have

$$\Theta_{\mathbf{k}}^2(\eta_{rec}) \simeq \left[\cos^2\left(\frac{\ell\,\eta_{rec}}{\sqrt{3}(\eta_0 - \eta_{rec})}\right) + \text{Doppler effect}\right] \tag{B.3.5}$$

Since the Doppler contribution in effective along the line of sight, we can neglect it with respect to the Sachs-Wolfe effect, hence after integration we get

$$C_\ell = \frac{8\pi A_s}{25\,\ell\,(\ell+1)} \cos^2\left(\frac{\ell\,\eta_{rec}}{\sqrt{3}(\eta_0 - \eta_{rec})}\right) \left(\frac{\ell}{\ell_*}\right)^{n_s - 1} \tag{B.3.6}$$

We have an oscillating spectrum exhibiting peaks at $(c_s\,\ell_n \eta_{rec})/\eta_0 \sim n\pi$.
The rough approximation of neglecting baryon contribution requires this estimate to be corrected.

Including he effect of the baryons can be done observing that they provide extra inertia in the Euler equation for pressure and potential gradients. Since inertial and gravitational mass are equal, all the terms in the Euler equation but the pressure one should be multiplied by $1 + R$ where $R = (P_b + \rho_b)/(P_\gamma + \rho_\gamma) = 3\rho_B/4\rho_\gamma$. The effect is then to reduce the sound speed by $c_s^2 \mapsto 1/(3(1+R))$.

The observational consequences and a qualitative understanding of the physics involved can be found in the text.

Appendix C

vDVZ discontinuity and Vainshtein mechanism in massive gravity

The attempt to give a mass to the graviton has a long history that dates back to a classical paper by Fierz and Pauli [54], who first wrote an action describing a free massive graviton at the linearised level. To reach the next significant achievement in the field we have however to jump to the 70's, when van Dam, Veltman and Zacharov [55], [75] realized the bizarre fact that the $m \to 0$ limit is not smooth, i.e., this theory makes predictions that do not recover those of GR even for $m = 0$. In particular, we shall show that the prediction for light bending is off by 25% from the GR prediction, which is strongly confirmed by experiments. This phenomenon is known as *vDVZ discontinuity*. This argument seem to rule out any massive extension of GR.
However, the linear approximation is the first step to construct a fully non-linear theory. The introduction of non-linearities is due to Vainshtein [69], who found that non-linearities become stronger as the mass decreases, and start dominating below a distance scale $r_V = (M/(m^4 M_{Pl}^2))^{1/5}$ (the "*Vainshtein radius*"), so the predictions of the linear theory are simply not applicable. The vDVZ discontinuity is therefore an artifact of a non valid expansion and could disappear due to non-linear effects.

C.1 Linearized massive gravity

As in the more familiar case of a spin-1 field, the kinetic term for a massless spin-2 field is uniquely determined by the requirement of locality, Lorentz invariance and absence of ghosts. This uniquely fixes it to [67, 57, 76]

$$S = \frac{1}{2} \int d^4x \, h_{\mu\nu} \mathcal{E}^{\mu\nu,\rho\sigma} h_{\rho\sigma} \,, \tag{C.1.1}$$

where the factor 1/2 is fixed requiring the canonical normalization, and the Lichnerowicz operator $\mathcal{E}^{\mu\nu,\rho\sigma}$ is defined as

$$\begin{aligned}\mathcal{E}^{\mu\nu,\rho\sigma} &\equiv \frac{1}{2}\left(\eta^{\mu\rho}\eta^{\nu\sigma}+\eta^{\nu\rho}\eta^{\mu\sigma}-2\eta^{\mu\nu}\eta^{\rho\sigma}\right)\Box+\left(\eta^{\rho\sigma}\partial^{\mu}\partial^{\nu}+\eta^{\mu\nu}\partial^{\rho}\partial^{\sigma}\right)+\\ &- \frac{1}{2}\left(\eta^{\mu\rho}\partial^{\sigma}\partial^{\nu}+\eta^{\nu\rho}\partial^{\sigma}\partial^{\mu}+\eta^{\mu\sigma}\partial^{\rho}\partial^{\nu}+\eta^{\nu\sigma}\partial^{\rho}\partial^{\mu}\right), \end{aligned} \tag{C.1.2}$$

so

$$\mathcal{E}^{\mu\nu,\rho\sigma}h_{\rho\sigma}=\Box h^{\mu\nu}-\eta^{\mu\nu}\Box h+\eta^{\mu\nu}\partial_{\rho}\partial_{\sigma}h^{\rho\sigma}+\partial^{\mu}\partial^{\nu}h-\partial_{\rho}\partial^{\nu}h^{\mu\rho}-\partial_{\rho}\partial^{\mu}h^{\nu\rho}\,. \tag{C.1.3}$$

In this action we have given to $h_{\mu\nu}$ the canonical dimension 1 of QFT, and the dimensionless metric can be recovered with the rescaling $h_{\mu\nu}\mapsto h_{\mu\nu}/(\sqrt{32\pi G})$ through which the action becomes exactly the linearized Einstein-Hilbert action, which appears then as the unique local, Lorentz-invariant, ghost-free action for a massless spin 2 field. This is possible thanks to a symmetry which projects out all unwanted dofs, namely diffeomorphism invariance

$$h_{\mu\nu}\mapsto h_{\mu\nu}+\partial_{(\mu}\xi_{\nu)} \tag{C.1.4}$$

In the case of a massive field, there exists two possible mass terms, $\propto h_{\mu\nu}^2$ and $\propto h^2$, so the most general is a combination of both,

$$\mathcal{L}_{mass}=-\frac{1}{2}m^2\left(h_{\mu\nu}^2-ah^2\right) \tag{C.1.5}$$

where a is a dimensionless parameter. The presence of this mass term breaks diffeomorphism invariance C.1.4, as it should, since we want to describe the 5 dof of a massive spin-2 particle while the gauge invariance leads to only two. Adding also the matter action in the form

$$S_M=\frac{\kappa}{2}\int d^4x\; h_{\mu\nu}T^{\mu\nu} \tag{C.1.6}$$

where κ is a coupling to be fixed below (in massless GR we would have $\kappa=\sqrt{32\pi G}$), the full action can be put in the form

$$S=\frac{1}{2}\int h_{\mu\nu}\mathcal{O}^{\mu\nu,\rho\sigma}h_{\rho\sigma}+\frac{\kappa}{2}\int d^4x\; h_{\mu\nu}T^{\mu\nu} \tag{C.1.7}$$

where $\mathcal{O}^{\mu\nu,\rho\sigma}=\mathcal{E}^{\mu\nu,\rho\sigma}-m^2(\eta^{\mu\rho}\eta^{\nu\sigma}+\eta^{\nu\rho}\eta^{\mu\sigma}-2\,a\,\eta^{\mu\nu}\eta^{\rho\sigma})/2$.

From the action C.1.7 we get the equations of motion in the form $\mathcal{O}^{\mu\nu,\rho\sigma}h_{\rho\sigma}=\frac{\kappa}{2}T^{\mu\nu}$, i.e.

$$\mathcal{E}^{\mu\nu,\rho\sigma}h_{\rho\sigma}-m^2(h^{\mu\nu}-a\eta^{\mu\nu}h)=-\frac{\kappa}{2}T^{\mu\nu} \tag{C.1.8}$$

Taking the trace we get

$$2\partial^{\mu}\partial^{\nu}(h_{\mu\nu}-\eta_{\mu\nu}h)=m^2\,h\,(1-4a)-\frac{\kappa}{2}T\,, \tag{C.1.9}$$

while taking the derivative of both sides and using $\partial_{\mu}T^{\mu\nu}=0$ one has

$$\partial^{\mu}(h_{\mu\nu}-a\eta_{\mu\nu}h)=0\,. \tag{C.1.10}$$

To count the propagating degrees of freedom, we compute the propagator of the theory, $\Delta_{\mu\nu\rho\sigma}$, defined in matrix notation as the solution of $\mathcal{O}(x)\cdot\Delta(y) = i\delta^4(x-y)\mathbb{1}$. Hence, $\Delta = i\mathcal{O}^{-1}$. The operator $\mathcal{O}^{-1}$ can be obtained from the equations of motion, since the solution of C.1.8 is just $h_{\mu\nu} = -(\kappa/2)\mathcal{O}^{-1}_{\mu\nu\rho\sigma}\,T^{\rho\sigma} = (\kappa/2)i\Delta_{\mu\nu\rho\sigma}T^{\rho\sigma}$.

Plugging C.1.10 in C.1.9 we get

$$[(2a-2)\Box + (4a-1)m^2]\,h = -\frac{\kappa}{2}T \tag{C.1.11}$$

We can solve in momentum space,

$$h(k) = \frac{\kappa}{2\left[k^2(-2a+2)+m^2(4a-1))\right]}T(k) \tag{C.1.12}$$

plug back into the equations of motion C.1.8 in momentum space and solve for $h_{\mu\nu}(k)$, neglecting terms proportional to $k_\mu k_\nu$ that give a null contribution when saturated with a conserved EM tensor. Putting the result in the form $h_{\mu\nu}(k) = (\kappa/2)i\,\Delta_{\mu\nu\rho\sigma}T^{\rho\sigma}$, we have

$$\Delta_{\mu\nu\rho\sigma} = \frac{-i}{k^2+m^2}\times\left[\frac{\eta_{\mu\rho}\eta_{\nu\sigma}+\eta_{\nu\rho}\eta_{\mu\sigma}}{2} - \frac{1}{2}\eta_{\mu\nu}\eta_{\rho\sigma} + \frac{(2a-1)m^2}{2\left[(2-2a)k^2+(4a-1)m^2\right]}\eta_{\mu\nu}\eta_{\rho\sigma}\right] \tag{C.1.13}$$

We then compute the saturated propagator, $T_{\mu\nu}(-k)\,\Delta_{\mu\nu\rho\sigma}T^{\rho\sigma}(k)$.

For massive gravitons, one can put the wave vector in the form $k_\mu = (-\omega, 0, 0, k)$ with $\omega^2 = k^2 + m^2$. We have $0 = k_\mu T^{\mu\nu} = -\omega T^{0\nu} + kT^{3\nu}$, so

$$T^{0\nu} = \frac{k}{\omega}T^{3\nu} \tag{C.1.14}$$

We can eliminate all the occurrences of $T^{0\nu}$. We introduce the helicity eigenstates

$$T_{\pm2} = \frac{1}{2}\left(T_{11} - T_{22} \mp 2iT_{12}\right) \tag{C.1.15}$$

$$T_{\pm1} = T_{13} \mp iT_{23} \tag{C.1.16}$$

$$\tag{C.1.17}$$

together with the scalars T_{33} and the trace

$$T = T_{11} + T_{22} + \frac{m^2}{\omega^2}T_{33} \tag{C.1.18}$$

Then we get

$$\begin{aligned} T_{\mu\nu}(-k)\,\Delta_{\mu\nu\rho\sigma}T^{\rho\sigma}(k) \;=\; & \sum_{q=-2,2} T_{-q}(-k)\frac{-i}{k^2+m^2}T_q(k) \\ & + \frac{m^2}{2\omega^2}\sum_{q=-1,1} T_{-q}(-k)\frac{-i}{k^2+m^2}T_q(k) \\ & + \frac{m^2}{6\omega^2}\begin{pmatrix} T_0(k), & T(k)\end{pmatrix}\frac{-i\,\mathcal{M}}{k^2+m^2}\begin{pmatrix} T_0(k) \\ T(k)\end{pmatrix} \\ & - \frac{1}{6}T(-k)\left[\frac{-i}{k^2+\frac{4a-1}{2-2a}m^2}\right]T(k) \end{aligned} \tag{C.1.19}$$

where $T_0 = 3T_{33}$ and

$$\mathcal{M} = \begin{pmatrix} \frac{m^2}{\omega^2} & -1 \\ -1 & \frac{\omega^2}{m^2} \end{pmatrix} \tag{C.1.20}$$

The first two lines describe the 4 components of the helicities 2 and 1, respectively. As for the scalar sector, the matrix $\mathcal{M}$ has the eigenvalues $\lambda_1 = 0$, $\lambda_2 = (m^4 + \omega^4)/(m^2\omega^2)$, hence it describes one scalar propagating degree of freedom carried by the eigenvector $t = T - (m^2/\omega^2)T_0$. The last line in C.1.19 instead describes a ghost-like degree of freedom with mass $\mu^2 = [(4a-1)/(2-2a)]m^2$.

C.2 The Fierz-Pauli point and the vDVZ discontinuity

The Fierz-Pauli Lagrangian is defined by $a = 1$. In this case, C.1.10 gives $\partial^\mu(h_{\mu\nu} - \eta_{\mu\nu}h) = 0$ which, used in C.1.9, implies $-3m^2h = \kappa T/2$. In vacuum, this gives $h = 0$. Then, starting from the 10 dof of $h_{\mu\nu}$, we can eliminate one scalar from the condition $h = 0$, and one scalar plus one vector from C.1.10 which now gives $\partial^\mu h_{\mu\nu} = 0$. Then we are left with the $10 - 4 - 1 = 5$ dof of a massive spin 2.
The Fierz-Pauli tuning is the only choice that allows to have the correct number of propagating degrees of freedom. Indeed, from the saturated propagator C.1.19 we see that only in the case $a = 1$ the ghost decouples and we are left with the correct number of dof. There is no way to get rid of the ghost otherwise. This shows that the Fierz-Pauli point is indeed special.

The surprise comes out if one takes the limit $m \to 0$ at $a = 1$. Then, the helicity 1 part decouples, since its saturated propagator is proportional to m^2/ω^2, while the helicity 2 part smoothly reduces to the GR contribution. In the scalar sector, the ghost has been removed by the FP tuning, but the eigenvector $t_{m=0} = T$ gives now a contribution

$$\frac{1}{6}T(-k)\,\frac{-i}{k^2+m^2}\,T(k) \tag{C.2.1}$$

Hence, the limit $m \to 0$ does not recover GR, but it is rather GR+scalar, the scalar being coupled with the trace of the EM tensor.

In order to compare with GR, we compute the potential induced by the exchange of a graviton between two static sources of masses m_1 and m_2 in the non-relativistic limit. In this limit, we can treat $T_{\mu\nu}$ as an external classical field. Thus, we set $T_{\mu\nu,\,i} = m_i U_{\mu,\,i} U_{\nu,\,i}$ in the limit $U_{\mu,\,i} \to (1,0,0,0)$.The relevant contribution from the propagator C.1.13 in the non relativistic limit is

$$\Delta_{0000} = \frac{2}{3}\frac{-i}{k^2+m^2}\,, \tag{C.2.2}$$

hence the amplitude is given by

$$A \propto \left(-i\frac{\kappa}{2}\right)^2 T_{\mu\nu}(-k)\,\Delta_{\mu\nu\rho\sigma}T^{\rho\sigma}(k) = \frac{\kappa^2}{4}\frac{2}{3}\frac{m_1 m_2}{k^2+m^2} \tag{C.2.3}$$

whereas in GR we have, setting $\sqrt{32\pi G} = \kappa_{GR}$,

$$A_{GR} \propto \left(-i\frac{\kappa_{GR}}{2}\right)^2 T_{\mu\nu}(-k)\,\Delta^{(GR)}_{\mu\nu\rho\sigma}T^{\rho\sigma}(k) = \frac{\kappa_{GR}^2}{4}\frac{1}{2}\frac{m_1 m_2}{k^2+m^2} \tag{C.2.4}$$

Hence, to fit Newton's law we must have m^{-1} much larger than the Solar System radius and

$$\kappa^2 = \frac{3}{4}\kappa_{GR}^2 \tag{C.2.5}$$

Next we examine the consequences on the deflection of light by m_1. The light radius is described by $T_{\mu\nu} = EU_\mu U_\nu$ with $U_\mu = (1,0,0,1)$. In the massive case we have the amplitude

$$\frac{\kappa^2}{4}\frac{m_1 E}{k^2+m^2} \tag{C.2.6}$$

while in the masses case

$$\frac{\kappa_{GR}^2}{4}\frac{m_1 E}{k^2} \tag{C.2.7}$$

Thus also in the limit $m \to 0$ the effect of the exchange of a massive graviton is 3/4 of the one due to the exchange of a massless graviton due to the relation C.2.5. This is the "*van Dam-Veltman-Zacharov discontinuity*". Experiments on light deflection agree with the exchange of a massless graviton, i.e. with general relativity.

The reason of the discontinuity can be traced back to the survival of the coupling between the trace of the EM tensor and a scalar degree of freedom. Since the EM tenor is traceless, the latter doesn't influence the scattering of light, but it affects the prediction for the Newtonian potential, so in light deflection we cannot have an effect that compensates the 25% difference.

C.3 Another special point

Note that another point of interest is the point $a = 1/2$, where the ghost contribution cancels exactly the contribution coming from the matrix element $\mathcal{M}_{22}$. Hence, we are left with a scalar sector of the form

$$\frac{m^2}{6\omega^2}\begin{pmatrix} T_0(k), & T(k) \end{pmatrix}\frac{-i\,\mathcal{M}^{(a=1/2)}}{k^2+m^2}\begin{pmatrix} T_0(k) \\ T(k) \end{pmatrix}$$

where

$$\mathcal{M}^{(a=1/2)} = \begin{pmatrix} \frac{m^2}{\omega^2} & -1 \\ -1 & 0 \end{pmatrix} \tag{C.3.1}$$

This is indeed the same result of reference [58], where the theory mentioned in the text (see eqn. 3.1.6), defined by the following equations of motion, was studied:

$$G_{\mu\nu} - m^2(\Box^{-1}G_{\mu\nu})^T = 8\pi G T_{\mu\nu} \tag{C.3.2}$$

The corresponding equations of motion at the linearized level are obtained from the action

$$S_{non-loc} = \frac{1}{2}\int d^4x\; h_{\mu\nu}\left(1 - \frac{m^2}{\Box}\right)\mathcal{E}^{\mu\nu,\rho\sigma}h_{\rho\sigma} \tag{C.3.3}$$

Then, the theory C.3.2 appears as a suitable "covariantization" of the linear Fierz-Pauli-like theory C.1.7 with $a = 1/2$. In reference [58], such theory was introduced as a promising non-local theory of massive gravity, and it was indeed recognised that it contains a ghost. Moreover, in this case the limit $m \to 0$ recovers smoothly the results of GR, as can be seen from the fact that the helicity 1 part and the scalar sector both smoothly decouple, while the helicity 2 part smoothly reduces to the GR contribution. Hence the point $a = 1/2$ removes the vDVZ discontinuity but at the price of introducing a light ghost. The correct approach to the problem is discussed in the text, where we show that theories such as C.3.2 involving non-local operators should not be considered as fundamental QFT but rather as effective classical equations, hence the existence of a "ghost" is simply a problem that cannot be consistently defined in this context. The real issue that lead to rule out such theory is rather its incapability to give a convincing cosmological evolution [44].

C.4 Vainshtein mechanism

An inadequacy in the argument that the graviton mass should be *exactly* zero to avoid the vDVZ discontinuity was found by Vainshtein [69]. He suggested that before applying the linear approximation to the massive theory one should discuss its applicability in a systematic way, i.e., we should start from the full GR action, add a mass term, and then study the corresponding solutions for a static metric generated by a mass M, which will be a suitable generalisation of the Schwarzschild metric. Then we start from

$$S = S_{EH} + S_{mass} \tag{C.4.1}$$

where S_{mass} is any mass term in the action that at the linearised level reduces to the Fierz-Pauli term,

$$S_{mass} \propto m^2 \int d^4x \, \left(h_{\mu\nu}^2 - h^2 + \mathcal{O}(h_{\mu\nu}^3)\right) \tag{C.4.2}$$

Then one should look for the solution for the metric generated by a source M, writing

$$ds^2 = -e^{2\alpha(r)}dt^2 + e^{2\beta(r)}dr^2 + e^{\mu(\rho)}r^2(d\theta^2 + \sin^2\theta\, d\phi^2) \tag{C.4.3}$$

The results are given e.g in [67], and we do not perform the calculation here since in the text we do the same for the more interesting case of our non-local theory. The steps are analogous, with the difference that, contrary to our theory, in the present case of massive gravity diff invariance is broken, hence one can't set to zero the function $\mu(\rho)$. With the definitions

$$r \equiv \rho e^{\mu/2}\,, \qquad e^{\lambda} \equiv \left(1 + \frac{\rho}{2}\frac{d\mu}{d\rho}\right)^{-2} e^{\sigma-\mu} \tag{C.4.4}$$

one gets, up to next-to leading-order in G (i.e. in the Schwarzshild radius r_S),

$$\nu(r) = -\frac{r_s}{r}\left[1 + \mathcal{O}\left(\frac{r_s}{m^4 r^5}\right)\right], \tag{C.4.5}$$

$$\lambda(r) = \frac{1}{2}\frac{r_s}{r}\left[1 + \mathcal{O}\left(\frac{r_s}{m^4 r^5}\right)\right], \tag{C.4.6}$$

$$\mu(r) = -\frac{1}{2}\frac{r_s}{m^2 r^3}\left[1 + \mathcal{O}\left(\frac{r_s}{m^4 r^5}\right)\right]. \tag{C.4.7}$$

To leading order, the difference from GR is the factor 1/2 in front of $\lambda(r)$, which is the origin of the vDVZ discontinuity. However, if we go to the next order, we discover that the corrections blow up for $m \to 0$. Hence, the linearised theory becomes meaningful only at scales larger than the *Vainshtein* radius r_V,

$$r_v = \left(\frac{r_s}{m^4}\right)^{1/5} \tag{C.4.8}$$

For the Solar System case, we have $r_{V\odot} \geq 40\,pC$ for a reasonable lower limit on m of $m^{-1} > 200\,kPc$, hence the Newtonian potential and the result for the scattering of light from the Sun found in the linearised massive case are simply not applicable.

On the other hand, well inside the Vainshtein radius, a tiny graviton mass has a negligible effect, since in the opposite limit $r << r_V$ one can find a consistent solution in powers of m in the form

$$\nu(r) = -\frac{r_s}{r} + \mathcal{O}\left(m^2\sqrt{r_s r^3}\right) , \tag{C.4.9}$$

$$\lambda(r) = \frac{r_s}{r} + \mathcal{O}\left(m^2\sqrt{r_s r^3}\right) , \tag{C.4.10}$$

$$\mu(r) = \sqrt{\frac{8r_s}{13r}} + \mathcal{O}\left(m^2 r^2\right) . \tag{C.4.11}$$

that approaches smoothly the Schwarzschild solution for GR as $m \to 0$. In this case, since the expansion in m reproduces the smoothly the massless limit, the results for light deflection and for the Newtonian potentials also reproduce the GR results, and no vDVZ discontinuity is present.

To prove that this mechanism actually works, one should however be able to show that the solutions found in the opposite regimes actually match. This is complicated by the fact that, as we approach r_V, the scalar mode becomes strongly coupled and perturbation theory breaks down.

In contrast, in the text we show that our theory is free of vDVZ discontinuity and there is no Vainshtein radius below which the theory becomes strongly coupled. Then, our results do match smoothly those of GR in the $m \to 0$ limit.

Bibliography

[1] M. Maggiore and M. Mancarella, "Non-local gravity and dark energy," 1402.0448. (document), 3, 3.2, 3.2, 3.5, 4.1.1, 4.2, 4.2, 4.2

[2] S. Carroll, *Spacetime and Geometry: An Introduction to General Relativity.* Addison-Wesley Longman, 2004. 1, 1.1, 3.5

[3] E. J. Copeland, M. Sami, and S. Tsujikawa, "Dynamics of dark energy," *Int.J.Mod.Phys.* **D15** (2006) 1753–1936, hep-th/0603057. 1.4, 3.1

[4] L. Amendola and S. Tsujikawa, *Dark Energy: Theory and Observations.* Cambridge University Press, 2010. 1.1, 2.1, 2.3.2, 2.3.2, 2.4.2

[5] R. Jimenez, P. Thejll, U. Jorgensen, J. MacDonald, and B. Pagel, "Ages of globular clusters: a new approach," *Mon.Not.Roy.Astron.Soc.* **282** (1996) 926–942, astro-ph/9602132. 2.1

[6] E. Carretta, R. G. Gratton, G. Clementini, and F. Fusi Pecci, "Distances, ages and epoch of formation of globular clusters," *Astrophys.J.* **533** (2000) 215–235, astro-ph/9902086. 2.1

[7] H. B. Richer, J. Brewer, G. G. Fahlman, B. K. Gibson, B. M. Hansen, *et. al.*, "The Lower main sequence and mass function of the globular cluster Messier 4," *Astrophys.J.* **574** (2002) L151–L154, astro-ph/0205086. 2.1

[8] H. E. Bond, E. P. Nelan, D. A. VandenBerg, G. H. Schaefer, and D. Harmer, "HD 140283: A Star in the Solar Neighborhood that Formed Shortly After the Big Bang," *Astrophys.J.* **765** (2013) L12, 1302.3180. 2.1, 2.5.3

[9] W. L. Freedman, B. F. Madore, B. K. Gibson, L. Ferrarese, D. D. Kelson, S. Sakai, J. R. Mould, J. Robert C. Kennicutt, H. C. Ford, J. A. Graham, J. P. Huchra, S. M. G. Hughes, G. D. Illingworth, L. M. Macri, and P. B. Stetson, "Final results from the hubble space telescope key project to measure the hubble constant," *Astrophys.J.* **553** (2001), no. 1 47. 2.1

[10] **WMAP Collaboration** Collaboration, G. Hinshaw *et. al.*, "Nine-Year Wilkinson Microwave Anisotropy Probe (WMAP) Observations: Cosmological Parameter Results," *Astrophys.J.Suppl.* **208** (2013) 19, 1212.5226. 2.1, 2.3.1, 2.6, 2.5.1, 2.5.3, 2.5.3, B.1

[11] **Planck Collaboration** Collaboration, P. Ade *et. al.*, "Planck 2013 results. XVI. Cosmological parameters," 1303.5076. 2.1, 2.3.1, 2.3.2, 2.8, 2.5.1, 2.5.2, 2.5.2, 2.5.2, 2.12, 2.13, 2.5.3, 3.3.2, 3.3.3, A, B.1

[12] **WMAP Collaboration** Collaboration, E. Komatsu *et. al.*, "Five-Year Wilkinson Microwave Anisotropy Probe (WMAP) Observations: Cosmological Interpretation," *Astrophys.J.Suppl.* **180** (2009) 330–376, 0803.0547. 2.1

[13] L. Perivolaropoulos, "Accelerating Universe: Observational Status and Theoretical Implications," in *The Invisible Universe: Dark Matter and Dark Energy* (L. Papantonopoulos, ed.). Springer, 2007. 2.2, 2.2.1

[14] **Supernova Cosmology Project** Collaboration, S. Perlmutter *et. al.*, "Measurements of the cosmological parameters Omega and Lambda from the first 7 supernovae at z>0.35," *Astrophys.J.* **483** (1997) 565, astro-ph/9608192. 2.3, 2.2.1

[15] **Supernova Cosmology Project** Collaboration, S. Perlmutter *et. al.*, "Measurements of Omega and Lambda from 42 high redshift supernovae," *Astrophys.J.* **517** (1999) 565–586, astro-ph/9812133. 2.2.2, 2.4, 2.5, 2.5.1

[16] **Supernova Search Team** Collaboration, A. G. Riess *et. al.*, "Observational evidence from supernovae for an accelerating universe and a cosmological constant," *Astron.J.* **116** (1998) 1009–1038, astro-ph/9805201. 2.2.2, 2.5.1

[17] **Supernova Search Team** Collaboration, A. G. Riess *et. al.*, "Type Ia supernova discoveries at z>1 from the Hubble Space Telescope: Evidence for past deceleration and constraints on dark energy evolution," *Astrophys.J.* **607** (2004) 665–687, astro-ph/0402512. 2.2.2

[18] E. V. Linder, "Exploring the expansion history of the universe," *Phys.Rev.Lett.* **90** (2003) 091301, astro-ph/0208512. 2.2.2

[19] M. S. Turner and A. G. Riess, "Do SNe Ia provide direct evidence for past deceleration of the universe?," *Astrophys.J.* **569** (2002) 18, astro-ph/0106051. 2.2.2

[20] **SNLS Collaboration** Collaboration, M. Sullivan *et. al.*, "SNLS3: Constraints on Dark Energy Combining the Supernova Legacy Survey Three Year Data with Other Probes," *Astrophys.J.* **737** (2011) 102, 1104.1444. 2.2.2

[21] A. G. Riess, L.-G. Strolger, S. Casertano, H. C. Ferguson, B. Mobasher, *et. al.*, "New Hubble Space Telescope Discoveries of Type Ia Supernovae at z>1: Narrowing Constraints on the Early Behavior of Dark Energy," *Astrophys.J.* **659** (2007) 98–121, astro-ph/0611572. 2.2.2

[22] **ESSENCE** Collaboration, W. M. Wood-Vasey *et. al.*, "Observational Constraints on the Nature of the Dark Energy: First Cosmological Results from the ESSENCE Supernova Survey," *Astrophys.J.* **666** (2007) 694–715, astro-ph/0701041. 2.2.2

[23] N. Suzuki, D. Rubin, C. Lidman, G. Aldering, R. Amanullah, *et. al.*, "The Hubble Space Telescope Cluster Supernova Survey: V. Improving the Dark Energy Constraints Above z>1 and Building an Early-Type-Hosted Supernova Sample," *Astrophys.J.* **746** (2012) 85, 1105.3470. 2.2.2, 2.10, 2.5.1, 2.5.1, 2.5.1, 2.11, 2.5.2, 2.5.2, 2.5.2, 2.12

[24] A. Rest, D. Scolnic, R. Foley, M. Huber, R. Chornock, *et. al.*, "Cosmological Constraints from Measurements of Type Ia Supernovae discovered during the first 1.5 years of the Pan-STARRS1 Survey," 1310.3828. 2.2.2, 2.10, 2.11, 2.5.2

[25] U. Seljak and M. Zaldarriaga, "A Line of sight integration approach to cosmic microwave background anisotropies," *Astrophys.J.* **469** (1996) 437–444, astro-ph/9603033. 2.3.1

[26] A. Lewis and A. Challinor, "http://camb.info." 2.3.1

[27] R. Sachs and A. Wolfe, "Perturbations of a cosmological model and angular variations of the microwave background," *Astrophys.J.* **147** (1967) 73–90. 2.3.1

[28] W. Hu and S. Dodelson, "Cosmic microwave background anisotropies," *Ann.Rev.Astron.Astrophys.* **40** (2002) 171–216, astro-ph/0110414. 2.3.1, 2.7

[29] R. Crittenden, "Dark Energy and the Microwave Background ," in *The Invisible Universe: Dark Matter and Dark Energy* (L. Papantonopoulos, ed.). Springer, 2007. 2.3.2

[30] **Planck Collaboration** Collaboration, P. Ade *et. al.*, "Planck 2013 results. XIX. The integrated Sachs-Wolfe effect," 1303.5079. 2.3.2

[31] H. Mo, F. van den Bosch, and S. White, *Galaxy Formation and Evolution*. Cambridge University Press, 2010. 2.4.1, B.2

[32] S. D. Landy and A. S. Szalay, "Bias and variance of angular correlation functions," *Astrophys.J.* **412** (1993) 64. 2.4.1

[33] F. Beutler, C. Blake, M. Colless, D. H. Jones, L. Staveley-Smith, *et. al.*, "The 6dF Galaxy Survey: Baryon Acoustic Oscillations and the Local Hubble Constant," *Mon.Not.Roy.Astron.Soc.* **416** (2011) 3017–3032, 1106.3366. 2.4.2, 2.4.2, 2.9, 2.5.3

[34] **SDSS Collaboration** Collaboration, D. J. Eisenstein *et. al.*, "Detection of the baryon acoustic peak in the large-scale correlation function of SDSS luminous red galaxies," *Astrophys.J.* **633** (2005) 560–574, astro-ph/0501171. 2.4.2, 2.9, 2.5.3

[35] D. H. Jones, W. Saunders, M. Colless, M. A. Read, Q. A. Parker, *et. al.*, "The 6dF Galaxy Survey: Samples, observational techniques and the first data release," *Mon.Not.Roy.Astron.Soc.* **355** (2004) 747–763, astro-ph/0403501. 2.4.2

[36] **SDSS Collaboration** Collaboration, D. G. York *et. al.*, "The Sloan Digital Sky Survey: Technical Summary," *Astron.J.* **120** (2000) 1579–1587, astro-ph/0006396. 2.4.2

[37] A. G. Riess, L. Macri, S. Casertano, H. Lampeitl, H. C. Ferguson, *et. al.*, "A 3% Solution: Determination of the Hubble Constant with the Hubble Space Telescope and Wide Field Camera 3," *Astrophys.J.* **730** (2011) 119, 1103.2976. 2.5.2, 2.5.3

[38] **BOSS** Collaboration, L. Anderson *et. al.*, "The clustering of galaxies in the SDSS-III Baryon Oscillation Spectroscopic Survey: Baryon Acoustic Oscillations in the Data Release 10 and 11 galaxy samples," 1312.4877. 2.5.2, 2.12

[39] D. L. Shafer and D. Huterer, "Chasing the phantom: A closer look at type Ia supernovae and the dark energy equation of state," 1312.1688. 2.5.3, 2.14, 2.5.3

[40] W. L. Freedman, B. F. Madore, V. Scowcroft, C. Burns, A. Monson, *et. al.*, "Carnegie Hubble Program: A Mid-Infrared Calibration of the Hubble Constant," *Astrophys. J.* **758** (2012) 24, 1208.3281. 2.5.3

[41] **BOSS** Collaboration, L. Anderson, E. Aubourg, S. Bailey, D. Bizyaev, M. Blanton, *et. al.*, "The clustering of galaxies in the SDSS-III Baryon Oscillation Spectroscopic Survey: Baryon Acoustic Oscillations in the Data Release 9 Spectroscopic Galaxy Sample," *Mon.Not.Roy.Astron.Soc.* **427** (2013), no. 4 3435–3467, 1203.6594. 2.5.3

[42] S. Nesseris and S. Tsujikawa, "Cosmological perturbations and observational constraints on non-local massive gravity," 1402.4613. 2.5.3

[43] L. Verde, P. Protopapas, and R. Jimenez, "Planck and the local Universe: Quantifying the tension," *Phys.Dark Univ.* **2** (2013) 166–175, 1306.6766. 2.5.3, 2.15, 3.3.3

[44] S. Foffa, M. Maggiore, and E. Mitsou, "Cosmological dynamics and dark energy from non-local infrared modifications of gravity," 1311.3435. 3, 3.1, 3.1, 3.2, 3.4.1, 3.4.1, 3.4.2, 3.4.2, 3.4.3, 4.2, 4.2, 4.2, C.3

[45] M. Maggiore, "Phantom dark energy from non-local infrared modifications of General Relativity," *Phys.Rev.* **D89** (2014) 043008, 1307.3898. 3, 3.1, 3.2, 3.4.1, 3.4.1, 4.2

[46] S. Foffa, M. Maggiore, and E. Mitsou, "Apparent ghosts and spurious degrees of freedom in non-local theories," 1311.3421. 3, 3.1, 3.2

[47] A. Kehagias and M. Maggiore, "Spherically symmetric static solutions in a non-local infrared modification of General Relativity," 1401.8289. 3, 3.5, 3.5, 3.5.1

[48] R. P. Woodard, "Avoiding Dark Energy with 1/R Modifications of Gravity," in *The Invisible Universe: Dark Matter and Dark Energy* (L. Papantonopoulos, ed.). Springer, 2007. 3.1

[49] S. Deser and R. Woodard, "Nonlocal Cosmology," *Phys.Rev.Lett.* **99** (2007) 111301, 0706.2151. 3.1, 3.4.1

[50] S. Deser and R. Woodard, "Observational Viability and Stability of Nonlocal Cosmology," *JCAP* **1311** (2013) 036, 1307.6639. 3.1, 3.2

[51] J. F. Donoghue and B. K. El-Menoufi, "Non-local quantum effects in cosmology 1: Quantum memory, non-local FLRW equations and singularity avoidance," 1402.3252. 3.1, 3.4.1, 3.4.1

[52] A. Barvinsky, "Nonlocal action for long distance modifications of gravity theory," *Phys.Lett.* **B572** (2003) 109–116, hep-th/0304229. 3.1, 3.4.1

[53] G. Dvali, S. Hofmann, and J. Khoury, "Degravitation of the cosmological constant and graviton width," *Phys.Rev.* **D76** (2007) 084006, hep-th/0703027. 3.1

[54] M. Fierz and W. Pauli, "On Relativistic Wave Equations for Particles of Arbitrary Spin in an Electromagnetic Field," *Proc. Roy. Soc. Lond.* **A173** (1939) 211. 3.1, C

[55] H. van Dam and M. Veltman, "Massive and massless Yang-Mills and gravitational fields," *Nucl.Phys.* **B22** (1970) 397–411. 3.1, C

[56] D. Boulware and S. Deser, "Can gravitation have a finite range?," *Phys.Rev.* **D6** (1972) 3368–3382. 3.1

[57] K. Hinterbichler, "Theoretical Aspects of Massive Gravity," *Rev.Mod.Phys.* **84** (2012) 671–710, 1105.3735. 3.1, 3.5.2, C.1

[58] M. Jaccard, M. Maggiore, and E. Mitsou, "A non-local theory of massive gravity," *Phys.Rev.* **D88** (2013) 044033, 1305.3034. 3.1, 3.4.1, 4, 4.2, 4.2, C.3, C.3

[59] S. Nesseris and S. Tsujikawa, "Cosmological perturbations and observational constraints on non-local massive gravity," 1402.4613. 3.1

[60] L. Modesto and S. Tsujikawa, "Non-local massive gravity," *Phys.Lett.* **B727** (2013) 48–56, 1307.6968. 3.1

[61] P. G. Ferreira and A. L. Maroto, "A few cosmological implications of tensor nonlocalities," *Phys.Rev.* **D88** (2013) 123502, 1310.1238. 3.1, 4, 4.2, 4.2

[62] A. O. Barvinsky, "Serendipitous discoveries in nonlocal gravity theory," *Phys.Rev.* **D85** (2012) 104018, 1112.4340. 3.2

[63] Y. Dirian, S. Foffa, N. Khosravi, M. Kunz, and M. Maggiore, "Cosmological perturbations and structure formation in nonlocal infrared modifications of general relativity," 1403.6068. 3.3.3, 3.3.3, 4.2

[64] C. Deffayet and R. Woodard, "Reconstructing the Distortion Function for Nonlocal Cosmology," *JCAP* **0908** (2009) 023, 0904.0961. 3.3.3, 4.1.2

[65] G. Vilkovisky, "Expectation values and vacuum currents of quantum fields," *Lect.Notes Phys.* **737** (2008) 729–784, 0712.3379. 3.4.1, 3.4.1

[66] A. Barvinsky and G. Vilkovisky, "The Generalized Schwinger-Dewitt Technique in Gauge Theories and Quantum Gravity," *Phys.Rept.* **119** (1985) 1–74. 3.4.1

[67] M. Maggiore, *Gravitational Waves: Volume 1: Theory and Experiments*. OUP Oxford, 2008. 3.4.1, C.1, C.4

[68] M. Jaccard, M. Maggiore, and E. Mitsou, "Bardeen variables and hidden gauge symmetries in linearized massive gravity," *Phys.Rev.* **D87** (2013), no. 4 044017, 1211.1562. 3.4.2, 3.4.3, 3.4.3

[69] A. Vainshtein, "To the problem of nonvanishing gravitation mass," *Phys.Lett.* **B39** (1972) 393–394. 3.5, 3.5.2, C, C.4

[70] D. Baumann, "TASI Lectures on Inflation," 0907.5424. A, A, A

[71] J. M. Bardeen, P. J. Steinhardt, and M. S. Turner, "Spontaneous Creation of Almost Scale - Free Density Perturbations in an Inflationary Universe," *Phys.Rev.* **D28** (1983) 679. A

[72] J. M. Maldacena, "Non-Gaussian features of primordial fluctuations in single field inflationary models," *JHEP* **0305** (2003) 013, astro-ph/0210603. A

[73] V. Mukhanov and S. Winitzki, *Introduction to Quantum Effects in Gravity*. Cambridge University Press, 2007. A

[74] M. White and W. Hu, "The Sachs-Wolfe effect," *Astron. Astrophys.* **321** (1997) 8–9, astro-ph/9609105. B.2

[75] V. I. Zakharov, "Linearized Gravitation Theory and the Graviton Mass," *JETP Letters (Sov. Phys.)* **12** (1970) 312. C

[76] C. de Rham, "Massive Gravity," 1401.4173. C.1